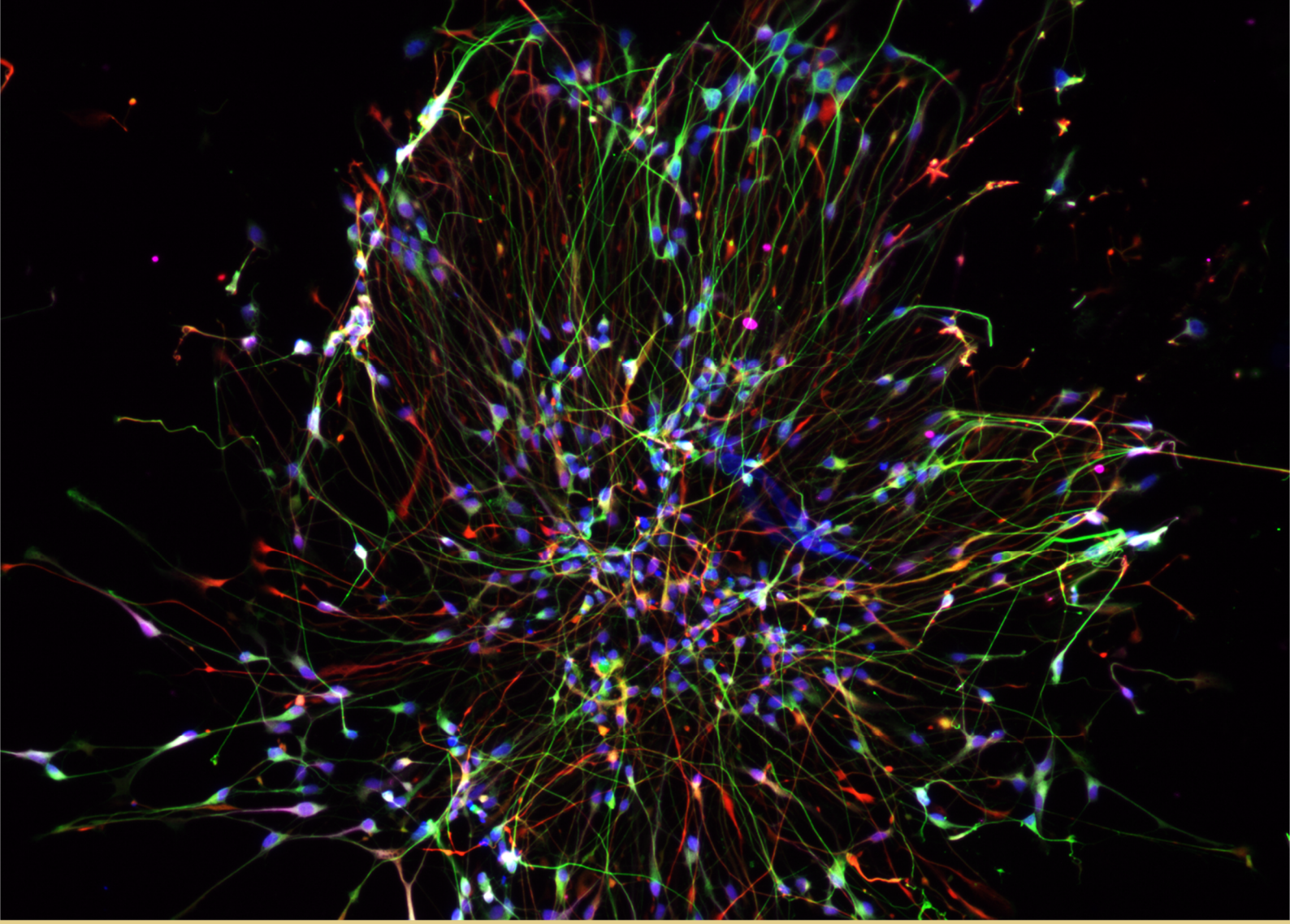

Vítor Manuel Martins Carmona

MICRORNAS TARGETING ATAXIN-3 MRNA IN MACHADO-JOSEPH DISEASE: FROM PATHOGENESIS TO THERAPY

Tese de doutoramento em Ciências Farmacêuticas, ramo de Biotecnologia Farmacêutica, orientada pelo Professor Doutor Luís Pereira de Almeida e apresentada na Faculdade de Farmácia da Universidade de Coimbra

Setembro de 2016

· U C ·

Universidade de Coimbra

MicroRNAs targeting Ataxin-3 mRNA in Machado-Joseph disease: from pathogenesis to therapy

Vítor Manuel Martins Carmona

Tese apresentada à Faculdade de Farmácia da Universidade de Coimbra para prestação de provas de doutoramento em Ciências Farmacêuticas, ramo de Biotecnologia Farmacêutica.

Thesis submitted to the Faculty of Pharmacy of the University of Coimbra for the attribution of the Doctor degree in Pharmaceutical Sciences, in the field of Pharmaceutical Biotechnology.

September 2016

· U C ·

UNIVERSIDADE DE COIMBRA

MicroRNAs targeting Ataxin-3 mRNA in Machado-Joseph disease: from pathogenesis to therapy

The research work presented in this thesis was performed at the Center for Neuroscience and Cell Biology of the University of Coimbra and at the Faculty of Pharmacy of the University of Coimbra, Portugal, under the supervision of Prof. Luís Pereira de Almeida.

O trabalho experimental apresentado nesta tese foi elaborado no Centro de Neurociências e Biologia Celular da Universidade de Coimbra e na Faculdade de Farmácia da Universidade de Coimbra, Portugal, sob a supervisão do Professor Luís Pereira de Almeida.

This work was supported by funds FEDER and the Competitive Factors Operational Program – COMPETE 2020 and by national funds through the Portuguese Foundation for Science and Technology UID/NEU/04539/2013, PTDC/SAU-NMC/116512/2010 and E-Rare4/0003/2012; by the Richard Chin and Lily Lock Machado Joseph Disease Research Fund; the National Ataxia Foundation and by the Marie Curie ITN –Treat PolyQ network. Vitor Carmona was the recipient of a FCT PhD fellowship SFRH/BD/87048/ 2012.

Este trabalho foi financiado por fundos FEDER através do Programa Operacional Factores de Competitividade – COMPETE 2020, por fundos nacionais, através da Fundação Portuguesa para a Ciência e Tecnologia (FCT) no âmbito do projecto Estratégico UID/NEU/04539/2013, PTDC/SAU-NMC/116512/2010 e E-Rare4/0003/2012; pelo Richard Chin and Lily Lock Machado-Joseph Research Fund; pela National Ataxia Foundation e pela rede Marie Curie ITN –Treat PolyQ. Vitor Carmona foi suportado por uma bolsa de doutoramento da FCT, referência SFRH/BD/87048/2012.

Front cover:

Microscope image of human induced pluripotent stem cells derived neurons obtained after neuronal differentiation. Staining was performed with anti-βIII tubulin (green) anti-GFAP (red), anti-MAP2 (yellow) and DAPI (blue).

“It’s a dangerous business, Frodo, going out your door. You step onto the road, and if you don’t keep your feet, there’s no knowing where you might be swept off to.”

J.R.R. Tolkien, The Lord of the Rings

Acknowledgements / Agradecimentos

Ao Professor Doutor Luís Pereira de Almeida, o meu mais sincero agradecimento pela confiança que depositou em mim desde o primeiro minuto, dando-me a oportunidade de fazer consigo o meu doutoramento mesmo sem nos termos conhecido anteriormente. Ao longo dos últimos quatro anos sempre me mostrou a sua disponibilidade, apoiando-me em todos os momentos e depositando em mim a confiança necessária para levar a cabo este projecto. Obrigado pelos ensinamentos científicos que me transmitiu e que me indicaram o caminho a seguir em cada passo, sem os quais este trabalho não se teria concretizado. Obrigado pela sua amizade e palavras de encorajamento que tanto me ajudaram ao longo desta importante etapa.

To Professor Beverly L. Davidson, I would like to acknowledge her contribution for the design of the studies presented in this thesis as well as for her important feedback regarding the interpretation of the results.

À Professora Doutora Catarina Resende de Oliveira e ao Professor Doutor João Ramalho de Sousa Santos agradeço a oportunidade de poder desenvolver este trabalho no Centro de Neurociências e Biologia Celular de Coimbra.

À Fundação para a Ciência e Tecnologia agradeço o seu financiamento sem o qual esta tese não teria sido possível.

A todos os meus colegas e amigos do Centro de Neurociências e Biologia Celular de Coimbra, agradeço a sua amizade, boa disposição, ajuda e encorajamento que tornaram todo este percurso a melhor experiência possível. A todos os "LAs", em especial à Mariana Conceição, Patrícia Rosado, Ana Cristina, Dina Pereira, Filipa Brito, Susana Paixão e Ana Teresa Simões por toda a amizade e companheirismo. Em particular agradeço à Joana Neves que desde o meu primeiro dia no laboratório me acolheu de forma calorosa no grupo, à Geetha pelos bons e maus momentos que partilhámos no mundo dos microRNAs, à Sara Lopes por me ajudar a controlar a minha (des)organização e à Isabel Onofre por me relembrar que a ciência consegue fazer coisas incríveis. Para além disso agradeço também a todos os membros JNs, CPLs e CCs cuja amizade demonstrada em nada ficou atrás da que foi expressa pelos LAs.

Acima de tudo, agradeço à Janete Santos, por todo o apoio incondicional que me deu ao longo de todos estes anos, pela indispensável ajuda que me deu na realização de todo o trabalho, pelas palavras de ânimo que me transmitiu nos maus momentos, pela re-orientação nas situações em que me sentia perdido, pela partilha do seu incomparável espírito científico mas, mais importante, por todo o carinho e amor que me transmitiu e que continuaremos a partilhar na nossa vida. Obrigado por viveres comigo todos estes momentos.

Por fim, um agradecimento especial a todos os amigos e familiares que sempre me incentivaram durante todo este percurso, em particular aos meus pais e à minha irmã que tanto me apoiaram em todos os bons e maus momentos e ao Nero, o felídeo mais popular da vizinhança, e que tanta boa disposição nos traz todos os dias.

Esta tese é-vos dedicada.

TABLE OF CONTENTS

Abbreviations

2'-F: 2' fluorine

2'-MOE: 2' methoxyethyl

2'-OMe: 2' methyl

AAV: Adeno-associated virus

ActD: Actinomycin D

Ago2: Argonaute-2

ALS: Amyotrophic lateral sclerosis

AR: Androgen receptor

ASO: Antisense oligonucleotide

ATN1: Atrophin-1

ATP: Adenosine triphosphate

ATXN: Ataxin

AURE: AU-rich element

BDNF: Brain-derived neurotrophic factor

BSA: Bovine serum albumin

CAA: Cytosine-adenine-adenine

CACNA1A: Calcium voltage-gated channel subunit alpha1 A

CAG: Cytosine-adenine-guanine

CARE: CA-rich element

CBP: CREB-binding protein

cDNA: Complementary DNA

CDS: Coding sequence

CMV: Cytomegalovirus

CNS: Central nervous system

CUG: Cytosine-uracil-guanine

CURE: CU-rich element

DARPP-32: dopamine- and cAMP-regulated neuronal phosphoprotein 32

DMEM: Dulbecco's Modified Eagle Medium

DRPLA: Dentatorubral-pallidoluysian atrophy

DTT: Ditiotreitol

ECF: Enhanced chemifluorescence

EDTA: Ethylenediamine tetraacetic acid

EGF: Epidermal growth factor

FBS: Fetal bovine serum

FGF: Fibroblast growth factor

FLAR: Firefly luciferase assay reagent

FLuc: Firefly luciferase

FTD: Frontotemporal dementia

GFAP: Glial fibrillary acidic protein

GFP: Green fluorescent protein

GURE: GU-rich element

HD: Huntington's disease

hIPSC: Human induced pluripotent stem cells

HTT: Huntingtin

Iba-1: Ionized calcium-binding adapter molecule 1

IRE: Iron responsive element

JD: Josephin domain

LTR: Long terminal repeat

MAP2: Microtubule-associated protein 2

MBNL1: Muscleblind like splicing regulator 1

MBS: MicroRNA binding site

MEM: Modified Eagle's Medium

MiRISC: miRNA-induced silencing complex

MJD: Machado-Joseph disease

mRNA: Messenger RNA

MutATXN3: Mutant ataxin-3

NES: Nuclear export signal

NEUN: Neuronal nuclei

NII: Neuronal intranuclear inclusions

NLS: Nuclear localization signal

PABP: Poly(A) binding protein

P-bodies: Processing bodies

PBS: Phosphate buffered saline

PEI: Polyethyleneimine

PFA: paraformaldehyde

PGK: Phosphoglycerate kinase

Pol II: RNA polymerase II

Pol III: RNA polymerase III

PolyQ: Polyglutamine

Pre-miRNA: Precursor miRNA

Pre-mRNA: Precursor mRNA

Pri-miRNA: Primary miRNA

QPCR: Quantitative PCR

RAB: Renilla assay buffer

RBP: RNA binding protein

REST: Repressor element-1 silencing transcription factor

RLuc: Renilla luciferase

RNAi: RNA interference

SBMA: Spinal and bulbar muscular atrophy

SCA: Spinocerebellar ataxia

SECIS: Selenocysteine insertion sequence elements

shRNA: Shot-hairpin RNA

SIN: Self-inactivating

siRNA: Small interfering RNA

snoRNA: Small nucleolar RNAs

SNP: Single nucleotide polymorphism

SOX2: SRY (sex determining region Y)-box 2

TBP: TATA binding protein

TBP: TATA binding protein

TBS: Tris-buffered saline

TDP-43: TAR DNA-binding protein 43

tRNA: Transfer RNA

TSH: Thyroid-Stimulating Hormone

UIM: Ubiquitin interacting motif

UPS: Ubiquitin-proteasome system

UTR: Untranslated region

VEGF: Vascular endothelial growth factor

WPRE: Woodchuck Hepatitis Virus Posttranscriptional Regulatory Element

WtATXN3: Wild-type ataxin-3

YAC: Yeast artificial chromosome

Summary

Machado-Joseph disease (MJD), also known as spinocerebellar ataxia type 3 (SCA3) is the most common autosomal dominantly-inherited ataxia worldwide. MJD belongs to the group of polyglutamine (polyQ) diseases, genetic disorders caused by an expansion in the number of CAG repetitions in the genes encoding for polyQ proteins. In the case of MJD, this expansion occurs in the *ATXN3* gene, leading to the formation of a mutated form of ataxin-3 (mutATXN3) protein. MutATXN3 will then trigger multiple pathogenic events, many of which are still unclear, culminating in neuronal dysfunction and neurodegeneration. So far, no treatment has been developed capable of delaying or blocking the progression of the disease. Current therapeutic approaches consist mainly in the use of physiotherapy and in the pharmacological alleviation of specific symptoms.

Nevertheless, promising therapeutic approaches have been recently discovered which hold great potential for the treatment of MJD. Among these, taking advantage of the RNA interference pathway (RNAi) allows the blockage of the production of disease-causing proteins therefore preventing its associated downstream toxic pathways. In fact, different studies based on the usage of the RNAi pathway in order to silence the expression of mutATXN3 have obtained encouraging results. However, none of these studies has elucidated how the endogenous RNAi pathway, particularly the microRNA (miRNA) based regulation of gene expression, is affected in MJD. Moreover, no study as evaluated whether endogenous miRNAs can be exploited as a novel therapeutic approach for MJD. For that reason, the aim of this project was to elucidate how the endogenous RNA regulatory mechanisms are involved in mutATXN3 regulation, whether this system is impaired in the context of MJD, and whether miRNA based regulation of ATXN3 could be useful as a novel therapeutic approach for MJD.

In the first part of this project, described in chapter 2, we started by generating a novel lentiviral mouse model of MJD which would allow us the study of the endogenous RNA regulatory mechanisms, in particular those which mediate their functions through the three prime untranslated region (3'UTR) of mutATXN3. The *in vitro* and *in vivo* characterization of this model clearly demonstrated the robust role that this non-coding region mediates in the control of mutATXN3 expression. Moreover, through a genetic and pharmacologic approach, we found compelling evidence that endogenous miRNAs are involved in the regulation of ATXN3 through its 3'UTR.

In chapter 3, we identified a set of miRNAs predicted to target ATXN3 3'UTR and evaluated their expression levels in multiple MJD models. In general, a global downregulation was observed for mir-9, mir-181a and mir-494, across different models including MJD neurons derived from patient fibroblasts and MJD transgenic mice. This raises important implications for the pathogenesis of MJD, but also opens a new opportunity for the development of a novel therapeutic approach for the treatment of MJD.

Accordingly, based on the data obtained in chapters 2 and 3, in chapter 4 we took advantage of miRNA mediated regulation of ATXN3 through its 3'UTR as a gene therapy tool for the reduction of mutATXN3 levels. After developing a lentiviral-based system for efficient overexpression of mir-9, mir-181a and mir-494 *in vitro* and *in vivo* and validating the direct interaction between these miRNAs with the 3'UTR of ATXN3, we demonstrated that viral delivery of mir-9, mir-181a and mir-494 effectively reduced the levels of mutATXN3 and simultaneously ameliorated the associated neuropathology *in vivo*, in a lentiviral mouse model of MJD.

In summary, in this thesis we have provided evidence that endogenous miRNAs play an important role in the regulation of mutATXN3 by targeting its 3'UTR and at the same time are dysregulated in MJD. Moreover, our data demonstrate that the reinstatement of the levels of endogenous miRNAs may be a promising therapeutic approach for the treatment of MJD.

Resumo

A doença de Machado-Joseph (DMJ), também conhecida como ataxia espinocerebelosa do tipo 3 é a ataxia hereditária autossómica dominante com maior prevalência a nível mundial. A DMJ pertence ao grupo das doenças poliglutamínicas (poliQ), um grupo de doenças genéticas causadas por uma expansão no número de repetições CAG nos genes codificantes para as proteínas poliQ. No caso da DMJ, esta expansão ocorre no gene *ATXN3,* levando à formação de uma forma mutada da proteína ataxina-3 (ATXN3MUT). A proteína ATXN3MUT desencadeia múltiplas vias patogénicas, muitas das quais ainda não totalmente esclarecidas, que culminam em disfunção neuronal e neurodegenerescência. Até ao momento não foi ainda desenvolvido nenhum tratamento capaz de atrasar ou impedir a progressão da DMJ. Assim sendo, o tratamento de doentes com DMJ baseia-se maioritariamente no recurso a fisioterapia e ao uso de fármacos com o objectivo de diminuir a incidência de alguns sintomas específicos.

Ainda assim, recentemente têm sido identificadas novas abordagens terapêuticas com bastante potencial para o tratamento da DMJ. Entre elas, a via de interferência de RNA (RNAi) permite bloquear a produção de proteínas mutadas causadoras de doenças e assim prevenir as vias fisiopatológicas a elas associadas. De facto, diferentes estudos baseados no silenciamento da ATXN3MUT através da via de RNAi, obtiveram resultados encorajadores. Ainda assim, nenhum destes estudos avaliou de que forma os mecanismos endógenos de RNAi, tais como a regulação da expressão génica por microRNAs (miRNAs), estariam alterados na DMJ. Para além disso, nenhum estudo avaliou se os miRNAs endógenos poderiam ser usados como nova estratégia terapêutica para a DMJ. Assim sendo, o objectivo deste projecto foi elucidar de que forma os mecanismos endógenos de regulação de RNA estariam envolvidos na regulação da ATXN3MUT, de que forma este sistema estaria alterado na DMJ, e se a regulação da ATXN3MUT por miRNAs poderia ser utilizada como nova abordagem terapêutica para o tratamento da DMJ.

Na primeira parte deste projecto, descrita no capítulo 2, começámos por gerar um novo modelo lentiviral da DMJ que nos permitisse estudar os mecanismos endógenos de regulação de RNA mensageiro através da região 3' não traduzida (3'UTR) da ATXN3MUT. A caracterização deste modelo *in vitro* e *in vivo* demonstrou um papel muito relevante da região não codificante 3'UTR no controlo da expressão da ATXN3MUT. Para além disso, recorrendo a uma abordagem genética e farmacológica,

encontrámos evidências do envolvimento dos miRNAs endógenos na regulação da ATXN3MUT através da sua região 3'UTR.

No capítulo 3, identificámos um conjunto de miRNAs tendo como alvo a 3'UTR da ATXN3 e avaliámos os seus níveis de expressão em múltiplos modelos da DMJ. Observámos uma diminuição nos níveis dos miRNAs mir-9, mir-181a e mir-494 em diferentes modelos incluindo neurónios MJD derivados de fibroblastos de doentes e em tecido de um modelo transgénico de MJD. Estes resultados não só têm importantes implicações para o conhecimento da patogénese da DMJ, como representam uma nova oportunidade para o desenvolvimento de uma nova estratégia terapêutica para a DMJ.

Assim sendo, tendo em consideração os resultados obtidos nos capítulos 2 e 3, no capítulo 4 tirámos partido da regulação da ATXN3MUT por miRNAs através da sua região 3'UTR para desenvolver uma nova estratégia de terapia génica visando a redução dos níveis de ATXN3MUT. Após o desenvolvimento de um sistema baseado em vectores lentivirais para a sobrexpressão de mir-9, mir-181a e mir-494 *in vitro* e *in vivo* e após validação da interacção directa entre os mesmos miRNAs com a 3'UTR da ATXN3, demonstrámos que a entrega destes miRNAs num modelo lentiviral da DMJ em murganho levou a uma diminuição dos níveis de ATXN3MUT e simultaneamente a uma diminuição da neuropatologia associada.

Em conclusão, nesta tese demonstrámos que os miRNAs endógenos não só desempenham um importante papel na regulação da ATXN3MUT através da sua região 3'UTR, como também estão desregulados na DMJ. Para além disso, os nossos resultados demonstram que a reposição dos níveis destes miRNAs é uma promissora estratégia terapêutica para o tratamento da DMJ.

CHAPTER 1

General Introduction

1. Introduction

1.1. Polyglutamine diseases

Among neurodegenerative disorders, polyglutamine (polyQ) diseases represent a family of neurodegenerative conditions caused by a cytosine-adenine-guanine (CAG) triplet repeat expansion in genes encoding several unrelated proteins (Shao and Diamond, 2007). This expansion at the DNA level, leads to the production of a pathogenic protein which will be responsible for the neurodegeneration of specific central nervous system (CNS) regions and ultimately for the development of the disease symptoms (Shao and Diamond, 2007).

In 1991, CAG repeat expansions were for the first time associated to the development of neurodegenerative disorders, when an expansion in the androgen receptor (AR) gene was linked to spinal and bulbar muscular atrophy (SBMA) (La Spada *et al.*, 1991). Since then, polyQ expansions in other genes were found to be associated to other disorders. Currently the group of polyQ diseases is comprised of nine different diseases: huntington's disease (HD), dentatorubral-pallidoluysian atrophy (DPRLA) and spinocerebellar ataxias (SCA) types 1, 2, 3, 6, 7 and 17, all caused by a CAG repeat expansion in a distinct gene (Table 1.1).

Table 1.1 – List of polyQ diseases with respective gene names, normal and pathogenic repeat length, most affected brain regions and main clinical features

Disease	Gene	CAG Repeat length		Most affected brain regions	Main clinical features
		Normal	Pathogenic		
SBMA	*AR*	9-36	38-62	Anterior horn and bulbar neurons, dorsal root ganglia	Motor weakness, swallowing, gynecomastia, decreased fertility
HD	*HTT*	6-34	36-121	Striatum, cerebral cortex	Chorea, dystonia, cognitive deficits, psychiatric problems
DRPLA	*ATN1*	7-34	49-88	Cerebellum, cerebral cortex, basal ganglia, Luys' body	Ataxia, seizures, choreoathetosis, dementia

SCA1	*ATXN1*	6-39	40-82	Cerebellar Purkinje cells, dentate nucleus, brainstem	Ataxia, slurred speech, spasticity, cognitive impairments
SCA2	*ATXN2*	15-24	32-200	Cerebellar Purkinje cells, brain stem, frontotemporal lobes	Ataxia, polyneuropathy, decreased reflexes, infantile variant with retinopathy
SCA3/MJD	*ATXN3*	12-44	55-87	Cerebellar dentate neurons, basal ganglia, brain stem, spinal cord	Ataxia, parkinsonism, spasticity
SCA6	*CACNA1A*	4-20	20-29	Cerebellar Purkinje cells, dentate nucleus, inferior olive	Ataxia, dysarthria, nystagmus, tremors
SCA7	*ATXN7*	4-35	37-306	Cerebellum, brain stem, macula, visual cortex	Ataxia, blindness, cardiac failure in infantile form
SCA17	*TBP*	25-42	47-63	Cerebelllar Purkinje cells, inferior olive	Ataxia, cognitive decline, seizures, and psychiatric problems

SBMA (Spinal and bulbar muscular atrophy), AR (Androgen receptor), HD (Huntington's disease), HTT (Huntingtin), DRPLA (Dentatorubral-pallidoluysian atrophy), ATN1 (Atrophin1), SCA (Spinocerebellar ataxia), MJD (Machado-Joseph disease), ATXN (Ataxin), CACNA1A (Calcium voltage-gated channel subunit alpha1 A), TBP (TATA-binding protein). Table was adapted from (Cummings and Zoghbi, 2000; Shao and Diamond, 2007)

Interestingly, other than the polyQ stretch, polyQ proteins don't share any sequence similarities between each other. Moreover, they have very different cellular localization and functions, which are likely responsible for the heterogeneous profile of polyQ disorders concerning the affected brain regions and associated clinical symptoms (Cummings and Zoghbi, 2000).

Even so, all of these diseases are characterized by a slowly progressive neurodegenerative profile which is likely due to a toxic gain-of-function generated by the polyQ stretch. In fact, both *in vitro* and *in vivo* evidence, demonstrated that the polyQ stretch alone induces increased apoptosis in cell lines, and neurodegeneration and behavioral impairments in mice (Ikeda *et al.*, 1996; Mangiarini *et al.*, 1996; Ordway *et al.*, 1997; Senut *et al.*, 2000). Another common feature in all of these diseases is repeat instability, which is more pronounced upon paternal transmission (McMurray, 2010). Moreover, somatic instability has also been described for many polyQ diseases and, in fact, neurons were identified as permissive cells for genetic instability in HD (Gonitel *et al.*, 2008). In general, the number of CAG repeats is associated with the age of onset of the disease. Longer polyQ tracts are associated with an earlier age of onset and

increased severity of symptoms (La Spada *et al.*, 1992; Andrew *et al.*, 1993; Ranum *et al.*, 1994; Maciel *et al.*, 1995; Gusella and MacDonald, 2000). Another shared feature of polyQ disorders is the formation of protein aggregates, frequently ubiquitinated, which have a predominantly intranuclear localization although they can also be found in the cytoplasm (Davies *et al.*, 1997; Paulson *et al.*, 1997b; Skinner *et al.*, 1997; Holmberg *et al.*, 1998). Interestingly, for SCA6, the presence of these inclusions has been mainly reported in the cytoplasm (Ishikawa *et al.*, 1999a; Ishikawa *et al.*, 1999b). The specific role played by protein aggregation in the disease progression is still controversial and will be discussed in greater detail in the sub-chapter regarding MJD.

1.1.1 Machado-Joseph disease

Machado-Joseph disease (MJD), also known as spinocerebellar ataxia type 3 (SCA3) is an autosomal dominant disease caused by a CAG expansion in the *ATXN3* gene, leading to the formation of a mutated form of the ataxin-3 (ATXN3) protein. It was originally described in 1972, in a family descendant of the Azorean William Machado, living in the United States of America (Nakano *et al.*, 1972). In the following years, other reports described the disease. However, due to the variable symptomatology, they were defined as distinct diseases: nigro-spino-dentatal-degeneration (Woods and Schaumburg, 1972), Joseph disease (Rosenberg *et al.*, 1976) and Azorean disease (Romanul *et al.*, 1977). Only in 1978, in a study of different families from the Azorean Islands, was the definition of “Machado-Joseph disease” proposed, suggesting that all the previously described diseases were in fact variations of a single disease which was characterized by significant clinical variability (Coutinho and Andrade, 1978).

Despite being a rare disorder, MJD is currently the most common form of autosomal dominantly inherited ataxia worldwide (Bird, 1993). Importantly, the highest prevalence worldwide occurs in the Azorean island of Flores, where it affects about 1 in 239 inhabitants. Nevertheless, MJD prevalence has been progressively decreasing in the last two decades (Lima *et al.*, 1998; Bettencourt *et al.*, 2008).

1.1.1.1 Clinical symptoms and progression

As previously mentioned, MJD is characterized by a highly variable profile of clinical manifestations. However, progressive cerebellar ataxia with dysfunction of motor coordination affecting gaze, speech, gait and balance is a hallmark of the disease (Rosenberg, 1992; Riess *et al.*, 2008). Other findings include a dystonic-rigid syndrome, a parkinsonian syndrome, or a combined syndrome of dystonia and peripheral neuropathy. More specific symptoms include ophtalmoplegia, bulging eyes, nystagmus, dystonia, amyotrophy, postural instability, dysarthria and facial and lingual fasciculations (Riess *et al.*, 2008). MJD patients may also be affected by other non-motor impairments such as sleep disorders, cognitive disturbances, chronic pain, cramps, olfactory dysfunction and fatigue (Pedroso *et al.*, 2013).

The age of onset for MJD is also variable and, as for other polyQ diseases, is associated with the extent of CAG over-repetition. In this disease the average age of onset is between 20 and 50 years (Paulson, 2012). More specifically, in a recent study evaluating 366 patients, the average age of onset was 36.37 years (Kieling *et al.*, 2007).

The variability in the clinical profile and in the age of onset between MJD patients led to the organization of five different disease sub-types (Table 1.2) (Coutinho and Andrade, 1978; Rosenberg, 1992; Landau *et al.*, 2000; Riess *et al.*, 2008; Wang *et al.*, 2009). Although having limited clinical relevance, the existence of these different subtypes illustrates the heterogeneity of MJD.

Table 1.2 – MJD different clinical subtypes

Subtype	Characteristics	Age of onset
Type I	Pyramidal and extrapyramidal deficits. Fast disease progression	10–30 years
Type II	Pyramidal and cerebellar deficits without extrapyramidal signs	20–50 years
Type III	Cerebellar deficits and neuropathy	40–75 years
Type IV	Neuropathy and slow progressive parkinsonism	38-47 years
Type V	Spastic paraplegia with or without ataxia	20-30 years

With the progression of the disease, patients are bound to a wheelchair and have severe dysarthria, dysphagia, facial and temporal atrophy, poor cough, often dystonic posturing and ophthalmoparesis. Death may occur due to pulmonary complications and cachexia and has been reported to happen on average 21 years after disease onset (Sudarsky *et al.*, 1992; Kieling *et al.*, 2007).

1.1.1.2 Management of MJD

Currently there is no medication available capable of slowing down or preventing the course of the disease. Therefore, management of MJD is only supportive and based on alleviation of the disease symptoms. In particular, levodopa or dopamine agonists can be used for the alleviation of parkinsonism, and restless leg syndrome, while antispasmodic drugs such as baclofen, can be used to reduce spasticity (Paulson, 1993; Tuite *et al.*, 1995; Schols *et al.*, 1998). Moreover, dystonia and severe spasticity might be reduced with local botulinum toxin injections but it should be used as a last resort due to possible side effects, such as swallowing problems (Holzer and Ludlow, 1996; Freeman and Wszolek, 2005). Depression and sleep disturbances should be treated with antidepressants and benzodiazepines (D'Abreu *et al.*, 2010).

In most cases, non-pharmacological approaches such as physical therapy and exercise programs should be incorporated in order to help the patients cope with their disabilities and improve their strength, balance and gait (D'Abreu *et al.*, 2010). Occupational therapy has also been shown to have a clear beneficial effect on depression symptoms (Silva *et al.*, 2010). Physical aids, such as walkers and wheelchairs, can assist patients on their daily activities (D'Abreu *et al.*, 2010).

1.1.1.3 Neuropathological features

In MJD, neuronal loss occurs in selective regions of the CNS (Fig.1.1). In the cerebellum, the dentate nucleus shows moderate to severe neuronal loss accompanied by the degeneration of the pontocerebellar and spinocerebellar fibers. Regarding the brainstem, there is significant neurodegeneration in the pons, cranial nerve nuclei, reticular formation and in the locus coeruleus. The basal ganglia (*substantia nigra* and

globus pallidus) are also affected by severe neurodegeneration (Rosenberg *et al.*, 1976; Sequeiros and Coutinho, 1993; Rub *et al.*, 2008; Rub *et al.*, 2013).

Although initial studies did not identify significant degeneration in the striatum or the cerebral cortex, the striatum in particular has been shown to present metabolic alterations such as reduced glucose uptake and decreased dopaminergic metabolism (Taniwaki *et al.*, 1997). Moreover, striatal neuronal dysfunction has been identified in multiple MJD mouse models (Bichelmeier *et al.*, 2007; Alves *et al.*, 2008b). Brain atrophy of these selective brain regions has been associated with disease progression and clinical symptoms in MJD (Schulz *et al.*, 2010).

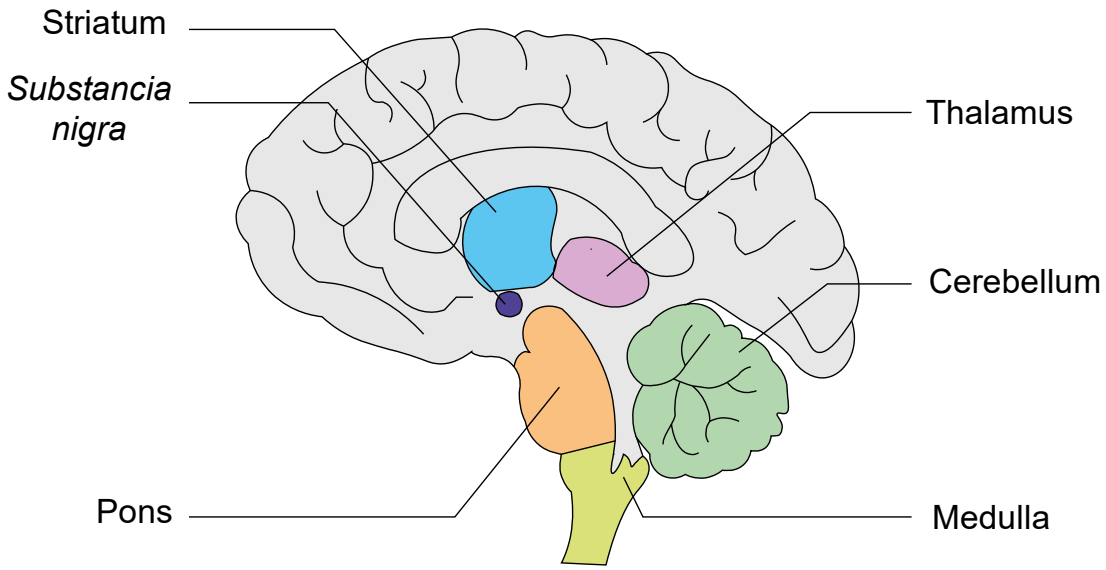

Figure 1.1 – Brain regions affected in MJD. Schematic representation of the main regions of neuronal loss and neuronal dysfunction in MJD are: cerebellum, brainstem (pons and medulla), *substantia nigra*, thalamus and striatum.

Interestingly, although wild-type ATXN3 (wtATXN3) is a cytoplasmatic protein expressed throughout the whole brain, upon expansion of the polyQ tract, it's location is aberrantly shifted to the nucleus where it is responsible for the formation of neuronal intranuclear inclusions (NII). These occur in specific neuronal populations such as the pontine neurons and, although in a smaller number, in the brainstem, thalamus, *substantia nigra* and in the striatum (Paulson *et al.*, 1997b; Schmidt *et al.*, 1998; Munoz *et al.*, 2002). Predominantly intranuclear, ubiquitinated inclusions have also been detected in the cytoplasm (Suenaga *et al.*, 1993; Yamada *et al.*, 2004).

Besides mutant ATXN3 (mutATXN3), these inclusions sequester other proteins and can also contain ubiquitin, wtATXN3, chaperones, proteasomal subunits and transcription factors, which might contribute to the pathogenesis of MJD (Paulson *et al.*, 1997b; Chai *et al.*, 1999a; Chai *et al.*, 1999b; Chai *et al.*, 2001; Takahashi *et al.*, 2001).

Despite being a recognized hallmark of the disease, the formation of NII has generated great controversy regarding their role in disease pathogenesis. Although NIIs are present in the affected brain regions in MJD patients and animal models, other reports have shown the development of neuronal dysfunction and associated motor abnormalities even without the formation of NIIs (Boy *et al.*, 2010; Silva-Fernandes *et al.*, 2010). Moreover, other studies have suggested that aggregates can function as a protective mechanism for containing the mutant protein (Evert *et al.*, 2006b). In fact, a morphometric study on pontine neurons of Machado-Joseph disease patients showed that neurons containing NIIs presented lower shrinkage and deformities, suggesting that NII are not necessarily toxic (Uchihara *et al.*, 2002). The question of whether mutATXN3 aggregates are harmful or protective still remains a disputed issue in the study of MJD.

1.1.1.4 Genetics of MJD

In 1993, eleven years after the description of the disease as an autonomous entity, the disease locus of MJD was mapped to the long arm of chromosome 14 (14q24.3-q32) (Takiyama *et al.*, 1993). However, only in the following year was the CAG expansion identified at the coding region of *MJD1* gene (now designated *ATXN3*), and confirmed to be present in individuals of MJD families (Kawaguchi *et al.*, 1994). In 2001, the genomic structure of the *ATXN3* gene was characterized (Fig. 1.2). The gene was found to span a region of 48,240bp in length and to be composed of 11 exons, with the CAG repeats location being identified to exon 10 (Ichikawa *et al.*, 2001). In the same study, multiple messenger RNA (mRNA) isoforms of ATXN3 were identified with approximate sizes of 1.4, 1.8, 4.5, and 7.5 kb. The authors demonstrated that exons 10 and 11 are used variably in the generation of ATXN3 transcripts due to alternative splicing mechanisms and alternative polyadenylation leading to the formation of different transcripts (Ichikawa *et al.*, 2001).

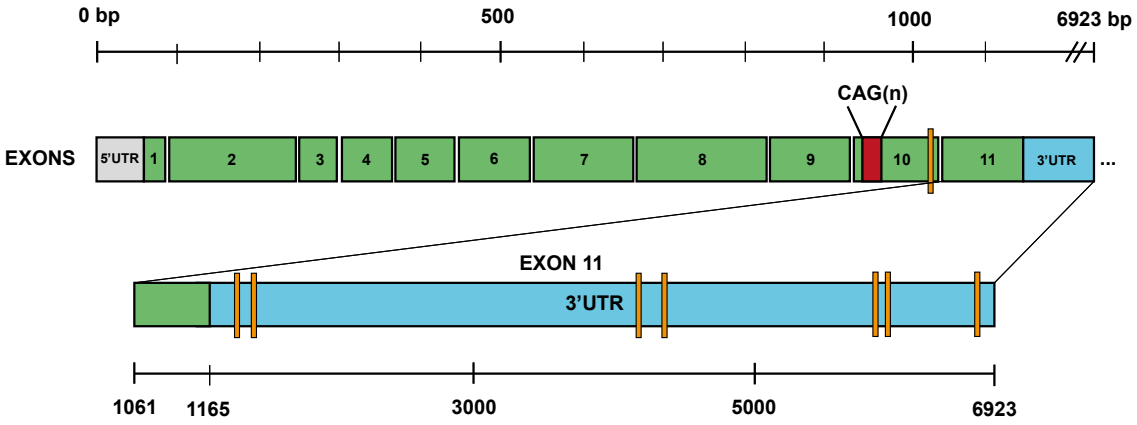

Figure 1.2 – Schematic representation of the reference exonic profile of the *ATXN3* gene. The *ATXN3 gene* is constituted by 11 exons that can undergo multiple types of alternative splicing. The expansion of the trinucleotide CAG is located in exon 10. Multiple alternative polyadenylation sites are also present, mainly in the 3' untranslated region (3'UTR) (depicted by orange bars), contributing for additional transcript diversity other than alternative splicing. The 3'UTR of ATXN3 is particularly long, having a much greater size than all of the other exons combined.

More recently, novel exons have been identified in the *ATXN3* gene. Bettencourt and colleagues reported the presence of two additional exons, 6a and 9a. Simultaneously, fifty new ATXN3 splicing variants were described, generated by four types of splicing events: exon skipping, new exons and usage of alternative 5' or 3' splice sites (Bettencourt *et al.*, 2010). This study focused only on the first 10 exons and did not account for eventual alternative splicing or polyadenylation in exon 11 which suggests the existence of a greater number of existing ATXN3 mRNA variants. Still the possible involvement of alternative splicing in the pathogenesis of MJD remained unclear. Recent work in two mouse models of MJD has identified an aberrant splicing isoform that is produced upon the presence of the expanded CAG tract, in which the intron immediately downstream of the CAG repeat is retained. This event might contribute to the pathogenesis of MJD either by leading to the production of a more toxic protein form or by changing the endogenous regulation of ATXN3 mRNA (Ramani *et al.*, 2015).

1.1.1.5 ATXN3 protein

The wtATXN3 protein has a molecular weight of approximately 42 kDa and is ubiquitously expressed throughout all types of tissues, either neuronal or non-neuronal (Paulson *et al.*, 1997a; Paulson *et al.*, 1997b; Wang *et al.*, 1997; Schmidt *et al.*, 1998).

Depending on the brain regions, ATXN3 is expressed at different levels (Trottier *et al.*, 1998). In the amino-terminal, the protein contains a highly conserved Josephin domain (JD) which consists of a catalytic triad of amino acids characteristic of cysteine proteases (Burnett *et al.*, 2003; Albrecht *et al.*, 2004; Nicastro *et al.*, 2005). In the carboxyl terminal, ATXN3 has two ubiquitin interacting motifs (UIM) followed by a nuclear localization signal (NLS) and the polyQ tract of variable length (Tait *et al.*, 1998; Burnett *et al.*, 2003; Masino *et al.*, 2003; Albrecht *et al.*, 2004; Berke *et al.*, 2005; Mao *et al.*, 2005). The presence of this NLS has been shown to promote nuclear importation of ATXN3 (Macedo-Ribeiro *et al.*, 2009). Interestingly the JD has been suggested to incorporate a nuclear export signal (NES) which actively promotes the transport of ATXN3 into the cytoplasm (Albrecht *et al.*, 2004; Macedo-Ribeiro *et al.*, 2009). These findings are consistent with the observation that although ATXN3 protein is mainly cytoplasmatic, it can be detected in both the nucleus and in the cytoplasm (Paulson *et al.*, 1997a; Trottier *et al.*, 1998).

Depending on the isoform produced by the already described alternative splicing events in ATXN3 mRNA, there can be the presence of a third UIM after the polyQ tract (Goto *et al.*, 1997). Previous evidence suggests that the isoform with three UIMs is the most abundant form in the human brain (Harris *et al.*, 2010) (Fig.1.3).

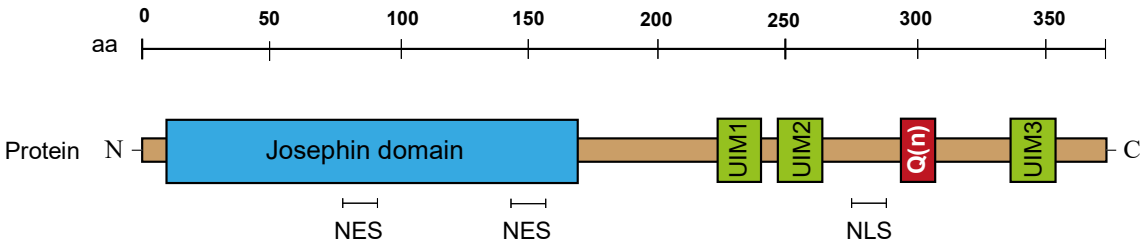

Figure 1.3 – Schematic representation of the ATXN3 protein structure. In the N-terminal, ATXN3 protein contains a Josephin domain which is essential for its enzymatic activity and two nuclear export signals (NES). In the C-terminal portion, depending on the isoform, ATXN3 can contain either 2 or 3 ubiquitin interacting motifs (UIM) and a nuclear localization signal (NLS). The polyQ tract is also located in the C-terminal portion of the protein.

Although the precise cellular role of ATXN3 is still unclear, the JD contains two binding sites for ubiquitin and has been predicted to cleave isopeptide bonds between ubiquitin monomers (Scheel *et al.*, 2003). This property has later been confirmed, validating ATXN3 has a deubiquitinating enzyme (Burnett *et al.*, 2003; Mao *et al.*, 2005; Nicastro *et al.*, 2005). This has linked ATXN3 to the ubiquitin-proteasomal system (UPS),

where ATXN3 is thought to contribute to the degradation of ubiquitinated proteins through the UPS by removing the poly-ubiquitin chains prior to digestion (Burnett *et al.*, 2003; Schmitt *et al.*, 2007; Winborn *et al.*, 2008; Todi *et al.*, 2009). By modulating the cellular ubiquitin-dependent mechanisms, ATXN3 might interfere with neuronal fate determination, axonal path finding and synaptic communication and plasticity (Todi and Paulson, 2011).

Besides the direct involvement in the UPS, ATXN3 physiological functions have also been related to other pathways which are involved with polyQ toxicity such has the oxidative stress response (Reina *et al.*, 2010; Araujo *et al.*, 2011; Rodrigues *et al.*, 2011), transcriptional regulation (Li *et al.*, 2002; Evert *et al.*, 2006a; Rodrigues *et al.*, 2007) and cytoskeletal organization and aggresome formation (Burnett and Pittman, 2005; Mazzucchelli *et al.*, 2009).

However, knock-out animal models for ATXN3 do not present any obvious abnormalities. In a C. elegans knock-out model, although no phenotype was observed, microarray analysis revealed a dysregulation of genes involved the ubiquitin-proteasome pathway, structure/motility, and signal transduction (Rodrigues *et al.*, 2007). Regarding the knock-out of ATXN3 in mice, no gross phenotype abnormality was observed, only displaying a reduction in their exploratory behavior. However, increased levels of ubiquitinated proteins were found in the tissues of ATXN3 knock-out mice, particularly in the brain (Schmitt *et al.*, 2007). These studies suggest that although ATXN3 performs important physiological functions, it is not essential for cell survival, maybe due to having a redundant function which is likely compensated by other proteins. Nevertheless, a study in *Drosophila melanogaster* showed that wtATXN3 was protective against polyQ neurotoxicity (Warrick *et al.*, 2005). However, this effect was not observed in MJD mouse models (Alves *et al.*, 2010; Hubener and Riess, 2010).

All in all, these studies support the idea that MJD is mainly caused by a toxic gain-of-function of mutATXN3 and only in a lesser extent by a loss-of-function of wtATXN3.

1.1.1.6 Models of disease

As in other human diseases, the development of cellular and animal models of MJD has been crucial for the elucidation of the mechanisms involved in MJD pathogenesis and for the employment of therapeutic strategies directed at blocking the progression of MJD.

1.1.1.6.1 *In vitro* models

Many cellular models have been developed by either transient or stable expression of full-length or truncated versions of ATXN3 coding sequence under control of different promoters. Although cellular models are in general easier to manipulate, these models do not completely recapitulate the pathological events of the disease. However, they do offer other advantages such as the ability to study isolated cells of one particular type and the study of possible pathogenic or protective pathways. Moreover, *in vitro* models are also very useful platforms for the screening of new drugs.

Regarding the use of non-neuronal cell lines, COS-7 and HEK293T cells have been used for the overexpression of full-length and truncated ATXN3. Increased apoptosis, formation of NII and sequestration of proteasomal subunits and chaperones have been described in these models (Ikeda *et al.*, 1996; Paulson *et al.*, 1997b; Perez *et al.*, 1998; Chai *et al.*, 1999a).

Neuronal cell lines such as the CSM14.1, PC-12, Neuro2A and SK-N-SH have also been used together with the overexpression of full-length and truncated mutATXN3. Besides confirming the observations in non-neuronal cell lines, these models allowed the identification of other pathogenic features such as mitochondrial dysfunction, ultrastructural and electrophysiological abnormalities, and activation of pro-inflammatory genes (Evert *et al.*, 1999; Chai *et al.*, 2001; Evert *et al.*, 2001; Yoshizawa *et al.*, 2001; Wen *et al.*, 2003; Tsai *et al.*, 2004; Jeub *et al.*, 2006; Chang *et al.*, 2009). Primary cells such as mouse and rat cerebellar, striatal and nigral cultures, and human MJD fibroblasts have also been used for *in vitro* studies (Chou *et al.*, 2006; Chen *et al.*, 2008; Chou *et al.*, 2011; Onofre *et al.*, 2016).

More recently, with the breakthrough development of human induced pluripotent stem cell (hIPSC) technology, a new opportunity for the development of improved *in vitro* models has arisen (Takahashi and Yamanaka, 2006). hIPSC technology offers the opportunity for physiological expression of mutant genes, under control of endogenous regulatory elements and in their native genetic background (Fig. 1.4). Moreover, this can be combined with specific differentiation protocols which allow for the investigation of molecular disease pathways in specific cellular populations (Avior *et al.*, 2016). This strategy has recently been employed in the context of MJD, where IPSC derived neurons obtained from human MJD patients were used to clarify the mechanism behind neuronal specific pattern of aggregate formation (Koch *et al.*, 2011).

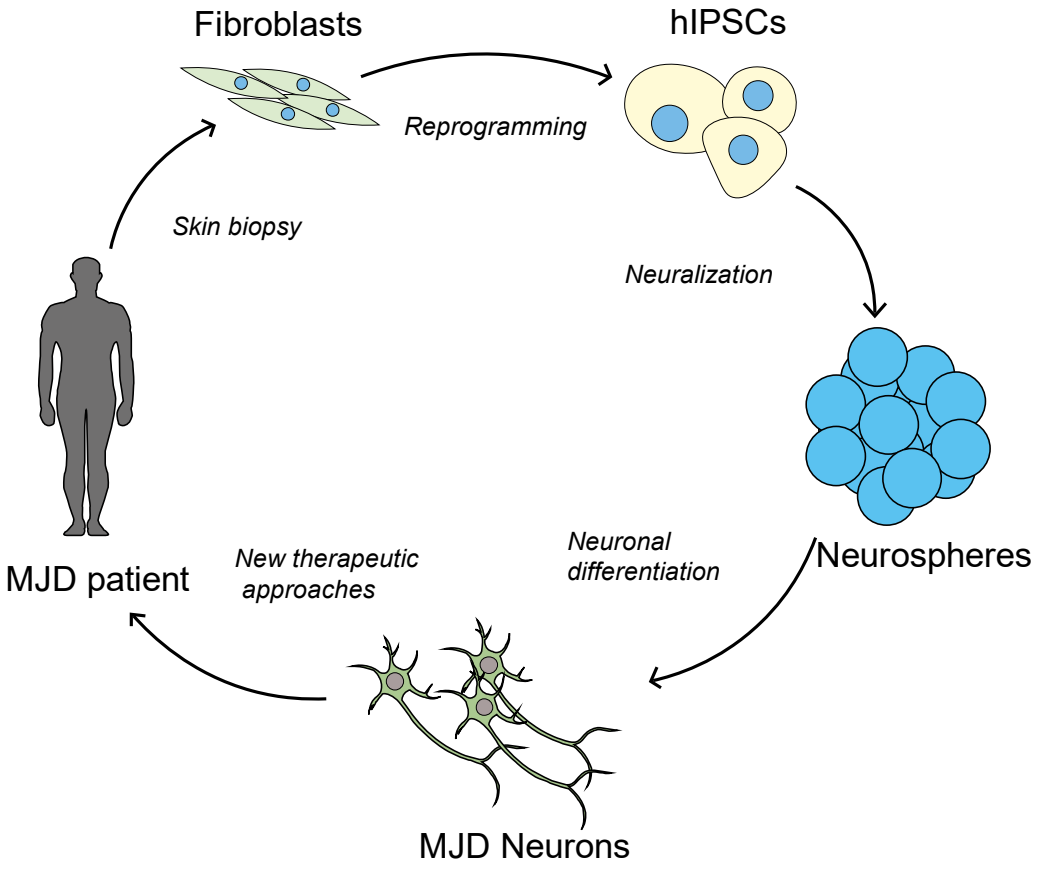

Figure 1.4 – Schematic representation of the generation and use of hIPSC modelling in MJD. Somatic cells from MJD patients can be isolated from a skin biopsy and then reprogrammed to a pluripotent state (hIPSCs). These cells can then be neuralized into neurospheres or neural progenitor cells which can be differentiated into mature neuronal cells. MJD neurons can then be used as a tool for the elucidation of pathogenic mechanisms or as a platform for drug screening, retaining their native genetic background.

1.1.1.6.2 *In vivo* models

Although rodents are the most commonly used animals to model MJD, other organisms have been used in MJD studies. In particular, multiple invertebrate models have been developed, either in *Drosophila melanogaster* or in *Caenorhabditis elegans*. In *drosophila*, the expression of either full length or truncated mutATXN3 resulted in the formation of intranuclear aggregates and neuronal loss, with associated locomotor dysfunction and premature death (Warrick *et al.*, 1998; Kim *et al.*, 2004; Warrick *et al.*, 2005). In the case of the worms, the overexpression of mutATXN3 also resulted in aggregation of the mutant protein, neuronal dysfunction and motor impairments (Khan *et al.*, 2006; Teixeira-Castro *et al.*, 2011).

Rodent models have been developed in greater number due to their closer genomic, anatomical and physiological profile when compared to humans (see Table 1.3). The first mouse model of MJD was developed in 1996 by Ikeda and colleagues. Two transgenic lines were developed either expressing full-length ATXN3 or a truncated form of ATXN3, both under control of the specific Purkinje cell specific L7 promoter. Interestingly, while mice expressing the full-length protein developed no phenotype, the transgenic line expressing the truncated form developed an ataxic and neurodegenerative phenotype at an early age (Ikeda *et al.*, 1996). In an effort to better replicate the human context, another mouse model was developed which included the whole human mutATXN3 gene together with its native regulatory elements. This model displayed a mild phenotype with wide gait, tremors, improper body positioning and reduced weight gain (Cemal *et al.*, 2002). Overall, this model correlated many features observed in MJD patients.

Since then, many other rodent models were developed taking advantage of the expression of different transcript variants of ATXN3 and using different promoters in order to drive expression in specific cell populations. Altogether, they have contributed with significant information to the understanding of MJD. Firstly, as in humans, the number of CAG repeats could be associated to the severity of the disease (Bichelmeier *et al.*, 2007; Silva-Fernandes *et al.*, 2010; Silva-Fernandes *et al.*, 2014). Secondly, truncated forms were found to be more toxic inducing a more severe phenotype with an earlier age of onset. Moreover, not only the C-terminal truncated forms were toxic, but also a N-terminal fragment of ATXN3 which was able to promote neurodegeneration, behavioral impairments and premature death (Hubener *et al.*, 2011). Moreover, taking advantage of a Tet-Off system, it was demonstrated that shutting-off the expression of the mutated protein was capable of reverting the motor symptoms after the onset of the disease (Boy *et al.*, 2009).

Regarding the presence of NIIs, their occurrence is consistent across many of the transgenic animals (Warrick *et al.*, 1998; Cemal *et al.*, 2002; Goti *et al.*, 2004; Warrick *et al.*, 2005; Bichelmeier *et al.*, 2007; Alves *et al.*, 2008b; Chou *et al.*, 2008; Torashima *et al.*, 2008; Boy *et al.*, 2009; Boy *et al.*, 2010). Nevertheless, there is no clear correlation between inclusion formation and neurodegeneration (Silva-Fernandes *et al.*, 2010). In fact, motor symptoms have been detected before the formation of NII (Boy *et al.*, 2010).

Table 1.3 – Rodent models of MJD

Species	Transgene	Promoter / Expression	Neuropathology	Motor phenotype	Reference
Mus musculus	Truncated and full-length human ATXN3 CDS with 79 CAGs	L7 promoter – expression in cerebellar Purkinje cells	Cerebellar atrophy	Ataxia Gait disturbances	(Ikeda *et al.*, 1996)
	Full-length human ATXN3 genomic locus with 76 / 84 CAGs	Endogenous human promoter in YAC system – Ubiquitous expression	Ubiquitinated NIIs in cerebellar neurons. Degeneration and mild gliosis of dentate and pontine nerve nuclei	Mild and progressive: abnormal gait, tremor, hypoactivity, limb clasping, reduced grip strength.	(Cemal *et al.*, 2002)
	Full-length ATXN3 CDS with 71 CAGs	Mouse prion promoter – Expression in several brain regions	NIIs in deep cerebellar and pontine nuclei and spinal cord. Abundant mutATXN3 fragments	Progressive postural instability, gait and limb ataxia, weight loss, premature death	(Goti *et al.*, 2004) (Colomer Gould *et al.*, 2007)
	Full length ATXN3 CDS with 70/ 148 CAGs with or without NLS and NES	Mouse prion promoter – Expression in several brain regions	Degeneration of Purkinje cells, reduced turnover of dopamine and serotonin.	Tremor, reduced activity, premature death.	(Bichelmeier *et al.*, 2007)
	Full length ATXN3 CDS with 79 CAGs	Mouse prion promoter - Expression in several brain regions	NIIs in dentate nucleus of the cerebellum, pontine nucleus and *substantia nigra*. Downregulated gene expression	Reduced motor coordination, ataxic gait and weight loss.	(Chou *et al.*, 2008)

	Truncated ATXN3 CDS with 69 CAGs	L7 promoter – expression in cerebellar Purkinje cells	Severe cerebellar atrophy with defects in Purkinje cells synaptic transmission	Severe ataxia	(Torashima *et al.*, 2008; Oue *et al.*, 2009)
	Full length ATXN3 CDS with 77 CAGs under control of a Tet-Off system	Hamster prion protein promoter - Expression in several brain regions	NIIs in cerebellar cortex. Neuronal dysfunction in the cerebellum	Reduced motor coordination, ataxic gait.	(Boy *et al.*, 2009)
	Full length ATXN3 CDS with 148 CAGs	Rat huntingtin promoter	NIIs in pons and cerebellum. Cell degeneration of Purkinje cells.	Hyperactivity, reduced motor coordination, impaired motor learning	(Boy *et al.*, 2010)
	Full-length ATXN3 cDNA with 94 CAGs	CMV promoter – Ubiquitous expression	Neurodegeneration in the absence of necrosis or apoptosis in thalamus, dentate and pontine nuclei.	Motor coordination impairments	(Silva-Fernandes *et al.*, 2010)
	Truncated N-terminal ATXN3 CDS	Endogenous mouse ATXN3 promoter – Expression in several brain regions	Neuronal cytoplasmic inclusions. Impaired endoplasmic reticulum-mediated unfolded response.	Premature death, tremor, clasping, gait ataxia, weight loss	(Hubener *et al.*, 2011)
	LV-mediated overexpression of full-length ATXN3 CDS with 72 CAGs in striatum	PGK promoter – expression at injection site	Abundant ubiquitinated NIIs. Loss of neuronal markers such as DARPP-32 and NeuN	-	(Simoes *et al.*, 2012)

	LV-mediated overexpression of full-length ATXN3 CDS with 72 CAGs in cerebellum	PGK promoter - expression at injection site	Ubiquitinated NIIs. Loss of neuronal markers. Shrinkage and degeneration of Purkinje cells.	Reduced motor coordination, ataxic gait, hyperactivity.	(Nobrega *et al.*, 2013a)
	Full-length ATXN3 with 135 CAGs	CMV promoter – ubiquitous expression	Neuronal loss in the pontine nuclei	Abnormal gait and body posture, limb clasping and limb tonus deficit.	(Silva-Fernandes *et al.*, 2014)
	Full-length humanized ATXN3 CDS with 91 CAGs and small portion of human 3'UTR region	Endogenous mouse ATXN3 promoter – Ubiquitous expression	Cerebellar degeneration. Astrogliosis in the cerebellar white matter and substantia nigra	Mild motor coordination impairment	(Switonski *et al.*, 2015)
	Full-length mouse ATXN3 gene with 82 CAGs	Endogenous mouse ATXN3 promoter – Ubiquitous expression	Abundant nuclear inclusions	Absence of behavioral deficits	(Ramani *et al.*, 2015)
Rattus norvegicus	LV-mediated overexpression of full-length ATXN3 CDS with 72 CAGs in striatum and substantia nigra	PGK promoter - expression at injection site	Abundant nuclear Inclusions. Loss of neuronal markers such as DARPP-32 and NeuN	Apomorphine- induced turning behavior when injected in *substantia nigra*	(Alves *et al.*, 2008b)

CDS (Coding sequence), YAC (Yeast artificial chromosome), NII (Neuronal intranuclear inclusions), NLS (Nuclear localization signal), NES (Nuclear export signal), CMV (Cytomegalovirus), LV (Lentiviral), PGK (Phosphoglycerate kinase), DARPP-32 (dopamine- and cAMP-regulated neuronal phosphoprotein 32) and NeuN (Neuronal nuclear antigen).

More recently two novel knock-in mouse models of MJD were developed. These models offer the advantage of combining the molecular and phenotypic features of MJD with the native genetic context of ATXN3 (Ramani *et al.*, 2015; Switonski *et al.*, 2015).

Altogether, although no animal model fully replicates the human disease, they represent valuable tools that have contributed to the understanding of MJD pathogenesis, and to the development of novel candidate therapeutic strategies.

1.1.1.6.2.1 Viral based MJD models

Viral vectors offer great potential for the disease modelling of multiple neurodegenerative disorders using lentiviral or adeno-associated viral vectors, having been employed not only in rodent models but also in non-human primates (Kirik and Bjorklund, 2003; Deglon and Hantraye, 2005). Although these models are not free of limitations, they do offer a set of advantages when compared to classical transgenic models such as: 1) allowing for specific control of the onset and time-course of the degeneration, 2) resulting in a rapid phenotype generation due to robust and sustained gene expression, 3) being easily employed between different species, 4) allowing for a selective evaluation of the role of specific disease regions and 5) controlling the severity of the phenotype through manipulation of the viral titers (Senut *et al.*, 2000).

Taking this into account, multiple MJD lentiviral-based animal models were developed. In the rat, striatal lentiviral overexpression of mutATXN3 resulted in the formation of ubiquitinated NII and neuronal dysfunction, while injections in the *substantia nigra* were able to induce a mild motor deficit (Alves *et al.*, 2008b). Other lentiviral models were later employed in mice replicating the results observed in the rat (Simoes *et al.*, 2012). Moreover, the injection of lentiviral particles encoding for mutATXN3 in the cerebellum of mice induced an ataxic phenotype and cerebellar neuropathology (Nobrega *et al.*, 2013a).

1.1.1.7 Pathogenesis of MJD

1.1.1.7.1 Protein toxicity

Although the genetic cause of MJD is well described, the molecular pathways leading to disease are still unclear. Several mechanistic hypotheses have emerged from numerous *in vitro* and *in vivo* studies.

Evidence has shown that proteolytic cleavage of the mutATXN3 by caspases or calpains might be the initial step in a series of processes which will lead to the formation of different toxic species (Wellington *et al.*, 1998; Berke *et al.*, 2004; Haacke *et al.*, 2007; Simoes *et al.*, 2012; Simoes *et al.*, 2014). These smaller fragments may facilitate translocation to the nucleous and undergo conformational changes required for the formation of aggregates. Nevertheless, polyglutamine monomers of full-length ATXN3 have been shown to acquire β-strand conformations and assemble into oligomers and to cause cytotoxicity in cell cultures (Bevivino and Loll, 2001; Nagai *et al.*, 2007; Takahashi *et al.*, 2008). The deposition of either full-length or cleaved mutATXN3 in NIIs can result in the impairment of axonal trafficking, nuclear function, recruitment and impairment of transcription factors and proteasome subunits (Chai *et al.*, 1999a; Chai *et al.*, 1999b; Gunawardena *et al.*, 2003). Nevertheless, the exact contribution of each distinct species is still a matter of debate (Fig.1.5).

One of the main effects of these toxic protein species is transcriptional dysregulation. Taking into account that mutATXN3 tends to accumulate in the nucleus, this favors its interaction with transcription factors and cofactors. In fact, nuclear inclusions in MJD were found to contain the transcription factor TBP and co-factor CBP (CREB-binding protein) (McCampbell *et al.*, 2000). The action of ATXN3 as a transcriptional corepressor or activator also appears to be compromised (Evert *et al.*, 2006a; Araujo *et al.*, 2011). Current studies have detected transcriptional alterations caused by mutATXN3 *in vitro* and *in vivo,* comprising genes involved with inflammation, glutamatergic signaling and signal transduction (Evert *et al.*, 2001; Evert *et al.*, 2003; Chou *et al.*, 2008; Mendonca *et al.*, 2015). More recently, a set of blood-based transcriptional biomarkers has also been identified (Raposo *et al.*, 2015).

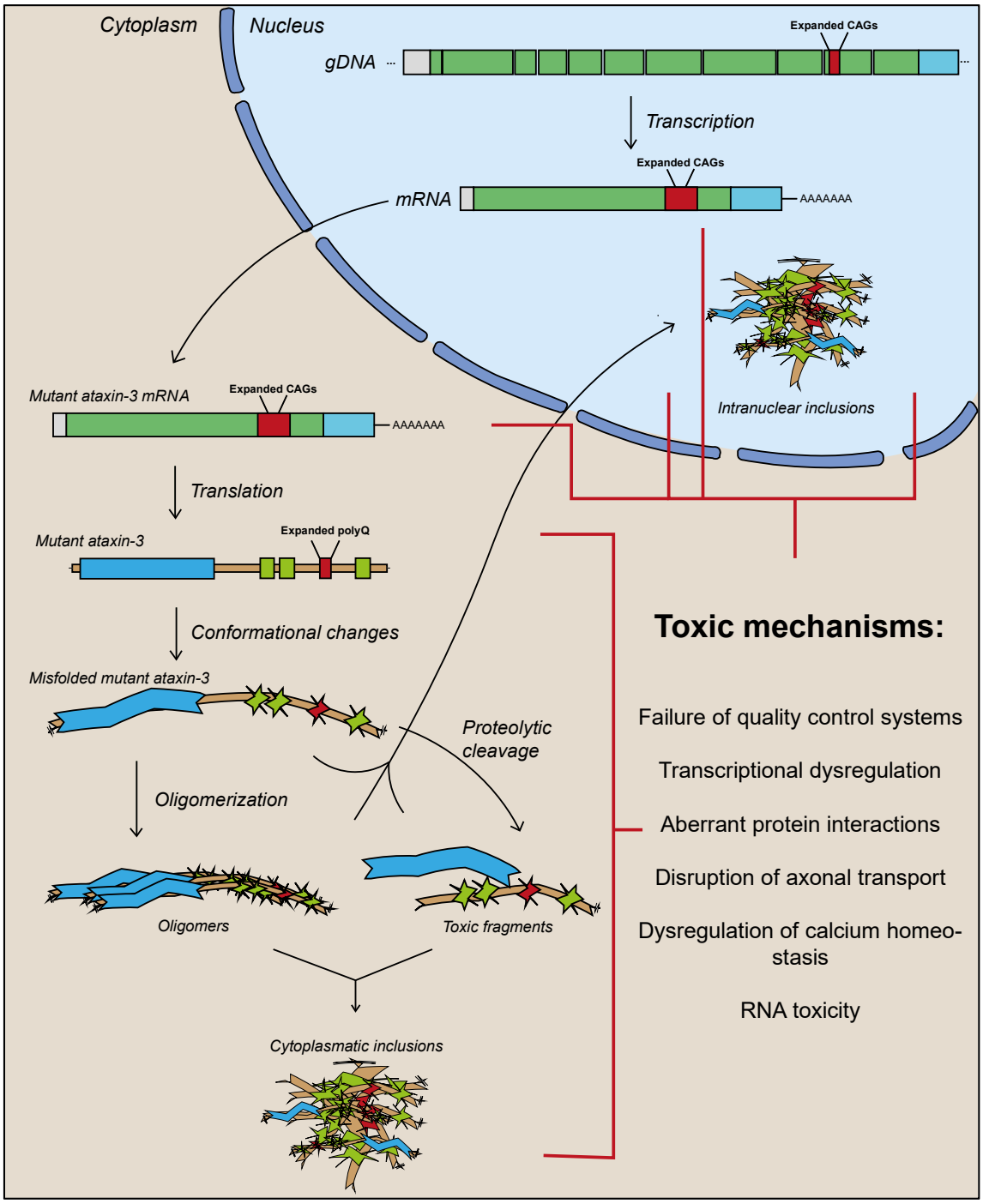

Figure 1.5 – Schematic representation of molecular mechanisms responsible for MJD pathogenesis. Starting from the transcription of the gene encoding for mutATXN3, multiple species are generated that contribute to toxic pathways. Upon expansion of the polyQ tract, mutATXN3 can undergo conformational changes, promote the formation of oligomers and ultimately lead to the formation of protein inclusions. Moreover, mutATXN3 can also be the target of proteolytic enzymes leading to the formation of smaller toxic fragments which not only can also oligomerize and lead to the formation of inclusions, but may also be more efficiently transported into the nucleus where they can also promote aggregation. In addition to protein toxicity, multiple evidence has now also attributed a toxic role to the mutATXN3 mRNA. Altogether, all these protein and RNA species can lead to the failure of quality control systems, transcriptional dysregulation, aberrant protein interactions, disruption of axonal transport, dysregulation of calcium homeostasis among others, which will culminate in neuronal dysfunction and death.

Among the multiple pathogenic mechanisms involved in MJD, the impairment of protein quality control systems such as the UPS and autophagy have generated great attention. In the case of the UPS, the fact that the normal function of ATXN3 has been linked to this protein surveillance pathway, suggests that a loss of function of mutATXN3 could lead to an impairment in the UPS system contributing for neurodegeneration (Burnett *et al.*, 2003). In fact, evidence suggests an impairment in proteostasis systems in later stages of disease, while at an earlier stage there is an activation of stress pathways with associated increase in molecular chaperones (Chai *et al.*, 1999b; Huen and Chan, 2005; Chou *et al.*, 2008). Moreover, the presence of ubiquitin and proteasome components in NIIs suggests that the UPS may be disrupted in MJD (Paulson *et al.*, 1997b; Chai *et al.*, 1999b).

Macroautophagy is a cellular pathway responsible for the degradation of insoluble aggregation-prone proteins which has been shown to be essential for neuronal survival (Hara *et al.*, 2006; Komatsu *et al.*, 2006). Blockage of autophagy has been shown to induce abnormal accumulation of intracellular proteins and extensive neuronal loss in mice (Hara *et al.*, 2006; Komatsu *et al.*, 2006). In the case of MJD, multiple studies have now demonstrated that autophagy is impaired in MJD (Nascimento-Ferreira *et al.*, 2011; Nascimento-Ferreira *et al.*, 2013; Cunha-Santos *et al.*, 2016; Onofre *et al.*, 2016). Autophagy components such as LC3, p62 and ATG16L are recruited to the mutATXN3 inclusions and an accumulation of autophagosomes has been detected in human brain tissue from MJD patients and in MJD animal models (Nascimento-Ferreira *et al.*, 2011). Moreover, MJD fibroblasts present an autophagy impairment with an underlying mechanism of decreased autophagosome production (Onofre *et al.*, 2016). Simultaneously, the SIRT1 pathway, which is highly associated with the autophagy process, has been found to be highly compromised in MJD (Cunha-Santos *et al.*, 2016).

Nevertheless, the mechanisms involved in the pathogenesis of MJD are diverse and still unclear. Other important toxic pathways are also very important to MJD pathogenesis such as mitochondrial dysfunction, aberrant protein-protein interactions, calcium homeostasis dysregulation, axonal transport disruption and repeat-associated non-ATG-initiated translation (extensively reviewed in: (Costa Mdo and Paulson, 2012), (Matos *et al.*, 2011), (Evers *et al.*, 2014) and (Paulson, 2012).

1.1.1.7.1 RNA toxicity

Although the main research focus has been the study of the mutATXN3 protein and its causative role in MJD pathogenesis, a more recent perspective has taken a look at the role of the ATXN3 mutated mRNA. An increasing number of studies have suggested that along with protein toxicity, there is also RNA toxicity involved in polyQ disease pathogenesis and in particular in MJD.

In *Drosophila*, the expression of an untranslated expanded CAG repeat led to progressive neuronal dysfunction. However, the expression of CAG repeats interspersed by CAA codons dramatically reduced the toxic phenotype (Li *et al.*, 2008). Moreover, a study in *C. elegans* expressing untranslated CAG repeats also supported a toxic role for RNA CAG repeats in a length-dependent manner (Evers *et al.*, 2014). In addition, repeat expanded mRNA accumulates in intranuclear foci formations which were found to co-localize with the muscleblind-like 1 splicing factor (MBNL1), suggesting a misregulation of alternative splicing as a pathogenic mechanism in MJD (Li *et al.*, 2008; Mykowska *et al.*, 2011; Evers *et al.*, 2014).

More recently, short RNAs of about 21 nucleotides containing CAG repeats were found to be cytotoxic. These short RNAs originated from CAG repeat mRNA and were found to be produced through a dicer-mediated mechanism. Upon formation, these short RNAs are capable of inducing RNA gene silencing through the RNA interference pathway leading to a decrease in the levels of CUG containing transcripts (Banez-Coronel *et al.*, 2012).

1.1.1.8 Promising therapeutic strategies for Machado-Joseph disease

As mentioned before, there are currently no available therapies capable of delaying or blocking the progression of MJD. Nevertheless, the identification of multiple pathogenic pathways in MJD has granted an opportunity for the development of different rational therapeutic approaches. In general, these strategies have focused on: 1) reducing the levels of mutATXN3 mRNA and protein, 2) preventing mutATXN3 cleavage, oligomerization and aggregation, 3) promoting clearance of mutATXN3, 4) modulating the downstream toxic pathways responsible for neurodegeneration such as oxidative stress, calcium homeostasis and transcriptional dysregulation, 5) promoting

neuroprotection and 6) promoting tissue regeneration with cell-therapy (Matos *et al.*, 2011; Costa Mdo and Paulson, 2012) (Fig. 1.6).

Taking into account the scope of this thesis, RNA interference mechanisms and applications will be discussed in greater detail in section 1.3.

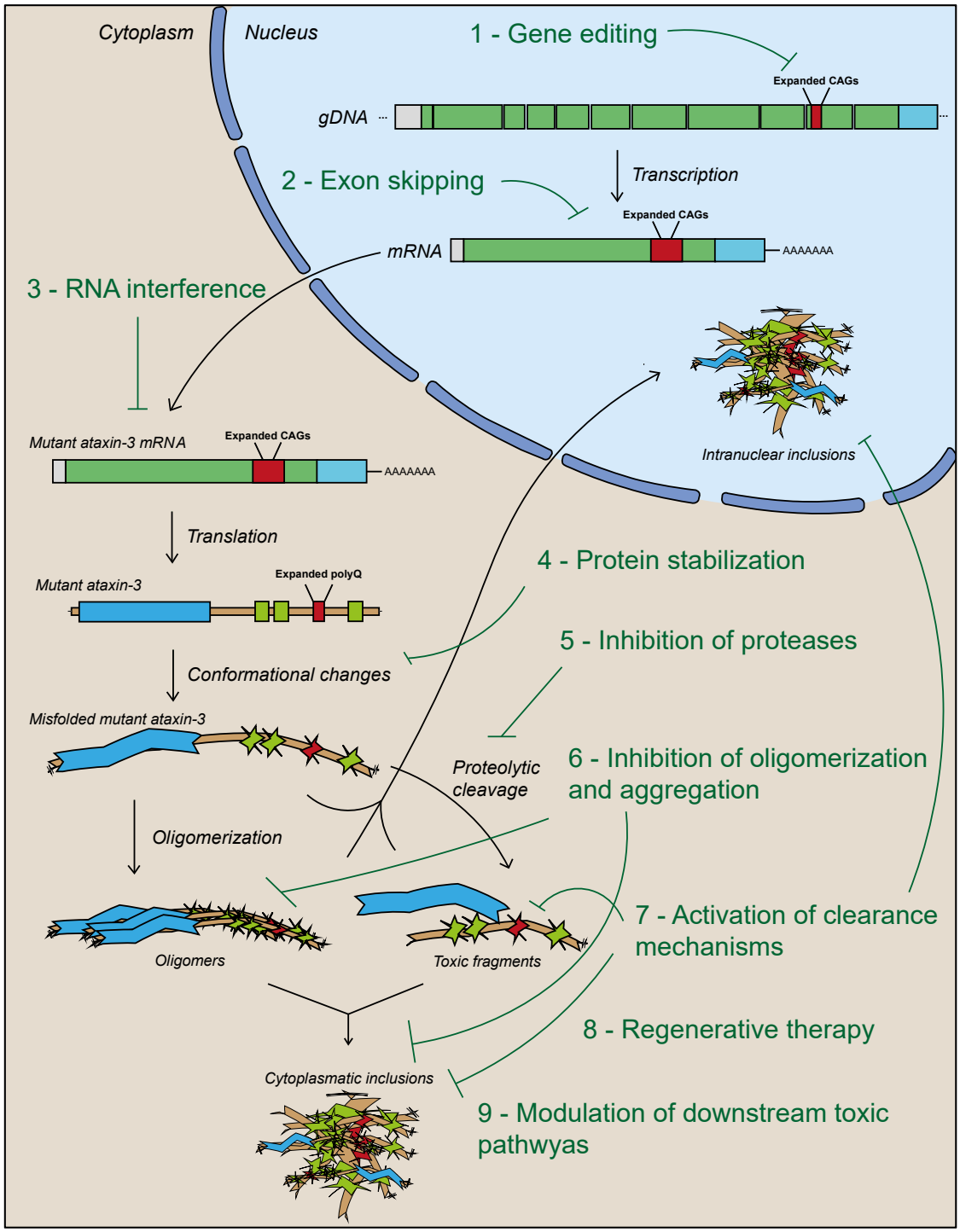

Figure 1.6 – Schematic representation of the potential therapeutic strategies for the treatment of MJD. The most straightforward therapeutic approach is the prevention of the production of the mutant protein. This can be achieved through different approaches such as: gene editing, exon skipping or RNAi. Other approaches can act at the protein level preventing processes such as misfolding (conformation stabilizers), oligomerization (oligomerization

inhibitors), cleavage (protease inhibitors) and aggregation (aggregation inhibitors). Alternatively, cellular clearance mechanisms such as the autophagy or the UPS can be activated. Neuroprotection and cell replacement strategies can also be used to alleviate MJD.

1.1.1.9 Clinical trials in MJD

Clinical trials in MJD have been mainly focused on symptomatic treatments. However, with the continuous progression in the knowledge of MJD pathogenic mechanism together with increased pre-clinical data, some clinical trials based on disease-modifying approaches such as autophagy activation have now been performed which should pave the way for the evaluation of other therapeutic options (Table 1.4).

Table 1.4 – Clinical trials in MJD

Drug / treatment	Proposed mechanism of action	Outcomes	Reference
Sulfamethoxazole-trimethoprim	Increase in the levels of brain biopterin	Mild improvements of hyperreflexia of knee jerks and of rigospasticity of the legs. beneficial effect on gait and coordination	(Correia *et al.*, 1995; Sakai *et al.*, 1995)
Sulfamethoxazole-trimethoprim	-	No improvements	(Schulte *et al.*, 2001)
Fluoxetine	Inhibition of serotonin reuptake	No improvements	(Monte *et al.*, 2003)
Taltirelin hydrate	Increase in TSH secretion	Speech improvements	(Shirasaki *et al.*, 2003)
Tandospirone citrate	Agonist of 5-HT1A receptor	Improvements in ataxia and depression. Alleviation of insomnia and leg pain.	(Takei *et al.*, 2004)
Lamotrigine	Decrease in the levels of mutATXN3	Gait improvements	(Liu *et al.*, 2005)
Varenicline	Agonist at α4β2 neuronal nicotinic acetylcholine receptors	Improved axial symptoms and rapid alternating movements	(Zesiewicz *et al.*, 2012)
Lithium carbonate	Increase the expression of molecular chaperones and promotion of autophagy	Minor improvements in limb coordination and speech	(Saute *et al.*, 2014)
Valproic acid	Increase of histone acetylation levels and modulation of gene expression	Improvements in locomotor function	(Lei *et al.*, 2016)

TSH (thyroid-stimulating hormone), 5-HT1A (5-hydroxytryptamine receptor 1A)

Although many drugs that have shown efficacy in mouse models are now moving toward clinical trials, the use of gene therapy and RNAi strategies for the treatment of MJD are still undergoing further preclinical studies in order to improve their efficacy and safety, before they can be introduced in clinical trials for MJD.

1.2 Post-transcriptional regulation of gene expression

In eukaryotic cells, the production and maturation of mRNA is a very regulated process. After transcription, the precursor mRNA transcript (pre-mRNA), undergoes multiple processing events before it is recognized as a template for protein synthesis. These mechanisms include formation of 5'cap structure, intron splicing, RNA editing, endonucleolytic cleavage and polyadenylation (Licatalosi and Darnell, 2010). In particular, non-coding regions such as the untranslated regions (UTRs) were found to cause a strong impact in the regulation of gene expression. UTRs have been reported to regulate mRNA stability, export to cytoplasm, localization and translation, altogether strongly affecting the total amount of translated protein (Matoulkova *et al.*, 2012).

1.2.1 3'UTR role in mRNA structure and function

The 3'UTR in particular has generated great research interest as accumulating evidence has implicated the 3'UTR of mRNA in the regulation of gene expression. Taking into account that, unlike the CDS and the 5'UTR sequence, the 3'UTR does not need to accommodate the translational machinery, this region is therefore available for the regulatory action of trans-acting factors such as RNA binding proteins (RBPs) or microRNAs (miRNAs) (Grimson *et al.*, 2007; Gu *et al.*, 2009).

The formation of the 3'UTR region is dependent on the polyadenylation process, a step in which the primary mRNA transcript is endonucleolytically cleaved at the 3' end. Cleavage is usually performed upon detection of a polyadenylation signal which is located about 10 to 30 nucleotides upstream of the cleavage site (Proudfoot and Brownlee, 1976). Most frequently, the polyadenylation signal is the hexamer "AAUAAA) (Graber *et al.*, 1999). The poly(A) tail comprising from 50 to about 250 adenines is then attached to the transcript by the action of poly(A) polymerase (Brawerman, 1981; Wahle, 1991; Bienroth *et al.*, 1993). Poly(A) binding protein (PABP) recognizes the poly(A) tail

and mediates the transport of the mRNA molecule to the cytoplasm while ensuring protection form degrading exonucleases (Eliseeva *et al.*, 2013).

Alternative polyadenylation is a process which occurs in more than half of human genes (Tian *et al.*, 2005; Derti *et al.*, 2012). This event leads to the production of different mRNA transcripts containing distinct 3' ends (Erson-Bensan, 2016). Depending on the location of the alternative poly(A) sites, the resulting alternative transcripts might have 3'UTR sequences of variable length or result in the translation of different protein isoforms (Edwalds-Gilbert *et al.*, 1997). Earlier studies have shown that the length of the 3'UTR is inversely correlated with the stability of the mRNA (Tian *et al.*, 2005). This was thought to be due to the increased presence of binding sites for factors responsible for translational inhibition such as miRNAs (Matoulkova *et al.*, 2012). However, in more recent evidence this correlation could not be validated (Spies *et al.*, 2013; Gruber *et al.*, 2014). Nevertheless, miRNA binding sites were still identified as the motifs with higher impact in mRNA stability and translation (Spies *et al.*, 2013). Interestingly, the selection of the preferred sites for polyadenylation appears to be variable between different tissues and cell types and even during cell cycle or developmental stages (Edwalds-Gilbert *et al.*, 1997).

The post-transcriptional regulation of gene expression at the 3'UTR level is the combined result of the interplay between cis-acting regulatory elements existing in the 3'UTR regions, which are then recognized by other binding factors known as trans-acting elements (Fig. 1.7). Among cis-acting sequences there are: 1) AU-rich elements, 2) GU-rich elements, 3) CU-rich elements, 4) CA-rich elements, 5) iron responsive elements and 6) selenocysteine insertion sequence elements (Matoulkova *et al.*, 2012). These sequences serve as molecular landmarks for both the activation or repression of gene expression. Among the trans-acting interacting partners there are: 1) RBPs and 2) miRNAs. RBPs are a very large class of proteins as estimates show that 7.5% of all protein coding genes are involved in binding or processing RNA (Gerstberger *et al.*, 2014). They have diverse structures and functions, controlling RNA stability, localization and translation (Gerstberger *et al.*, 2014). Regarding miRNAs, multiple aspects about their discovery, biogenesis and function will be described in the next following sections.

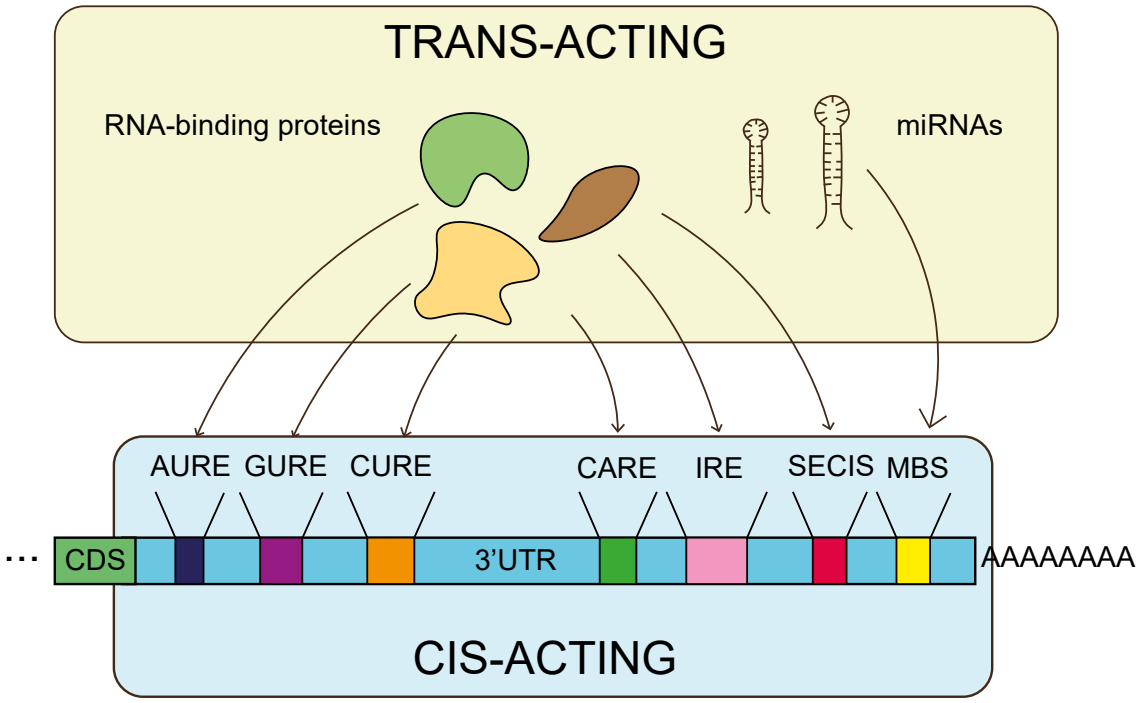

Figure 1.7 – Schematic illustration of the 3'UTR with its regulatory elements. The 3'UTR can contain sequences functioning as cis-acting elements such as: AU-rich elements (AURE), GU-rich elements (GURE), CU-rich elements (CURE), CA-rich elements (CARE), iron responsive elements (IRE), selenocysteine insertion sequence elements (SECIS) and miRNA binding sites (MBS) which will then interact with their trans-acting regulators such as multiple RBPs and miRNAs. Unlike miRNAs which only mediate a negative regulation of their target genes, RBPs can either promote the stabilization or the degradation of their target mRNAs.

1.2.2 MiRNAs

MiRNAs are a very large class of regulatory non-coding RNAs with approximately 22 nucleotides in size. They are endogenously expressed from miRNA-encoding genes and have been found to play important roles in many physiological and pathological processes in eukaryotes (Flynt and Lai, 2008).

1.2.2.1 Discovery of miRNAs and RNA-mediated gene silencing mechanisms

In 1993, the first member of the miRNA family, lin-4, was identified in *C. elegans* using a genetic screen for defects in the temporal control of post-embryonic development (Lee *et al.*, 1993). The authors observed that this gene encoded for a small non-coding RNA with antisense complementarity to another gene's 3'UTR, lin-14 (Lee *et al.*, 1993).

This was an early step towards the discovery of the RNAi mechanism and the identification a new regulatory layer of post-transcriptional gene control.

Five years later, the experiments of Fire and Mello, demonstrated the existence of RNA interference control of gene expression after observing a decrease in mRNA transcripts upon delivery of small non-coding RNAs to *C. elegans* (Fire *et al.*, 1998). Their discovery would award them the Nobel Prize in Physiology of Medicine in 2006.

Only in 2000, almost 7 years later after the discovery of lin-4, was the second miRNA (let-7) discovered, again in *C. elegans*. The let-7 miRNA was found to inhibit translation of lin-41 and hbl-1 mRNAs by binding to their 3'UTR (Reinhart *et al.*, 2000; Abrahante *et al.*, 2003; Lin *et al.*, 2003). Importantly, the let-7 miRNA was identified to be conserved in vertebrate, ascidian, hemichordate, mollusk, annelid, and arthropod organisms (Pasquinelli *et al.*, 2000). In humans, let-7 is expressed in the vast majority of tissues including the brain (Pasquinelli *et al.*, 2000). This was the starting point for the creation and establishment of miRNAs as a new class of molecules with diverse regulatory functions affecting almost every biological pathway (Filipowicz *et al.*, 2008). Currently, thousands of miRNAs have been identified in humans and other organisms. The current version of MiRbase (Release 21: June 2014), an online sequence repository, currently lists a total of 28,645 miRNA entries. Regarding the human sequences, 1881 precursors and 2588 mature sequences have been currently deposited (Kozomara and Griffiths-Jones, 2014). Accordingly, the number of research publications related with miRNAs has increased dramatically since 2000 (Fig. 1.8).

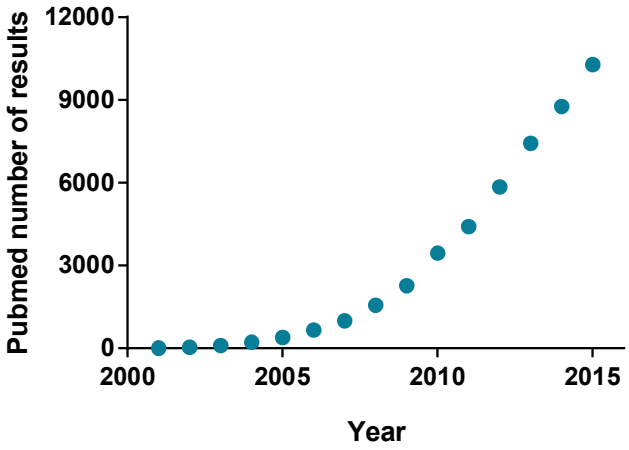

Figure 1.8 – Evolution of miRNA research. Ever since their discovery, miRNAs have generated great research interest. Since 2000, with the expansion of the miRNA class, the number of studies involving miRNA research has been continuously increasing, as demonstrated by the number of studies about miRNAs listed on PubMed.

1.2.2.2 MiRNA annotation

Due to the dramatic increase in the number of discovered miRNAs, a system was developed to ensure proper miRNA annotation. With the exception of a very limited number of miRNAs, most of them are designated with the abbreviation “mir”, followed by an identification number, attributed in accordance to their discovery date. A prefix indicates the species of the miRNA (for example: hsa is used for *Homo sapiens* and mmu is used for *Mus musculus*). Very similar miRNAs that only differ in some nucleotides are distinguished by the addition of a letter in front of the number (for example: hsa-mir-181a and hsa-mir-181b). Upon maturation, each miRNA hairpin can give rise to two mature miRNAs being differentiated by a 5p or 3p designation according to the position of each chain in the pre-miRNA hairpin. In addition, multiple miRNAs located in a single genomic cluster may be named together by indicating the first and last miRNA in the cluster (for example: mir-17-92) (Ambros *et al.*, 2003; Kozomara and Griffiths-Jones, 2014).

Pri and pre-miRNA molecules can also have an extra number as a suffix. This is done in order to differentiate the genomic origin of each hairpin (for example (mir-9-1 and mir-9-2), in the cases of miRNAs that are encoded by multiple genomic locus (Ambros *et al.*, 2003; Kozomara and Griffiths-Jones, 2014).

1.2.2.3 MiRNA biogenesis

In the main canonical pathway for the generation of mature miRNAs, their expression starts with the formation of primary miRNA (pri-miRNA) transcripts typically from RNA Polymerase II (Pol II) transcription. These pri-miRNA encoding sequences may exist either within non-coding RNAs or in the introns of mRNA. Importantly, a single transcript might contain multiple pri-miRNAs (Lagos-Quintana *et al.*, 2001; Cai *et al.*, 2004) (Fig. 1.9).

Pri-miRNAs will then be the target of a series of enzymatic processing events before they lead to the formation of mature miRNA sequences. These events start with the cleavage of the pri-miRNA by the enzyme Drosha with the help of its partner DGCR8. This cleavage at the base of the pri-miRNA will lead to the formation of the precursor miRNA (pre-miRNA), a hairpin sequence with about 55-70 nt in length (Lee *et al.*, 2003; Han *et al.*, 2006).

The pre-miRNA hairpins are then recognized by Exportin-5 promoting the nuclear export to the cytoplasm (Yi *et al.*, 2003; Lund *et al.*, 2004). In the cytoplasm, Dicer RNase III enzyme cleaves the pre-miRNA leading to the formation of the mature miRNA, a small RNA duplex with approximately 22 nt in size (Grishok *et al.*, 2001; Hutvagner *et al.*, 2001). Both of these strands might then be individually incorporated into a miRNA associated induced silencing complex (miRISC) (Perron and Provost, 2008).

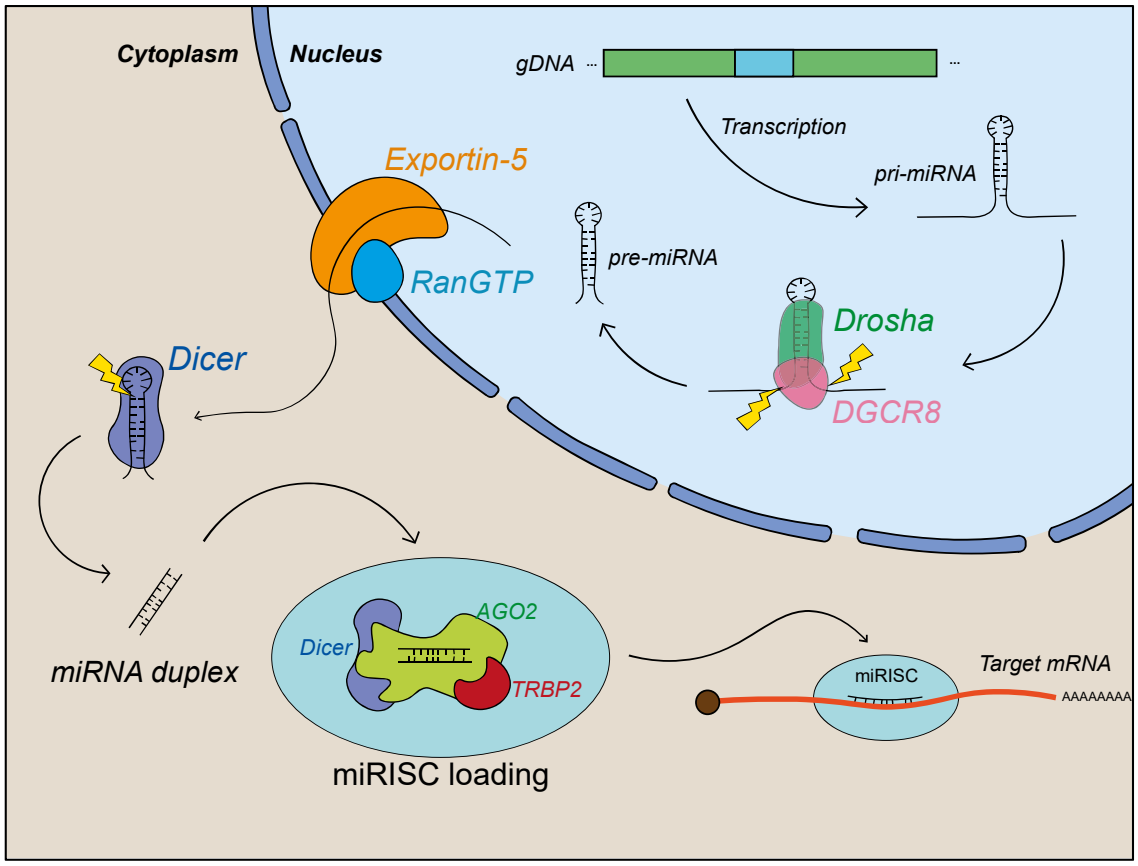

Figure 1.9 – Schematic representation of the miRNA biogenesis pathway. MiRNA expression starts from the transcription of miRNA encoding genes by RNA polymerase II leading to the formation of the primary miRNA (pri-miRNA). The pri-miRNA is then enzymatically processed by the complex Drosha-DGCR8 which will cleave the base of the hairpin resulting in the formation of the pre-miRNA and then exported into the cytoplasm by the complex Exportin-5 and RanGTP. In the cytoplasm, the mature miRNA duplex is generated after cleavage of the pre-miRNA by the enzyme Dicer. The mature miRNA is then loaded in the miRNA induced silencing complex (miRISC), a dynamic process mediated by Dicer and TRBP and in which one of the miRNA strands is associated with Ago2. The miRNA strand will then guide the complex to its target mRNAs which will also incorporate other proteins other than Ago2 in order to mediate translational repression.

Besides the canonical pathway, there are other less common pathways for the biogenesis of miRNAs. In particular, multiple pathways of Drosha-independent miRNA biogenesis were identified such as: the mirtron pathway, snoRNA-derived miRNAs, tRNA-derived miRNAs and endo-shRNAs (Yang and Lai, 2011). Even more, at least one miRNA (mir-451) has been shown to be generated in a Dicer independent pathway (Cheloufi *et al.*, 2010). This information is supported by the different phenotypes observed in knockout models of either Drosha or Dicer enzymes (Yang and Lai, 2011). Altogether, a combinatorial Dicer and Drosha knockout or knockdown might be more relevant in studies of miRNA loss-of-function.

1.2.2.4 miRISC: assembly and function

After enzymatic processing, the miRNA pathway shares many similarities with the RNAi mechanism (Bartel, 2004). The guide strand of the mature miRNAs is incorporated into the miRISC complex through a dynamic process involving Dicer, TRBP and the argonaute-2 protein (Ago2). Other components are also recruited to the miRISC such as argonaute-bound GW182 family proteins (Schwarz *et al.*, 2003; Eulalio *et al.*, 2008). In its core, it is the miRNA sequence which guides the ribonuclear complex to its target mRNAs based on perfect or imperfect complementarity, where it will mediate the silencing activity on target mRNAs (Fabian and Sonenberg, 2012). Besides Ago and GW182 proteins, the miRISC complex can also contain other proteins responsible for mRNA translation inhibition, such as the fragile X mental retardation protein (FMRP) a known modulator of translation in neurons which is thought to be responsible for a strand exchange mechanism in which the passenger strand of the miRNA is swapped for the mRNA target sequence (Jin *et al.*, 2004; Sontheimer, 2005).

In the majority of cases, miRNAs have a preferential interaction within the 3'UTRs of their target mRNAs. The complementarity between the 2nd and 8th nucleotides of the 5' end of the miRNA (known as *seed region*) with the sequence of the mRNA (known as *seed site*) is vital for target recognition. However, it has been shown that only six consecutive matches are required to achieve proper targeting and post-translational repression (Stefani and Slack, 2012). Moreover, the presence of bulged sites is frequent (Chi *et al.*, 2012).

In fact, depending on the degree of complementarity between the miRNA sequence and the target mRNA, the mechanisms by which gene silencing will occur can

be different. When there is a perfect complementarity between the miRNA seed region and the mRNA seed site, this will trigger mRNA degradation via Ago2. This enzyme with endonuclease activity will promote the cleavage of the mRNA while the miRNA remains intact (Hutvagner and Zamore, 2002; Liu *et al.*, 2004). The cleaved mRNA will then be degraded via 5'-exonucleases and 3'-exonucleases (Liu *et al.*, 2008).

The mRNA cleavage mechanism has been described mostly in plants, however, in what concerns animal miRNAs, they usually regulate gene expression through imperfect base pairing with their target mRNA (Millar and Waterhouse, 2005). This leads to the occurrence of different silencing mechanisms such as inhibition of translation and mRNA destabilization (Fig. 1.10). Although these mechanisms are still not completely understood, they can essentially be divided in two types. The first type of miRNA mediated silencing is through a direct effect on translation. This can be mediated by: 1) preventing ribosome association with the target mRNA, 2) promoting premature ribosome drop off, 3) slowing or stopping elongation and 4) cotranslational degradation of nascent polypeptides. The second type is based on indirect effects on translation, including: 1) promotion of de-adenylation, which induces mRNA degradation and 2) sequestration into P-bodies where it can be stored or degraded (Nilsen, 2007; Wu and Belasco, 2008).

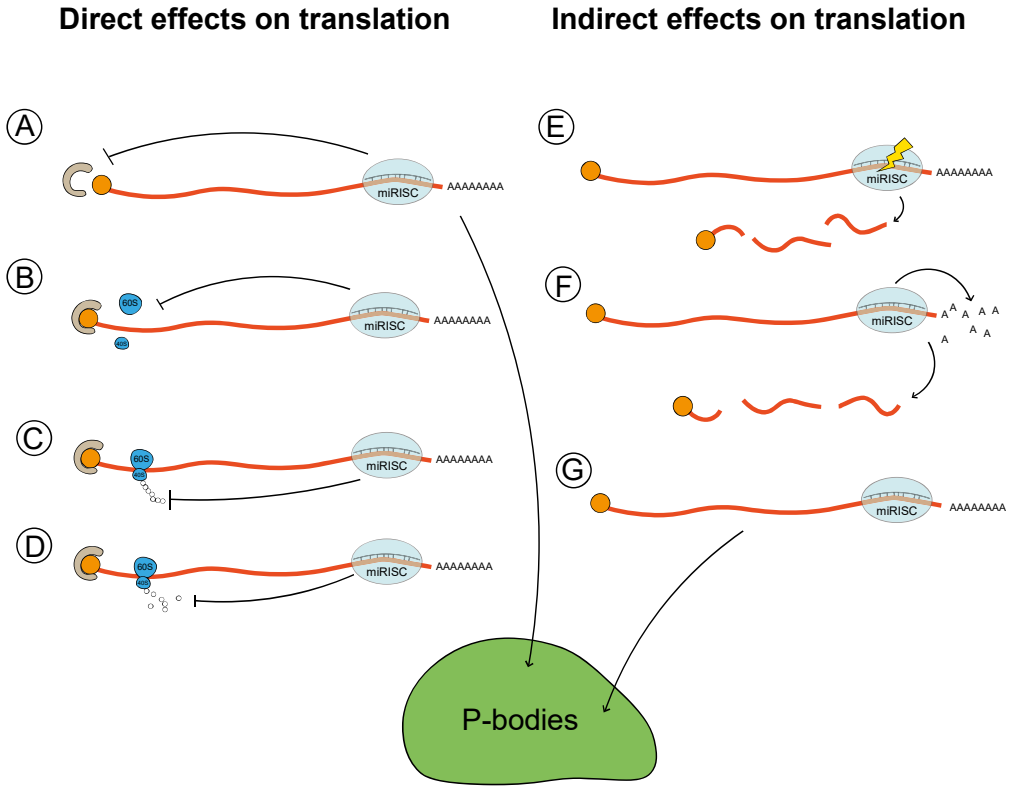

Figure 1.10 – Schematic representation of the miRNA silencing mechanisms in animals. The interaction of the miRISC complex with its target mRNAs can result in different effects, either

directly affecting the translation process, or through indirect effects. Direct inhibition of translation can be mediated by: **A)** Inhibiting the translation initiation by competing with cap binding proteins such as EIF4E (Eukaryotic translation initiation factor 4E), **B)** Blocking the association of small and large ribosome units, **C)** Slowing of stalling the elongation process and premature termination of translation. **D)** Promoting the degradation of nascent polypeptides. Other mechanisms not directly related with translation include: **E)** Cleavage of the mRNA molecule by Ago2 in cases of near-perfect or perfect complementarity which results in mRNA degradation, **F)** Removal of the poly(A) tail and consequent mRNA degradation and **G)** sequestration of the mRNA molecules to the P-bodies where they can be either stored or degraded.

One important feature in the regulation process mediated by miRNAs is the fact that a single miRNA can have hundreds of target mRNAs, a characteristic which is mainly due to their ability to imperfectly bind to mRNAs (Peter, 2010). Moreover, each mRNA can also be the target of multiple miRNAs, generating highly complex regulatory networks involving miRNAs: mRNA interactions where multiple miRNAs can synergistically regulate the expression of multiple genes (Peter, 2010).

MiRNAs have emerged as important players in gene regulation. Evidence suggests more than 30% of all protein-coding genes are regulated by miRNAs implicating their function in processes such as development, metabolism, and cell death (Stark *et al.*, 2005). In most cases, miRNAs are responsible for the subtle regulation of multiple cellular processes, contributing for the fine-tuning of protein output (Baek *et al.*, 2008; Selbach *et al.*, 2008). Nevertheless, some miRNAs are capable of strongly repressing their target genes leading to robust changes in gene expression and dramatically affecting associated cellular functions such as those involved in differentiation and development (Kloosterman and Plasterk, 2006).

1.2.2.5 MiRNA target prediction

The increased knowledge about the interaction between miRNAs and their target mRNAs has enabled the development of bioinformatic algorithms that allow the prediction of miRNA targets. Several online tools are available which are based on experimentally validated factors that improve the performance of these algorithms (Krek *et al.*, 2005; Saito and Saetrom, 2010; Agarwal *et al.*, 2015).

The Watson and Crick base-pairing is naturally the most important factor for target prediction. Prediction algorithms take into account not only the degree of complementarity between the seed region of the miRNA with the seed site of the mRNA but may also account for compensatory binding in other regions of the miRNA/mRNA.

Depending on the criteria used by the algorithm, very strict binding rules will lead to high specificity at the cost of lower sensibility. However, allowing more imperfect binding rules will cause an increase in sensibility at the cost of an increased number of false positives (Saito and Saetrom, 2010).

The location of the binding sites is also an important factor. As previously mentioned most miRNAs bind preferentially to the 3'UTR of target mRNAs (Bartel, 2009). Due to this fact, many tools give a preferential score for predictions in the 3'UTR. Moreover, binding sites conserved between multiple organisms have an increased chance of higher relevance due to their evolutionary preservation (Maziere and Enright, 2007). Finally, the existence of multiple binding sites for a miRNA in a single mRNA will likely have an additive effect, increasing the regulatory effect mediated by the miRNA. Other algorithms will also account for secondary structure of the mRNA molecules, using RNA folding packages to predict the accessibility of miRNA binding sites (Maziere and Enright, 2007; Saito and Saetrom, 2010; Witkos *et al.*, 2011).

1.2.2.6 Role of miRNAs in polyQ diseases

Taking into account the broad functions of miRNAs, it would be expected that they would be important players in neurodegenerative diseases and in particular in the case of polyQ diseases. Moreover, previous evidence has shown that the depletion of miRNAs in differentiated cerebellar neurons, mediated by Dicer knockdown, causes neuronal cell death, cerebellar degeneration and development of ataxia (Schaefer *et al.*, 2007). In fact, accumulating evidence has identified important roles for different miRNAs in polyQ diseases, either as mediators of pathogenic mechanisms, direct regulators of polyQ proteins or as useful biomarkers for the evaluation of disease progression.

1.2.2.6.1 Role of miRNAs in Huntington's disease

Multiple studies have identified different miRNAs which are relevant for HD pathogenesis. The first study was performed by Johnson and colleagues who detected a dysregulation in the levels of multiple miRNAs in samples from HD transgenic mice and human *post-mortem* brain tissue (Johnson *et al.*, 2008). Four miRNAs displayed significantly reduced expression in R6/2 mice: mir-29a, mir-124a, mir-132 and mir-135b.

Regarding human samples, mir-132 levels were significantly lower in the HD samples while in contrast, mir-29a and mir-330 were significantly higher in HD samples (Johnson *et al.*, 2008). Packer and colleagues also identified multiple miRNAs that were dysregulated in HD. Importantly this dysregulation could be associated with the disease progression. Among dysregulated miRNAs, four miRNAs were found to be downregulated: mir-9, mir-9*, mir-29b, mir-124a while one miRNA, mir-132, was found to be upregulated (Packer *et al.*, 2008). Interestingly, both studies associated the observed dysregulation in miRNA levels with increased REST repression, implicating miRNA dysregulation as an important component in polyQ mediated neurodegenerative pathways (Johnson *et al.*, 2008; Packer *et al.*, 2008). Recently, an in vitro study demonstrated that miR-214 overexpression contributes to HD pathogenesis by promoting a downregulation of beta catenin (Ghatak and Raha, 2015).

Other studies have extensively characterized the miRNA profile in other models and brain regions. One study reported nine miRNAs (miR-22, miR-29c, miR-128, miR-132, miR-138, miR-218, miR-222, miR-344, and miR-674*) which were commonly down-regulated in both 12-month-old YAC128 and 10-week-old R6/2 mice (Lee *et al.*, 2011). Interestingly, they also observed an abnormal expression in the genes encoding for the miRNA biogenesis machinery (Lee *et al.*, 2011). More recently miR-128a was observed to be downregulated in a HD monkey model and in the brains of pre-symptomatic and post-symptomatic HD patients (Kocerha *et al.*, 2014) while many other miRNA alterations were found in HD brain which were related to the clinical manifestations of the disease (Hoss *et al.*, 2015).

Another study has detected increased levels of miR-34b in pre-manifest HD plasma and in mHTT-expressing, NT2-derived neurons (Gaughwin *et al.*, 2011). This illustrates the potential of miRNAs to be used as biomarkers for disease progression using easy to obtain samples such as plasma.

Taking advantage of miRNA regulation of gene expression, miRNAs have been exploited as a therapeutic approach for HD. Mir-196a overexpression was an effective strategy for the reduction of mutant HTT and associated aggregates *in vitro* and *in vivo* (Cheng *et al.*, 2013). Mir-124 was also capable of slowing down the progression of HD by promoting neurogenesis in the striatum (Liu *et al.*, 2015).

1.2.2.6.2 Role of miRNAs in SBMA

Regarding SBMA, miRNAs have been successfully used as a therapeutic strategy in pre-clinical studies. Adeno-associated virus (AAV) mediated overexpression of mir-196a was capable of ameliorating disease manifestations in SBMA transgenic mice by downregulating CELF2, a protein capable of stabilizing the AR mRNA, and consequently reduce the levels and associated toxicity of the mutant AR (Miyazaki *et al.*, 2012). Another recent study has taken advantage of AAV overexpression of a miRNA directly targeting AR 3'UTR, mir-298, which was effective in reducing the levels of mutant AR and in ameliorating the disease phenotype in SBMA mice (Pourshafie *et al.*, 2016).

1.2.2.6.3 Role of miRNAs in Spinocerebellar ataxias

More and more evidence has been implicating miRNAs in the pathology of spinocerebellar ataxias. Nevertheless, their use as a therapeutic strategy has been very limited (Koscianska and Krzyzosiak, 2014).

Regarding SCA1, ATXN1 itself was identified to be the target of multiple miRNAs: mir-19, mir-101 and mir-130 which were found to co-regulate ATXN1 levels through its 3'UTR. Their inhibition enhanced the cytotoxicity of polyglutamine-expanded ATXN1 in human cells (Lee *et al.*, 2008). Moreover, mir-144, mir-101 and mir-130 levels were found to be increased in the cerebellum and cortex of SCA1 patients (Persengiev *et al.*, 2011). Another study has provided evidence for changes in miRNA expression of multiple miRNAs in pre- and post-symptomatic SCA1 transgenic mice cerebellum, and identified mir-150 upregulation as an event contributing to the pathogenesis of SCA1 by promoting a decrease in the levels of VEGF (Rodriguez-Lebron *et al.*, 2013b).

In MJD, the first study associating miRNAs and the development of the disease was performed in *Drosophila* where one miRNA, *bantam*, was demonstrated to modulate mutATXN3 toxicity, reducing its associated neurodegeneration (Bilen *et al.*, 2006). ATXN3 itself was also observed to be the target of two different miRNAs: mir-25 and mir-181a (Huang *et al.*, 2014; Koscianska and Krzyzosiak, 2014). Overexpression of mir-25 was capable of reducing the levels of mutant ATXN3 and apoptosis *in vitro* (Huang et al., 2014). MiRNA dysregulation has also been the target of intense research in MJD. The profiling of miRNAs in the brain of MJD transgenic mice revealed a dysregulation of

mir-15b, miR-181a, miR-361 and mir-674 (Rodriguez-Lebron *et al.*, 2013a). Analysis of serum samples from MJD patients identified a dysregulation for miR-25, miR-125b, miR-29a and miR-34b (Shi *et al.*, 2014).

Recently, in SCA6, Miyazaki and colleagues identified one miRNA, mir-3191-5p, that targets the CACNA1A IRES inhibiting the expression of IRES-driven translation of α1ACT. Moreover, *in vivo* AAV9-mediated delivery of mir-3191-5p was demonstrated to reduce motor deficits and Purkinje cell degeneration in a SCA6 mouse model (Miyazaki *et al.*, 2016).

Finally, in SCA7, mir-124 was found to be consistently downregulated across different models such has SCA7 transgenic mice and in SCA7 patient fibroblasts. This was caused by an impairment in mir-124 transcription caused by the polyQ mutation on *ATXN7.* However, ATXN7 itself is a target of mir-124, which, upon depletion, induced an upregulation in the levels of mutant ATXN7 (Tan *et al.*, 2014).

1.2.2.6.4 Role of miRNAs in DRPLA

Although data regarding the role of miRNAs in DRPLA is very limited, one study in *Drosophila* has identified a highly conserved miRNA (mir-8) which binds to atrophin 3'UTR, promoting a reduction in its levels, which in turn may have implications for DRPLA disease pathogenesis (Karres *et al.*, 2007).

1.3 RNA interference as a therapeutic approach

Many clinical trials based on the RNAi pathway are now being performed. However, the vast majority of these are based on the usage of siRNAs and not miRNAs (Lam *et al.*, 2015). Therapies based on siRNA technologies have been tested for the treatment of cancer, infectious diseases, ocular conditions cardiovascular and metabolic diseases, genetic disorders, among others (Lam *et al.*, 2015). In contrast, clinical trials based on miRNA technologies have only undergone clinical testing for a very limited number of applications, namely the treatment of cancer and infectious diseases (Table 1.5).

Table 1.5 – MiRNA therapeutics in clinical trials

Type of therapy	miRNA	Indication	Clinical trial identifier
miRNA inhibitors	Mir-122	Hepatitis C	NCT01200420 (Phase II)
miRNA mimics	Mir-34	Primary liver cancer or metastatic cancer with liver involvement	NCT01829971 (Phase I)
	Mir-16	Malignant pleural mesothelioma and advanced non-small cell lung cancer	NCT02369198 (Phase I)

Although sharing many similarities, this striking difference in the progress of miRNA therapeutics compared to siRNAs may be due to the uncertain specificity of miRNAs when compared to theoretical single-target specificity of siRNAs (Hydbring and Badalian-Very, 2013). This disadvantage may however represent one of the miRNAs greatest advantages. In complex diseases such as cancer, the ability of miRNAs to modulate entire gene pathways with a single sequence may prove beneficial. Moreover, in diseases where there is a depletion in the endogenous levels of specific miRNAs, miRNA replacement therapy might be the ideal approach in order to restore the normal translational activity of all the target genes (Bader *et al.*, 2010).

1.3.1 RNA interference as a therapeutic approach in MJD

In the past years, multiple studies have successfully taken advantage of RNA interference technology in order to silence the expression of mutATXN3 in MJD rodent models. Alves and colleagues designed shRNAs targeting a single nucleotide polymorphism (SNP) which has been proposed to differentiate wild-type and mutant transcripts in 70% of patients (Gaspar *et al.*, 2001; Miller *et al.*, 2003; Alves *et al.*, 2008a). Lentiviral delivery of these shRNAs was capable of efficiently reducing the levels of mutATXN3 and associated neuropathology in a lentiviral rat model of MJD while

preserving the levels of wtATXN3 (Alves *et al.*, 2008a; Alves *et al.*, 2008b). Interestingly, non-allele specific silencing of ATXN3 did not aggravate MJD pathology, suggesting that this approach may be safe and effective for the treatment of MJD (Alves *et al.*, 2010). A similar approach has later demonstrated the efficacy of shRNA based silencing of mutATXN3 in additional MJD mouse models (Nobrega *et al.*, 2013b; Nobrega *et al.*, 2014). More recently, an allele-specific strategy was employed through a non-invasive non-viral delivery approach using encapsulated siRNAs which were effective in alleviating the MJD phenotype in different MJD mouse models (Conceição *et al.*, 2015).

A different approach has employed AAV-mediated overexpression of artificial miRNAs encoding for non-allele specific silencing sequences in MJD transgenic mice. This strategy resulted in the amelioration of the molecular phenotype of the MJD mice (Rodriguez-Lebron *et al.*, 2013a). Nevertheless, no improvements were observed at the behavioral level (Costa Mdo *et al.*, 2013).

1.3.2 MiRNA modulation technologies

In order to exploit the regulatory role of miRNAs as a therapeutic approach, the development of technologies for efficient modulation of their levels is critical. Current systems for overexpression or inhibition of miRNAs are described in the next following sections.

1.3.2.1 Overexpression of miRNAs

In order to overexpress miRNAs in cells or tissues, two different strategies might be followed: plasmid or viral based overexpression or the use of artificial miRNA mimics.

DNA plasmid vectors and viral encoded miRNAs allow for stable or controlled expression of the miRNA transcript. These are usually expressed under the control of Pol II such as CMV or PGK or Pol III promoters such as H1 or U6. Pol II promoters offer the advantage of leading to the expression of a coding mRNA together with a non-coding miRNA sequence in a single transcript. This can be an advantage if co-expression of a reporter gene is desired (Lebbink *et al.*, 2011; Seyhan, 2016). However, considering that miRNAs can be expressed from Pol III promoters, and taking into account that these

promoters will, in most case scenarios, induce higher expression levels, it might be advantageous to express the miRNA under a Pol III promoter, and if required, drive the expression of the reporter gene under control of an independent Pol II promoter (Makinen *et al.*, 2006; Lebbink *et al.*, 2011).

Regarding the miRNA encoding sequence, multiple strategies may be followed. The most straightforward approach for miRNA expression is to clone the endogenous pre-miRNA encoding sequences together with their endogenous flanking sequences (usually up to 200 nt upstream and downstream of the pre-miRNA). This strategy will resemble endogenous miRNA expression, undergoing the same biogenesis events of endogenous miRNAs (Chen *et al.*, 2004; Furukawa *et al.*, 2011). Another strategy is to only express the endogenous pre-miRNA hairpin without flanking sequences or use artificial hairpins, in which only the regions encoding for the mature miRNA sequences are changed between each miRNA. Although technically attractive, these artificial hairpins will not mimic endogenous processing as they will bypass Drosha processing (Furukawa *et al.*, 2011). Depending on the selected DNA construct, both of the described miRNA encoding systems can be packaged into different types of viral vectors. The advantages and disadvantages of each type of viral vectors will be discussed in point 1.3.3.

Synthetic miRNA mimics are double-stranded RNA molecules which mimic the endogenous miRNA duplex formed after Dicer processing. They have however very poor physicochemical characteristics for *in vivo* administration (Behlke, 2008). In order to overcome this limitation, different chemical modifications can be performed in order to protect these sequences from nuclease degradation such as the adition of methyl (2'-O-Me), methoxyethyl (2'-MOE) or fluorine (2'-F) to the 2′ OH of the ribose ring (Henry *et al.*, 2011). Another chemical modification is the addition of aromatic benzene-pyridine analogs which also promote increased resistance to nucleases (Kitade and Akao, 2010). The presence of a 2 nucleotide 3′ overhang assists with miRISC loading and the degradation of the passenger strand (Henry *et al.*, 2011). Recent evidence suggests that miRNA mimics can also be delivered as single stranded molecules that are 5′-phosphorylated and that contain 2′-fluoro ribose modifications (Chorn *et al.*, 2012). Unlike expression-based miRNAs, these synthetic sequences main disadvantage is the need of repeated administration as they are rapidly cleared from the organism (Zhang *et al.*, 2013a).

1.3.2.2 Inhibition of miRNAs

Similarly to what was shown for miRNA overexpression, the inhibition of miRNA activity in cells or tissues may be performed by following two different strategies: 1) plasmid or viral based expression of anti-miR molecules and 2) use of synthetic anti-mir oligonucleotides.

The first gene expression system for miRNA inhibition were miRNA sponges, transgenes harboring multiple miRNA target sites in order to sequester endogenous miRNAs (Ebert *et al.*, 2007). This approach enables both transient and long-term inhibition of a single miRNA or miRNA family and allows for co-expression of reporter genes depending on the selection of either Pol II or Pol III promoters. In order to prevent cleavage of the sponge transcript, central mismatches in the miRNA binding sites were introduced (Ebert *et al.*, 2007; Ebert and Sharp, 2010).

In the following years other designs were developed for DNA encoded miRNA inhibitors. Scherr and colleagues developed an “antagomiR” inhibitor which contains a single miRNA target site (Scherr *et al.*, 2007). Another strategy, the tough-decoy inhibition was created by Haraguchi and colleagues. This strategy consists on the expression of a hairpin structure with a large, internal bulge exposing two miRNA target sites with imperfect base-pairing with the miRNA (Haraguchi *et al.*, 2009). This technology appears to outperform miRNA sponges on miRNA inhibition (Xie *et al.*, 2012; Bak *et al.*, 2013). One advantage of this type of expression constructs is that they can also be packaged into different types of viral vectors according to their desired application.

ASOs have been extensively characterized as a tool for mRNA degradation and inhibition (Bennett and Swayze, 2010). However, they also have the potential to mediate miRNA inhibition (Esau, 2008). ASOs are synthetic oligonucleotide sequences with sequence complementarity to their target miRNAs. Since unmodified oligonucleotides suffer from poor stability and limited affinity for their target, chemical modifications on their sequence are also essential to improve their stability, potency and specificity (Davis *et al.*, 2006; Lennox *et al.*, 2013). Among existing modifications, the antagomiR is a technology consisting of 2’-hydroxil modifications conjugated with phosphorothioate backbone which offers high resistance to nuclease degradation and improved binding affinity to miRNAs (Krutzfeldt *et al.*, 2005). Other chemical modifications have been developed such as the locked nucleic acids (LNAs). These consist of 2′-modified ASOs where the 4′-carbon has been tethered to the 2′-hydroxyl group (Wahlestedt *et al.*, 2000;

Sorensen *et al.*, 2002). This modification results in a stronger affinity with the target miRNA and associated higher activity (Davis *et al.*, 2006).

1.3.3 Delivery of miRNA modulators to the CNS – Viral vectors

Viral vectors encoding for shRNAs or miRNAs have been used in a large set of RNAi applications such as neurodegenerative diseases, retinal diseases, cardiac disease and cancer, among others (Couto and High, 2010). The most used viral vectors have been the lentiviruses, adenoviruses and adeno-associated viruses. The majority of these vectors can cross cellular membranes and deliver their genetic material to the host cells with very high efficiency making them excellent therapeutic vehicles in the field of gene therapy (Ginn *et al.*, 2013). The different characteristics of each viral vector should be accounted in order to select the most suitable type for each application (Table 1.6).

Table 1.6 – The main types of viral vectors used in gene therapy applications

Vector	Packaging capacity	Tropism	Inflammatory potential	Vector genome form
Retroviruses	8 kb	Dividing cells	Low	Integrated
Lentiviruses	8 kb	Broad	Low	Integrated
Herpes simplex virus	180 kb	Neurons	High	Episomal
Adeno-associated viruses	< 5 kb	Broad	Low	Mainly episomal
Adenoviruses	30 kb	Broad	High	Episomal

Table adapted from (Thomas *et al.*, 2003)

Taking into account the broad tropism and low inflammatory potential of both lentiviruses and AAVs, they both offer great potential as CNS therapies.

Lentiviral vectors persistent gene transfer represents an advantage in situations when continuous transgene expression is required, such as in most RNAi applications. Moreover, they have been used successfully *in vivo* for the transduction of most CNS

cell types (Jakobsson and Lundberg, 2006). However, their main disadvantage relies on their genomic integrative properties which will always carry an associated risk of causing insertional mutagenesis (Sinn *et al.*, 2005). In fact, insertional mutagenesis has led to the development of leukemia in children with X-linked SCID which were submitted to an *ex vivo* gene therapy using murine leukemia virus (MLV) vectors (Hacein-Bey-Abina *et al.*, 2003). These results have raised important concerns over the clinical application of gene therapy. However, unlike MLVs which integrate preferentially into promoter regions, leading to increased oncogenesis by influencing the promoter activity or by giving rise to new transcripts, lentiviral vectors integrate in the entire transcribed region being less likely to disturb the regulation of the host gene (Schroder *et al.*, 2002; Mitchell *et al.*, 2004). Nevertheless, integrase defective lentiviral vectors (IDLV) have now been developed which can overcome this limitation (Banasik and McCray, 2010). IDLVs have already been shown to efficiently transduce adult and fetal CNS cells (Rahim *et al.*, 2009). Moreover, they are also capable of achieving sustained expression in non-dividing cells populations such as those in the brain and in the retina (Philippe *et al.*, 2006; Yanez-Munoz *et al.*, 2006).

Regarding AAV vectors, one of their greatest advantages is the fact that they will not integrate in the host genome, bypassing the safety limitation of lentiviral vectors (Thomas *et al.*, 2003). Despite the fact that these vectors are non-integrative, their genome will remain in an episomal state and its expression can be sustained in non-dividing cell populations such as neurons. In fact, one study in non-human primates has reported sustained expression even after 6 years of a single AAV administration on the striatum (Bankiewicz *et al.*, 2006). Moreover, multiple serotypes of AAV have now been described that are characterized by different tropism, making them a flexible vector for distinct applications (Lisowski *et al.*, 2015). Regarding CNS delivery, AAVs also offer the potential for a non-invasive gene delivery route for specific serotypes or genetically engineered capsids (Lisowski *et al.*, 2015; Choudhury *et al.*, 2016; Deverman *et al.*, 2016). However, their greatest disadvantage lies in their cargo capacity which is limited to 4-5 kb (Thomas *et al.*, 2003). Nevertheless, taking into account that in RNAi applications, such as miRNA delivery, long expression cassettes are not required, this limitation should not be of great concern. Moreover, despite the fact that both AAV and lentiviral vectors only induce a minimal inflammatory response upon brain administration, the majority of humans have antibodies against wild-type AAV, which may prime an immune response against the vector and lead to diminished transgene expression (Bessis *et al.*, 2004; Peden *et al.*, 2004).

1.4 Objectives

The main goal of this thesis was the elucidation of the post-transcriptional regulatory mechanisms of ATXN3 mRNA and the evaluation of their role in the disease pathogenesis, taking advantage of their function as a novel gene therapy approach for the treatment of MJD.

To achieve this goal, the specific objectives of this thesis were the following:

- To develop and characterize a new lentiviral model of MJD which would mimic the endogenous regulatory functions of human ATXN3 3'UTR *in vitro* and *in vivo*.

- To evaluate the role of endogenous miRNAs on the regulation of ATXN3 through its 3'UTR.

- To identify and characterize the potential dysregulation of miRNAs predicted to target human ATXN3 3'UTR and of the miRNA machinery, in the context of *in vitro* and *in vivo* MJD models

- To develop a gene expression-based system for efficient modulation of miRNAs *in vitro* and *in vivo*.

- To exploit the regulatory functions of miRNAs targeting human ATXN3 3'UTR and to evaluate their therapeutic potential as a tool for the silencing of mutATXN3 *in vitro* and *in vivo*.

CHAPTER 2

Ataxin-3 3'UTR reduces levels and aggregation of mutant Ataxin-3 *in vitro* and *in vivo* by mediating microRNA regulation

2.1 Abstract

Machado-Joseph disease (MJD), is a genetic neurodegenerative disease caused by an expanded polyglutamine tract within the protein ataxin-3 (ATXN3). MJD's mechanism of pathogenesis is unclear and no disease-modifying treatment is available. Despite the numerous efforts to elucidate the underlying pathogenic mechanisms of MJD, the regulation of ATXN3 mRNA has remained largely unaddressed.

In order to further clarify ATXN3 mRNA regulatory mechanisms, we developed and characterized a novel lentiviral mouse model of MJD which includes the 3'UTR of human ATXN3. Moreover, we sought to understand the role of microRNAs (miRNAs) in the regulation of ATXN3 3'UTR by performing a genetic and pharmacologic inhibition of their function.

We found that the addition of the 3'UTR, drastically reduces ATXN3 expression and aggregation *in vitro,* and neurodegeneration and neuroinflammation *in vivo*. Moreover, the blockage of endogenous miRNA functions resulted in a reversal of the observed effects mediated by the 3'UTR.

Altogether, these findings indicate that miRNAs and the 3'UTR of ATXN3 play a crucial role in MJD pathogenesis and provide a promising opportunity for MJD treatment.

2.2 Introduction

Machado-Joseph disease (MJD) or spinocerebellar ataxia type 3 (SCA3), is the most common autosomal dominantly inherited ataxia worldwide (Schols *et al.*, 2004). MJD belongs to the group of polyglutamine (polyQ) diseases, a group of nine disorders caused by an expansion of the trinucleotide cytosine-adenine-guanine (CAG) in the genes encoding for polyQ proteins (Shao and Diamond, 2007). In the case of MJD this mutation occurs in the *ATXN3* gene, leading to the formation of a mutant messenger RNA (mRNA) and protein, which will be responsible for progressive neurodegeneration in selective brain regions and an associated impairment of motor coordination (Takiyama *et al.*, 1993; Kawaguchi *et al.*, 1994). Currently, treatment for the disease is only based on alleviation of the disease symptoms, as there is no available therapy capable of modifying or delaying the progression of the disease.

The severe lack of therapeutic solutions for the treatment of MJD has raised a strong interest from the scientific community in trying to clarify the mechanisms involved in MJD pathogenesis and to develop novel therapeutic strategies for the disease. In order to reach this goal, multiple models of MJD, both *in vitro* and *in vivo*, have been developed mostly through the expression of the coding region of human mutant ataxin-3 (mutATXN3) (Goti *et al.*, 2004; Bichelmeier *et al.*, 2007; Alves *et al.*, 2008b; Chou *et al.*, 2008; Torashima *et al.*, 2008; Boy *et al.*, 2009; Boy *et al.*, 2010; Silva-Fernandes *et al.*, 2010). However, despite the valuable information they provide for the study of the effects of mutATXN3, further studies in other models are required in order to understand the role of ATXN3 mRNA non-coding regions, such as the three prime untranslated region (3'UTR) (Conne *et al.*, 2000).

In fact, although regulation of gene expression is strongly performed at the transcriptional level, being associated with the activation of transcriptional factors and promoter regions at the DNA level, post-transcriptional regulation has generated intense research interest. In particular, UTRs of the majority of genes have been identified to perform an important role in post-transcriptional regulation of gene expression, affecting mRNA stability, localization and translation (Matoulkova *et al.*, 2012). Among UTRs, the 3'UTR has been recognized as a preferential location for the action of RNA-binding proteins (RBP) or microRNAs (miRNAs) (Gu *et al.*, 2009).

MiRNAs are a large class of trans-acting small non-coding RNAs with a big role in post-transcriptional regulation of gene expression (Bartel, 2004). They are

endogenously expressed from miRNA coding genes and their primary transcripts are processed into mature miRNAs through a series of highly regulated enzymatic steps involving key players such as Drosha and Dicer proteins (Kim, 2005). MiRNA-specific binding sites are denoted as "seed sites" and are usually localized within 3'UTRs. This privileged location has been attributed to the absence of the translational machinery usually bound to the 5'UTR and coding sequence (CDS) of the mRNA enabling more efficient binding and silencing activity of miRNAs in the 3'UTRs (Gu *et al.*, 2009).

In fact, recent *in vitro* evidence suggests that ATXN3 levels are transcriptionally regulated by miRNAs (Huang *et al.*, 2014; Koscianska and Krzyzosiak, 2014). However, the direct role of the ATXN3 3'UTR and possible interaction with miRNAs remains unclear and its investigation in both *in vitro* and *in vivo* models is crucial to understand MJD pathogenesis.

In this study, we evaluated the impact of the ATXN3 3'UTR, *in vitro* and *in vivo*, by developing and characterizing a novel lentiviral model of MJD that includes the 3'UTR non-coding region of human ATXN3. Our results suggest that the 3'UTR of ATXN3 allows endogenous miRNAs to exert a negative physiological regulation of mutATXN3, with crucial relevance in MJD neuropathology.

2.3 Materials and methods

2.3.1 Vector construction

Human ATXN3 3'UTR (1-3,434bp) was obtained by restriction digestion of the dual luciferase vector clone HmiT054676a-MT01 (Genecopoeia) using EcoRI and XhoI enzymes (New England Biolabs). The insert was gel purified using a DNA gel extraction kit (Macherey-Nagel), blunted using Klenow Polymerase (New England Biolabs), and later inserted into the previously described LTR-SIN-PGK-mutATXN3-LTR vector (Alves *et al.*, 2008b) using a SmaI site downstream of the mutATXN3 CDS in order to generate the LTR-SIN-PGK-mutATXN3-3'UTR-LTR vector (Fig. 2.1).

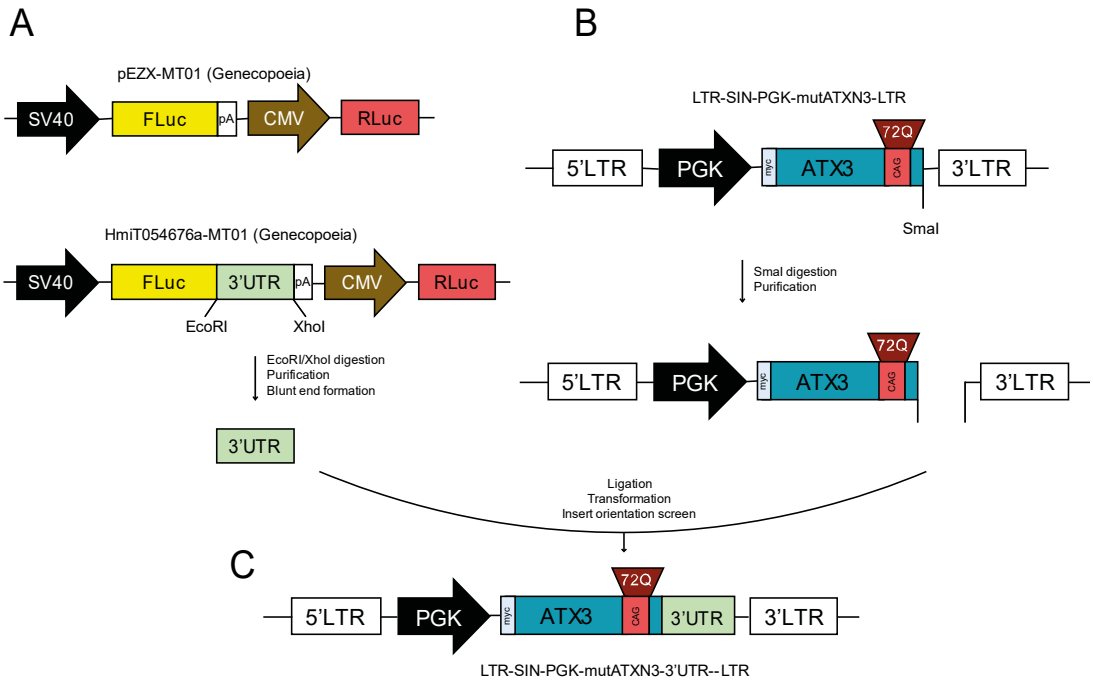

Figure 2.1 - Schematic representation of the procedure used to clone human ATXN3 3'UTR in a lentiviral vector. (A) Plasmid constructions encoding for firefly luciferase bound or not to human ATXN3 3'UTR were purchased from Genecopoeia. ATXN3 3'UTR was extracted from HmiT054676a-MT01 after EcoRI and XhoI digestion. The insert was later purified, and turned blunt using Klenow polymerase. **(B)** A lentiviral vector encoding for mutATXN3 (LTR-SIN-PGK-mutATXN3-LTR) was used as backbone for the introduction of ATXN3 3'UTR after being digested with SmaI. **(C)** The 3'UTR fragment was ligated downstream of ATXN3 CDS in order to generate LTR-SIN-PGK-mutATXN3-3'UTR-LTR.

Truncated C-terminal mutATXN3 with 72 glutamines (TmutATXN3) vectors were constructed using inverted PCR mutagenesis. Briefly, two 5' phosphorylated oligonucleotides (Forward: GCAGATCTCCGCAGGG; Reverse: GTCAATTTCTTGGCGACTTAGTG) (Eurofins Genomics) were designed in order to amplify the parental vectors full sequence (LTR-SIN-PGK-mutATXN3-LTR or LTR-SIN-PGK-mutATXN3-3'UTR-LTR), with the exception of the sequence corresponding to the first 252 amino acids (756bp), using Phusion DNA polymerase (Thermo Scientific) and a modified protocol for GC rich templates. Linear products were circularized using T4 DNA ligase (Thermo Scientific) and transformed into TOP10 chemically competent cells (Life Technologies) to generate LTR-SIN-PGK-TmutATXN3-LTR or LTR-SIN-PGK-TmutATXN3-3'UTR-LTR vectors (Fig. 2.2).

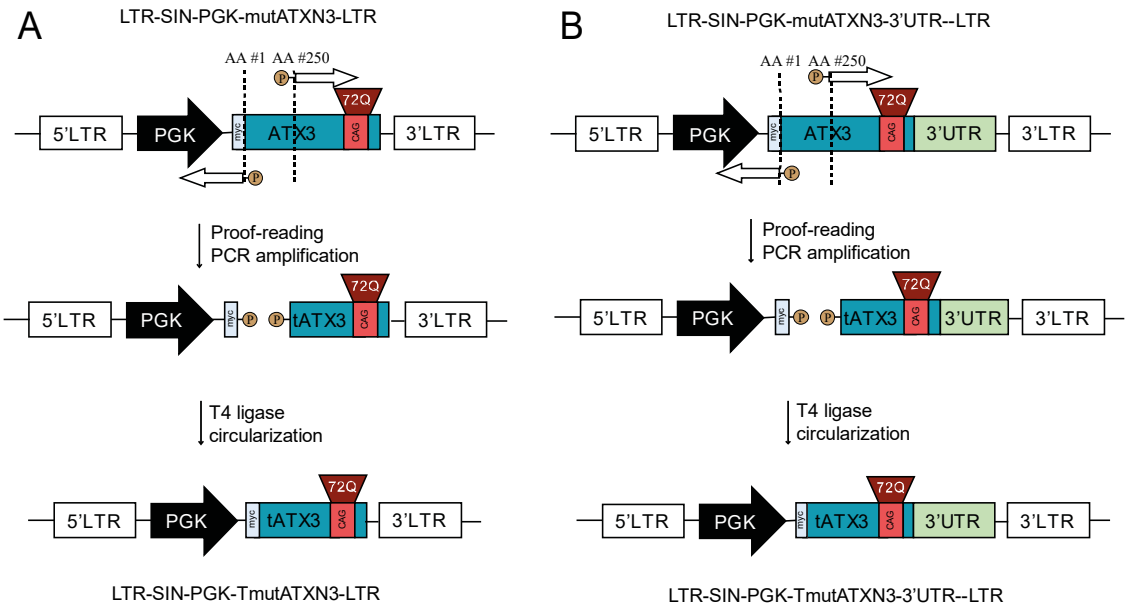

Figure 2.2 - Schematic representation of the procedure used to generate truncated isoforms of mutATXN3. (A) LTR-SIN-PGK-mutATXN3-LTR was used as PCR template for inverted PCR mutagenesis. Two phosphorylated oligonucleotides were designed in order to amplify the parental vector full sequence with the exception of the sequence correspondent to the first 252 amino acids of ATXN3. Linear PCR products were circularized with T4 DNA ligase in order to generate LTR-SIN-PGK-TmutATXN3-LTR. **(B)** LTR-SIN-PGK-mutATXN3-3'UTR-LTR was used as PCR template for inverted PCR mutagenesis. Two phosphorylated oligonucleotides were designed in order to amplify the parental vector full sequence with the exception of the sequence correspondent to the first 252 amino acids of ATXN3. Linear PCR products were circularized with T4 DNA ligase in order to generate LTR-SIN-PGK-TmutATXN3-3'UTR-LTR.

The protocol for the construction of short-hairpin (shRNA) lentiviral vectors has been described in our previous study (Cunha-Santos *et al.*, 2016). Briefly a shRNA negative (control), a shRNA targeting either human Dicer or Drosha were created. For each one, a pair of oligonucleotides was designed, annealed and ligated into linearized p-ENTR/pSUPER+ (AddGene 575-1) (Table 2.1). The H1-shRNA cassette was then transferred, into SIN-cPPT-PGK-EGFP-WHV-LTR, taking advantage of a LR clonase recombination system (Life Technologies). All constructs were verified by restriction analysis and sequencing.

Table 2.1 – Oligonucleotide sequences used for the generation of shRNA constructs

shRNA		Oligonucleotide sequence
hDicer	Top	GATCCCCGCTCGAAATCTTACGCAAATATTCAAGAGATATTTGCGTAAGATTTCGAGCTTTTTA
	Bottom	AGCTTAAAAAGCTCGAAATCTTACGCAAATATCTCTTGAATATTTGCGTAAGATTTCGAGCGGG
hDrosha	Top	GATCCCCCCAGCGTCCATTTGTACTATTTTCAAGAGAAATAGTACAAATGGACGCTGGTTTTTA
	Bottom	AGCTTAAAAACCAGCGTCCATTTGTACTATTTCTCTTGAAAATAGTACAAATGGACGCTGGGGG

2.3.2 Cell line culture, transfection, and transduction

HEK293T and Neuro2A cells were maintained in standard Dulbecco's Modified Eagle Medium (DMEM) (Sigma) supplemented with 10% fetal bovine serum (FBS) (Life Technologies) and 1% Penicillin/Streptomycin (Life Technologies).

For the transfection of HEK293T cell line, 2.75X104 cells were initially plated on 12-well cell culture treated multiwell plates (Fisher Scientific). After 24 hours, medium was changed and cells were transfected with a mixture of DNA/ polethyleneimine (PEI) complexes (MW40000, PolySciences) diluted in complete DMEM. Complex formation was performed by combining 750ng of plasmid DNA in 60µl of serum free DMEM and 4.5µl of PEI (1mg/ml) per well. This mixture was vortexed for 10 seconds and incubated at room temperature for 10 minutes. After that, DNA/PEI complexes were diluted in complete DMEM and added to cell culture. Cell collection was performed 48 hours post-transfection.

For the transduction of Neuro2A cells, 24 hours after plating, the culture medium was replaced with fresh medium containing lentivirus (400ng of P24 per 200 000 cells). Twelve hours later the medium was replaced with regular complete medium and cells were cultured and expanded in standard conditions.

2.3.3 Dual luciferase assay

A dual luciferase reporter construct including the 3'UTR of ATXN3 (FLuc-3'UTR) and a control vector (FLuc-CTRL) clone pEZX-MT01 were purchased from GeneCopoeia. To evaluate the role of ATXN3 3'UTR, 2.75X104 HEK293T cells were seeded per well in 12-well plates (Fisher Scientific). In the next day, cells were transfected with 375ng of the luciferase reporter constructs per well (in triplicates). Forty-eight hours after transfection, cells were washed with 1x Phosphate-buffered saline (PBS) and frozen at -80ºC. Collected cells were lysed with 100 µl of Firefly luciferase assay reagent – 0.1 %Triton (FLAR-T) buffer per well containing 20mM tricine, 100 µM Ethylenediamine tetraacetic acid (EDTA), 25 µM MgCl2, 2.67 mM MgSO4, 17 mM ditiotreitol (DTT) and 0.1% Triton in milli-Q grade water pH 7.8. For the luminescent reaction, 30 µl of cell lysates were loaded on an opaque 96well plate (Corning) and the firefly luminescence activity was measured on a LMax II 384 Luminometer (Molecular Devices) after automatic injection of 100 µl of FLAR buffer containing 20mM tricine, 100 µM EDTA, 25 µM MgCl2, 2.67 mM MgSO4, 17 mM DTT, 250 µM adenosine triphosphate (ATP) and 250 µM D-luciferin (Synchem). Renilla luminescence activity was used as a normalization control and was measured after automatic injection of 100 µl of renilla assay buffer (RAB) buffer containing 1.1 M NaCl, 2.2 mM Na2EDTA, 0.22 M KxPO4, 0.44 mg/ml bovine serum albumin (BSA), 1.3 mM NaN3, and 1.43 mM coelenterazine (Life Technologies) in milli-Q grade water pH 5.0 to 30 µl of cell lysate per microplate well. Integration times were 10 seconds for firefly luciferase signal capture and 5 seconds for renilla luciferase signal capture. Unless stated, all reagents were purchased from Sigma-Aldrich.

2.3.4 RNA stability assay

Actinomycin D (ActD) (10 mg/ml, Sigma-Aldrich) was used to inhibit *de novo*

mRNA synthesis. Neuro2A cells stably expressing either mutATXN3 or mutATXN3-3'UTR at 50–60% confluence were treated with ActD (10 mg/ml) for 0, 2, and 4h and collected for total mRNA extraction and analysis.

2.3.5 Lentivirus production, purification, and titer assessment

Lentiviral vectors encoding for human mutATXN3 (mutATXN3 and mutATXN3-3'UTR) were produced in HEK293T cells with a four-plasmid system, as previously described (de Almeida *et al.*, 2002). The lentiviral particles were resuspended in 1% BSA in PBS. The viral particle content of batches was determined by assessing HIV-1 p24 antigen levels (Retro Tek, Gentaur). Viral stocks were stored at -80ºC. For functional analysis of lentiviral transduction rates, genomic DNA from HEK293T was isolated 72 hours after cell transduction with equal amounts of p24 using a Genomic DNA Purification Kit (Thermo scientific). Quantitative real time polymerase-chain reaction (qPCR) analysis was performed with WPRE and Albumin primers (Table 2.2) using SsoAdvanced SYBR Green Supermix (Bio-Rad) and following manufacturers recommended conditions.

2.3.6 Animals

Four-week-old C57BL/6J mice were obtained from Charles River. The animals were housed in a temperature-controlled room maintained on a 12 h light/12 h dark cycle. Food and water were provided ad libitum. The experiments were carried out in accordance with the European Union Directive 2010/63/EU covering the protection of animals used for scientific purposes. The researchers received adequate training (FELASA certified course) and certification to perform the experiments from Portuguese authorities (Direção Geral de Veterinária).

2.3.7 Mouse surgery

Five-week-old C57BL/6J mice were anesthetized by intraperitoneal administration of avertin (14 µL/g, 250 mg/Kg). Mice were stereotaxically injected into

the striatum in the following coordinates calculated from bregma: anteroposterior: +0.6 mm; lateral: ±1.8 mm; ventral: -3.3 mm; tooth bar: 0, by receiving a single injection of concentrated lentiviral vectors in a final volume of 2 µL containing 400ng of p24 antigen for each vector encoding for the specific transgenes, at an infusion rate of 0.25 µl/min using a 10-µl Hamilton syringe. Five minutes after the infusion was completed the needle was retracted 0.3 mm and allowed to remain in place for an additional 3 minutes prior to its complete removal from the mouse brain.

2.3.8 Immunohistochemical analysis

2.3.8.1 Tissue preparation

Mice were sacrificed with an overdose of avertin (35 µl/g, 625 mg/kg, intraperitoneally), transcardially perfused with PBS and fixed with 4% paraformaldehyde (PFA). Brains were collected and post-fixed in 4% PFA for 24 hours, cryoprotected by incubation in 25% sucrose/PBS and frozen at -80ºC. Coronal sections of 25 µm thickness were obtained using a cryostat equipment (LEICA CM3050S, Leica Microsystems).

2.3.8.2 Bright-field Immunohistochemistry

Free-floating brain coronal sections were treated with a 0.1% phenylhidrazyne/PBS solution for the blockage of endogenous peroxidases for 30 minutes at 37ºC. After permeabilization in PBS/0.1% Triton X-100 with 10% normal goat serum (Gibco), sections were incubated overnight at 4ºC in blocking solution with primary antibodies: mouse monoclonal anti-ATXN3 antibody (1H9; 1:5000; Merck Millipore), rabbit anti-dopamine and cyclic AMP-regulated neuronal phosphoprotein 32 (DARPP-32) antibody (1:1000; Merck Millipore); followed by incubation with respective biotinylated secondary goat anti-mouse or anti-rabbit antibodies (1:200; Vector Laboratoires). Bound antibodies were visualized using the VECTASTAIN® ABC kit, with 3',3'-diaminobenzidine tetrahydrocloride (DAB metal concentrate; Pierce) as substrate. Dry sections were mounted in gelatin-coated slides, dehydrated with ethanol solutions

and Xylene Substitute (Sigma-Aldrich) and mounted in Eukit quick-hardening mounting medium (Sigma-Aldrich). Staining was visualized with Zeiss Axioskop 2 imaging microscope (Carl Zeiss MicroImaging) equipped with AxioCam HR color digital cameras (Carl Zeiss Microimaging) and Plan-Neofluar 5x/0.15 Ph 1 (440321), Plan-Neofluar 20x/0.50 Ph 2 (1004-989), Plan-Neofluar 40x/0.75 Ph 2 (440351) and Plan-Neofluar 63x/1.25 Oil (440460-0000) objectives using the AxioVision 4.7 software package (Carl Zeiss Microimaging).

2.3.8.3 Fluorescence Immunohistochemistry

Free-floating sections were incubated in PBS/0.1% Triton X-100 containing 10% normal goat serum (Sigma-Aldrich), and then incubated overnight at 4ºC in blocking solution with primary antibody: rabbit anti-ionized calcium binding adaptor molecule 1 (Iba-1) antibody (1:1000; Wako Chemicals USA). Sections were washed and incubated for 2h at room temperature with the secondary antibody: goat anti-mouse Alexa Fluor 594 (1:250, Molecular Probes-Invitrogen) diluted in the respective blocking buffer. The sections were washed and incubated during 10 min with 4',6'-diamidino-2-phenylindole DAPI (1:5000, Sigma), washed and mounted in mowiol on gelatin-coated slides. Immunoreactivity of mouse sections was analyzed as previously described (Goncalves *et al.*, 2013). Staining was visualized with Zeiss Axioskop 2 imaging microscope (Carl Zeiss MicroImaging) equipped with AxioCam HR color digital cameras (Carl Zeiss Microimaging) and Plan-Neofluar 5x/0.15 Ph 1 (440321), Plan-Neofluar 20x/0.50 Ph 2 (1004-989), Plan-Neofluar 40x/0.75 Ph 2 (440351) and Plan-Neofluar 63x/1.25 Oil (440460-0000) objectives using the AxioVision 4.7 software package (Carl Zeiss Microimaging). Quantitative analysis of fluorescence was performed with a semiautomated image-analysis software package and images were taken under the same image acquisition conditions and uniform adjustments of brightness and contrast were made to all images (ImageJ).

2.3.9 Fluorescence immunocytochemistry

Cell cultures were washed with PBS and fixed with PBS/4% PFA. After permeabilization in PBS/1% Triton X-100 (Sigma) solution for 5 minutes and blocking in

PBS/3% BSA, cells were incubated overnight at 4ºC with the primary antibodies: mouse anti-Myc tag clone 4A6 (1:1000, Millipore) diluted in PBS/3% BSA. On the next day, cells were washed and incubated for 2h at room temperature with the secondary antibody goat anti-mouse Alexa Fluor 594 (1:250, Molecular Probes-Invitrogen). Cells were washed and incubated during 5 min with 4',6'-diamidino-2-phenylindole DAPI (1:5000, Sigma), washed and mounted in mowiol on gelatin-coated slides. Staining in HEK293T was visualized using a Zeiss LSM 510 Meta confocal microscope (Carl Zeiss MicroImaging), equipped with EC Plan-Neofluar 40x/1.30 Oil DIC M27 (420462-9900) and Plan-Apochromat 63x/1.40 Oil DIC M27 (420782-9900) objectives and LSM Image software. In order to quantify mutATXN3 aggregates in transfected HEK293T cells, five images were randomly acquired per condition and total aggregates and nuclei were manually counted using ImageJ software. The total number of cells counted ranged from 800 to 1100 cells per experimental condition.

2.3.10 Quantification of mutATXN3 inclusions DARPP32 depleted volume

Quantitative analysis of the total number of mutATXN3 inclusions and the extent of DARPP-32 loss in the striatum was performed by scanning 12 stained-sections per animal that were distanced 200 µm from each other (to obtain representative images of the striatum). Total number of inclusions were manually counted in all 12 sections and multiplied by 8 to account for the intermediate sections. To calculate the DARPP-32 loss, sections were imaged using a x5 objective. The quantifications were then performed using an image-analysis software (Image J software). The DARPP-32-depleted volume was estimated using the following formula: Volume = d(a1 + a2 + a3 +…), where d is the distance between serial sections and a1, a2, a3 are the areas for individual serial sections.

2.3.11 Isolation of total RNA from cells and mouse tissue

Total RNA was isolated with miRCURY RNA isolation kit (Exiqon) according to manufacturer's instructions. Monolayer cell cultures were washed with PBS and stored at -80ºC before extraction. For the extraction from mouse tissue, mice were sacrificed with a lethal dose of avertin. The striatum of mice was dissected and stored at -80ºC until

RNA isolation. All samples were submitted to on-column DNAse I digestion (QIAGEN) during isolation. Total amount of RNA was quantified by optical density (OD) using a Nanodrop 2000 Spectrophotometer (Thermo Scientific) and RNA was stored at -80ºC.

2.3.12 cDNA synthesis and quantitative real time polymerase-chain reaction

Complementary DNA (cDNA) for mRNA quantification was obtained by conversion of total RNA with iScript cDNA Synthesis kit (Bio-Rad) according to manufacturer's instructions. qPCR was performed in the StepOne Plus Real-Time PCR System (Applied Biosystems) and SsoAdvanced SYBR Green Supermix (Bio-Rad). Primers for human ACTB and ATXN3 genes were pre-designed and validated by QIAGEN (QuantiTect Primers, QIAGEN). Primers for mouse 18S, human Dicer, Drosha and WPRE were designed using PrimerBlast Software (Table 2.2). Appropriate negative controls were also prepared. All reactions were performed in duplicate and using the following cycling conditions: 95ºC for 30 sec, followed by 45 cycles at 95ºC for 5 sec and 58ºC for 30 sec. The amplification rate for each target was evaluated from the cycle threshold (Ct) numbers obtained with cDNA dilutions. Differences between control and experimental samples were calculated using the $2^{-\Delta\Delta Ct}$ method.

Table 2.2 – Primer sequences used in qPCR

Gene		Primer Sequence	Amplicon size
hDicer	Forward	TTAACCTTTTGGTGTTTGATGAGTGT	98
	Reverse	GCGAGGACATGATGGACAATT	
hDrosha	Forward	AACCCTGGGACGAAACCAAG	118
	Reverse	TCAACTGTGCAGGGCGTATC	
WPRE	Forward	CCGTTGTCAGGCAACGTG	86
	Reverse	AGCTGACAGGTGGTGGCAAT	
Albumin	Forward	GCTGTCATCTCTTGTGGGCTGT	139
	Reverse	ACTCATGGGAGCTGCTGGTTC	
18S	Forward	CTCAACACGGGAAACCTCAC	110
	Reverse	CGCTCCACCAACTAAGAACG	

2.3.13 Protein extraction and western blotting

Monolayer cells were scraped in radioimmunoprecipitation lysis buffer (50mM Tris HCl, pH 8, 150mM NaCl, 1% NP-40, 0.5% sodium deoxycholate, 0.1% sodium dodecyl sulphate) containing protease inhibitors (Roche) followed by sonication by 2 series of 4s pulses. Protein lysates were stored at -20ºC and protein concentration was determined with Bio-Rad Protein Assay. Protein samples were denatured with 6x sample buffer (0.375M Tris pH 6.8 (Sigma-Aldrich), 12% SDS (Sigma-Aldrich), 60% glycerol (Sigma-Aldrich), 0.6M DTT (Sigma-Aldrich), 0.06% bromophenol blue (Sigma-Aldrich)) and 40 µg were resolved by electrophoresis on 12% SDS-PAGE and transferred onto polyvinylidene fluoride (PVDF) membranes (GE Healthcare). Membranes were blocked by incubation in 5% non-fat milk powder in 0.1% Tween 20 in Tris buffered saline (TBS-T), and incubated overnight at 4°C with primary antibody: mouse monoclonal anti-ATXN3 antibody (1H9; 1:5000; Merck Millipore); mouse monoclonal antibody anti-myc tag (4A6; 1:1000; Merck Millipore) and mouse anti-β-actin antibody (AC74; 1:10.000; Sigma-Aldrich), followed by the incubation with alkaline phosphatase-linked secondary goat anti-mouse antibody (1:10.000; Thermo Scientific Pierce). Bands were visualized with Enhanced Chemifluorescence substrate (ECF) (GE Healthcare) and chemifluorescence imaging (Chemidoc Imaging System, Bio-Rad). Semi-quantitative analysis was carried out based on the optical density of scanned membranes (ImageLab version 5.2.1; Bio-Rad). The specific optical density was then normalized with respect to the amount of β-actin loaded in the corresponding lane of the same gel.

2.4 Results

2.4.1 Strategy used to generate a 3'UTR regulated model of MJD

Our group has previously developed a lentiviral vector system used to induce the expression of mutATXN3 *in vitro* and *in vivo* (LTR-SIN-PGK-mutATXN3-LTR) (Alves *et al.*, 2008b). Therefore, to evaluate the role of the human ATXN3 3'UTR, this 3'UTR sequence (1-3,434 bp) was inserted immediately downstream of the mutATXN3 CDS (LTR-SIN-PGK-mutATXN3-3'UTR-LTR) (Fig2.3A). Furthermore, in order to potentiate ATXN3 aggregation *in vitro*, particularly in HEK293T cells, we generated two lentiviral vector constructs encoding a C-terminal fragment of mutATXN3 with 72 glutamines, with (LTR-SIN-PGK-TmutATXN3-3'UTR-LTR) and without the 3'UTR (LTR-SIN-PGK-TmutATXN3-LTR), respectively.

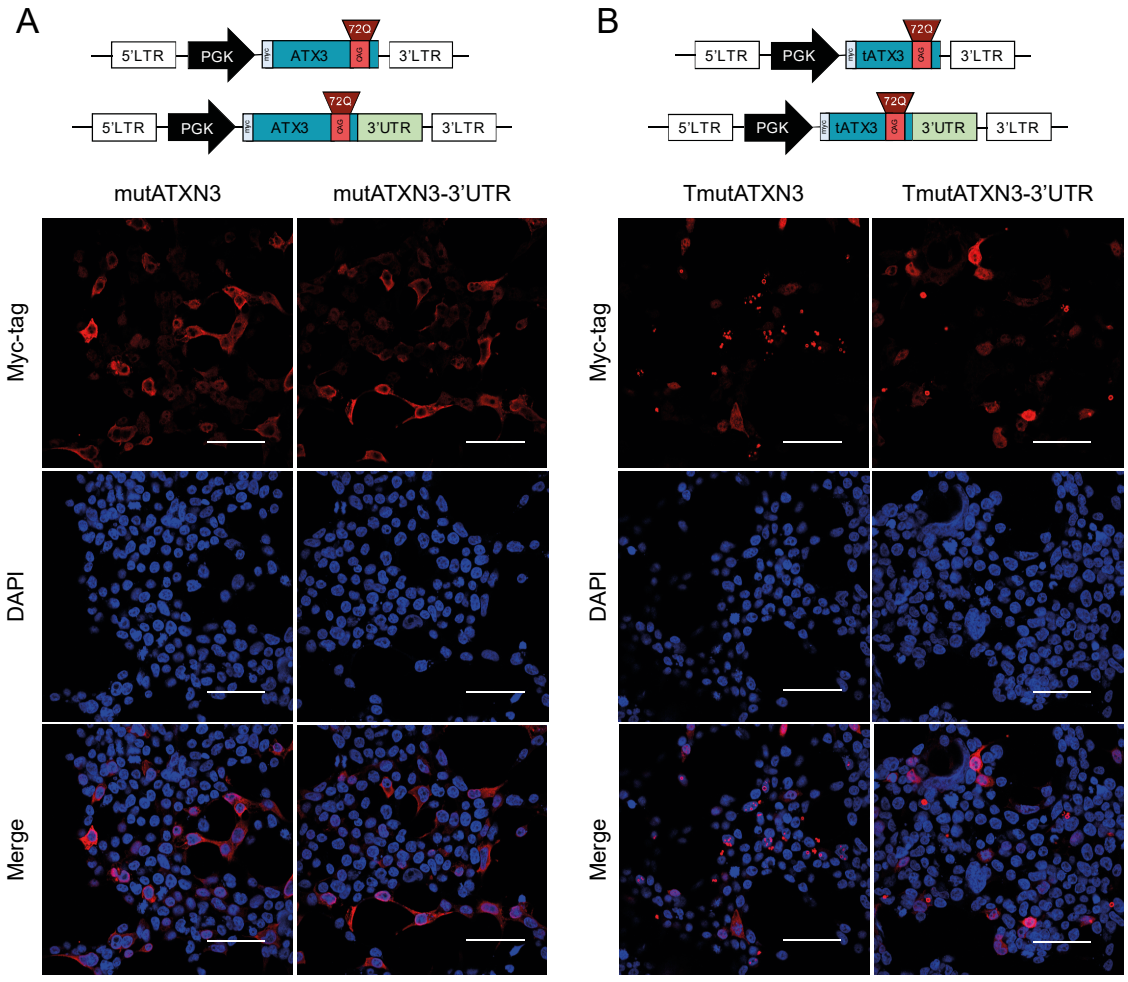

Figure 2.3 – Generation of constructs encoding for a truncated form of mutATXN3 enhance aggregation *in vitro*. (A) Schematic representation of the lentiviral constructs used for the

evaluation of the role of ATXN3 3'UTR *in vitro*. Human ATXN3 3'UTR (1-3,434 bp) was cloned immediately downstream of mutATXN3 (72Q) CDS. These constructs do not aggregate *in vitro* upon transfection of HEK293T. **(B)** Truncated versions of mutATXN3 with and without the 3'UTRs were constructed in order to promote aggregation of mutATXN3 *in vitro*. Upon transfection of HEK29T cells, both constructs result in the formation of characteristic mutATXN3 inclusions. Scale bars represent 50µm.

As expected, transfection of truncated constructs in HEK293T cells induced the formation of extensive mutATXN3 aggregation after 48 hours (Fig. 2.3B).

2.4.2 Inclusion of human ATXN3 3'UTR reduces levels and aggregation of mutATXN3 in HEK293T cells.

In order to evaluate any differences promoted by the 3'UTR of ATXN3, HEK293T cells were transfected with equimolar amounts of TmutATXN3 or TmutATXN3-3'UTR plasmid DNA. Immunoblotting of total protein extracts revealed striking differences not only in aggregate levels (Fig. 2.4A and B; TmutATXN3: 2063 ± 0.1455 vs TmutATXN3-3'UTR: 0.8594 ± 0.2843) but also in soluble mutATXN3 (Fig. 2.4A and C; TmutATXN3: 1.917 ± 0.1906 vs TmutATXN3-3'UTR: 1.181 ± 0.3388).

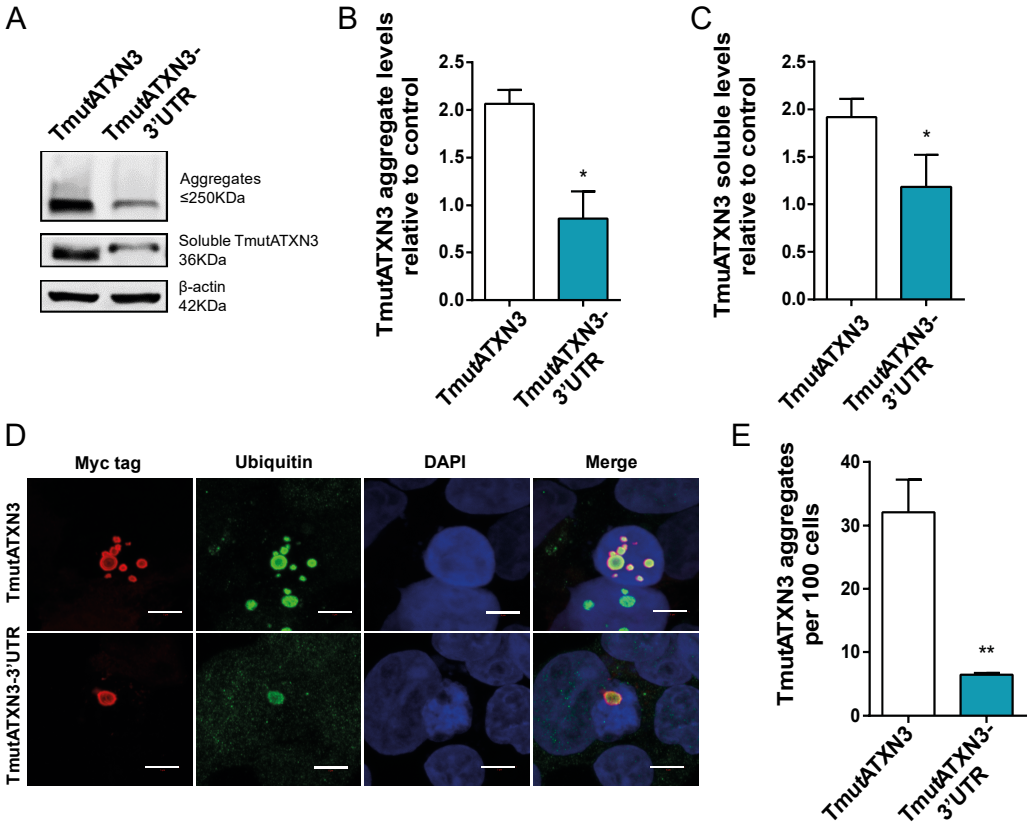

Figure 2.4 – Addition of human ATXN3 3'UTR reduces levels and aggregation of TmutATXN3 in HEK293T cells. (A) Western blot analysis of HEK293T transfected with

equimolar amounts of TmutATXN3 and TmutATXN3-3'UTR constructs showing aggregated (stacking gel) and soluble forms of TmutATXN3 (~36kDa). **(B-C)** Optical densitometry analysis of ATXN3 fractions normalized with actin showing a significant reduction in aggregated and soluble TmutATXN3 protein levels (n=3). **(D)** Representative images from laser confocal microscopy of HEK293T transfected with equimolar amounts of TmutATXN3 and TmutATXN3-3'UTR constructs. Analysis was performed by staining TmutATXN3 (red), ubiquitin (green) and nuclei (blue). **(E)** Quantification of TmutATXN3 aggregates per cell was normalized by nuclei counts, confirming western blot results (n=4). Statistical significance was evaluated with paired Student's t-test (*P < 0.05, **P < 0.01). Data are expressed as mean ± SEM. Scale bars represent 5µm.

Confocal microscopy analysis confirmed this result showing a marked decrease in the number of ubiquitinated mutATXN3 inclusions numbers upon inclusion of ATXN3 3'UTR. (Fig. 2.4D-E; TmutATXN3: 32.10 ± 5.147 aggregates/100 cells vs TmutATXN3-3'UTR: 6.426 ± 0.3043 aggregates/100 cells).

2.4.3 Effects of human ATXN3 3'UTR on a reporter gene assay and on mutATXN3 mRNA stability.

In order to evaluate whether this effect of ATXN3 3'UTR was linked exclusively to ATXN3 mRNA, HEK293T cells were transfected with a construct encoding for firefly luciferase (FLuc-CTRL) or firefly luciferase bound to ATXN3 3'UTR (FLuc-3'UTR) (Fig. 2.5A).

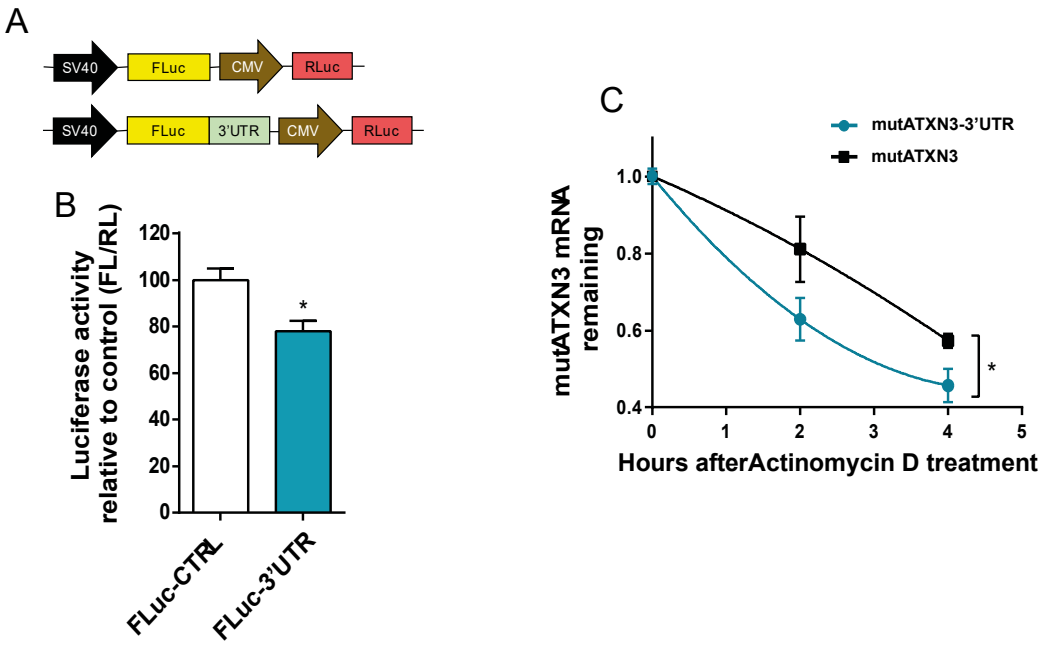

Figure 2.5 – Effects of human ATXN3 3'UTR on a reporter gene assay and on mutATXN3 mRNA stability. (A) Schematic representation on the luciferase constructs encoding for Firefly

luciferase bound or not to ATXN3 3'UTR. Both vectors contain as internal normalizer the gene encoding for Renilla luciferase. **(B)** Dual-luciferase activity evaluation from HEK293T transfected with a control construct encoding for firefly luciferase and renilla luciferase (FLuc-CTRL) or a construct encoding for firefly luciferase bound to ATXN3 3'UTR and renilla luciferase (FLuc-3'UTR). Quantitative analysis presented as firefly/renilla ratio (FL/RL) relative to control shows a reduction in FLuc-3'UTR luminescence activity (n=4). **(C)** MutATXN3 mRNA stability assay from Neuro2A cells stably expressing mutATXN3 or mutATXN3-3'UTR after treatment with ActD for 0, 2 and 4 hours. QPCR analysis for mutATXN3 mRNA levels normalized with endogenous control (18S) and relative to t=0 showing a faster decay rate for mutATXN3-3'UTR mRNA (n=4 for each time-point). Statistical significance was evaluated with paired Student's t-test (B) and unpaired Student's t-test (C) (*P < 0.05). Data are expressed as mean ± SEM.

As expected, the 3'UTR induced a reduction in the expression of a luciferase reporter gene, even in the absence of ATXN3 CDS, suggesting the involvement of other independent endogenous regulators. Moreover, internal normalization with Renilla luciferase control gene confirmed that the observed results were not due to differences in transfection efficiencies (Fig. 2.5B; FLuc-CTRL: 100.0 ± 4.95 vs FLuc-3'UTR: 77.80 ± 4.70).

Taking into account that both constructions have the same CDS, leading to the expression of the same protein, these results led us to hypothesize that the ATXN3 3'UTR was promoting a reduction in the expression of mutATXN3, either by promoting mRNA decay or through translational inhibition. To investigate whether the inclusion of ATXN3 3'UTR changed mutATXN3 mRNA stability, Neuro2A cells stably expressing either mutATXN3 or mutATXN3-3'UTR were treated with ActD in order to block transcription. As shown in Fig. 2.5C, we observed a significantly faster decay of mutATXN3-3'UTR mRNA compared to mutATXN3 which persisted until 4 hours post-treatment with ActD (Fig. 2.5C; mutATXN3: 0.57 ± 0.018 vs mutATXN3-3'UTR: 0.46 ± 0.04).

Overall, these data indicate that mutATXN3 mRNA and protein levels are strongly negatively regulated by its 3'UTR.

2.4.4 Genetic and pharmacologic blockage of miRNA biogenesis reverts ATXN3 3'UTR regulatory effects

Given that miRNAs are one of the most relevant class of molecules capable of inducing mRNA degradation and inhibition of translation, we wanted to assess whether they would be the mediators of the regulation of ATXN3 expression through its 3'UTR.

In order to deplete cells from endogenous miRNAs, we simultaneously silenced two key enzymes for the biogenesis of miRNAs, Dicer and Drosha.

Forty-eight hours after co-transfecting TmutATXN3-3'UTR and either Dicer or Drosha shRNAs-encoding vectors or two control shRNA encoding vectors (Fig. 2.6A-B), we observed, in the knock-down condition, a significant decrease in the levels of both Drosha and Dicer mRNA levels (Fig. 2.6C: hDrosha shCTRL: 1.00 ± 0.05 vs hDrosha shDrosha/Dicer: 0.50 ± 0.01; hDicer shCTRL: 1.02 ± 0.16 vs hDicer shDrosha/Dicer: 0.38 ± 0.03).

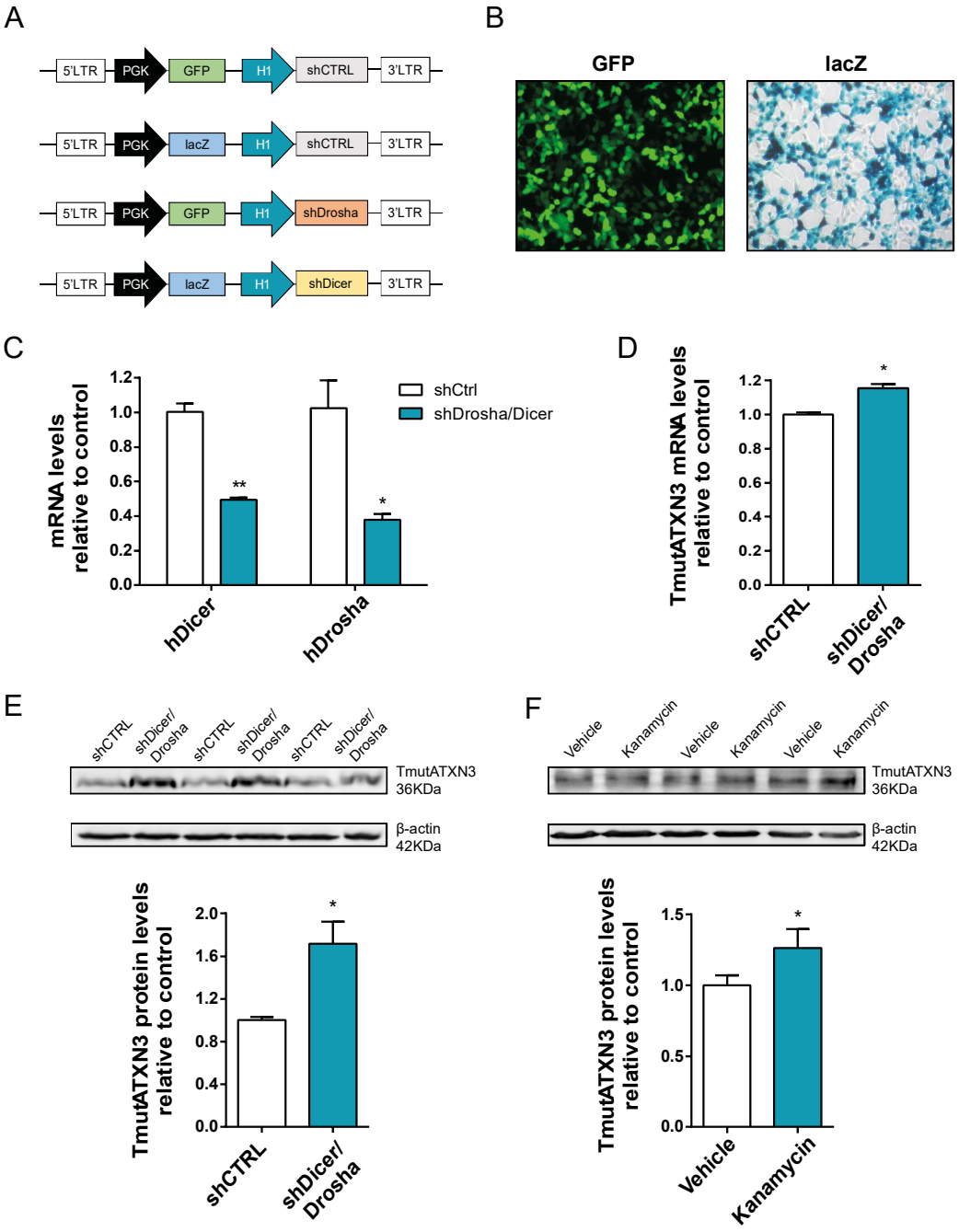

Figure 2.6 – Blockage of endogenous miRNAs increases the levels of mutATXN3. (A) Schematic representation of the lentiviral constructs used for the modulation of endogenous

hDrosha and hDicer through H1 mediated expression of shRNAs targeting hDrosha and hDicer. Green fluorescent protein (GFP) or lacZ expression cassettes were inserted in order to follow gene expression in both targeting shRNAs and negative shRNAs (predicted not to target any known human or mouse gene). **(B)** HEK293T co-transfected with TmutATXN3 and either shRNAs against hDrosha and hDicer or neg shRNAs are efficiently co-transfected as can be observed via reporter gene expression of GFP and lacZ. **(C)** QPCR analysis of endogenous hDrosha and hDicer mRNA levels 48 hours after co-transfection with shRNAs against hDrosha and hDicer compared to control showing efficient gene knock-down (n=3). **(D)** QPCR analysis of TmutATXN3 mRNA levels after hDicer and hDrosha knock-down displays a significant increase in TmutATXN3 mRNA levels (n=3). **(E)** Western blot evaluation of TmutATXN3 protein levels (n=6) in the knock-down conditions when compared to control. TmutATXN3 levels were increased after hDrosha / hDicer knockdown. **(F)** Western blot analysis of TmutATXN3 protein levels in Neuro2A cells stably expressing TmutATXN3-3'UTR. Cells were maintained during 48 hours in complete DMEM as the control condition or in complete DMEM containing kanamycin at a final concentration of 100nM (n=7). TmutATXN3 protein levels were significantly increased in kanamycin treated cells. QPCR analysis was normalized with endogenous control (ACTB). Statistical significance was evaluated with paired Student's t-test (*P < 0.05, **P < 0.01). Data are expressed as mean ± SEM.

Simultaneously, we observed a significant increase in TmutATXN3 mRNA (Fig. 2.6D; shCTRL: 1.00 ± 0.01 vs shDicer/Drosha: 1.15 ± 0.02) and protein levels (Fig. 2.6E; shCTRL: 1.00 ± 0.03 vs shDicer/Drosha: 1.72 ± 0.21). Taking into account the comparatively smaller changes of TmutATXN3 mRNA relative to protein levels, these results suggest a dominant effect of miRNAs on mutATXN3 3'UTR through translational inhibition and in a lesser extent through mRNA degradation, although suggesting an implication for both mechanisms.

Moreover, in order to pharmacologically reproduce the previous results, we took advantage of the previously described properties of aminoglycoside antibiotics, reported to inhibit Dicer-mediated precursor miRNA (pre-miRNA) processing (Davies and Arenz, 2008; Schmidt, 2014). In accordance with the genetic silencing results, Kanamycin A-treated cells stably expressing TmutATXN3-3'UTR presented an upregulation in TmutAtxn3 protein levels when compared to PBS (Vehicle) treated cells. (Fig. 2.6F; Vehicle: 1.00 ± 0.07 vs Kanamycin A: 1.26 ± 0.13).

Altogether, these results suggest an important role for endogenous miRNAs in controlling mutATXN3 expression through interaction with its 3'UTR.

2.4.5 ATXN3 3'UTR reduces mutant ATXN3 inclusions and associated neuropathology in a lentiviral-based mouse model of MJD

Although our *in vitro* results suggest an important role for ATXN3 3'UTR mediated through the action of endogenous miRNAs, they were performed in cellular models. Being known that the endogenous miRNA profile changes extensively between different cell types and tissues (Lagos-Quintana *et al.*, 2002), and taking into account the neurodegenerative profile of MJD, we wanted to address whether these results could be replicated in a neuronal *in vivo* context. To do this we employed our previously characterized lentiviral-based mouse model of MJD (Alves *et al.*, 2008b; Simoes *et al.*, 2012). In this experiment, lentiviral vectors encoding for mutATXN3 or mutATXN3-3'UTR (Fig. 2.7A) were stereotaxically injected in each hemisphere of the striatum of five-week-old mice that were later sacrificed 5 weeks post-injection.

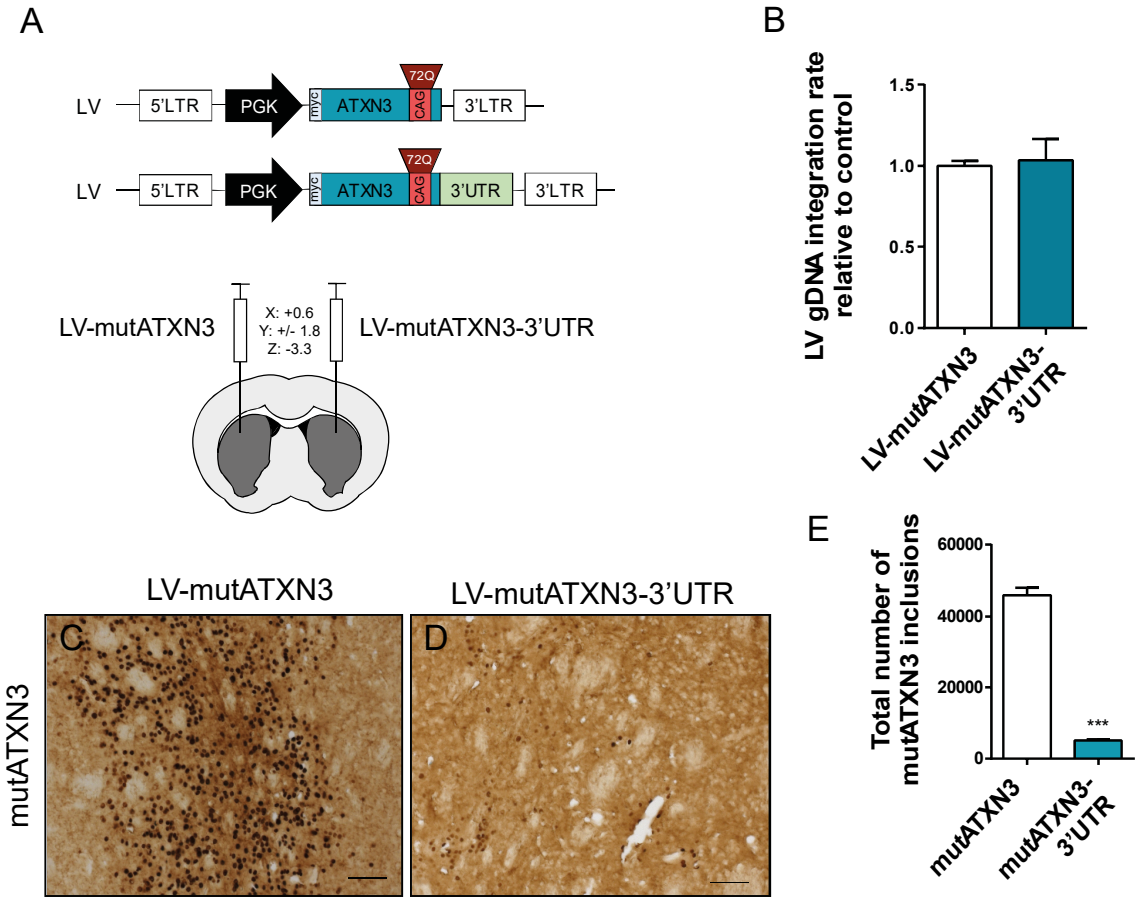

Figure 2.7 - ATXN3 3'UTR reduces mutATXN3 inclusions in a lentiviral mouse model of MJD. (A) Schematic representation of the lentiviral vectors used for the production of lentivirus used in the evaluation of the role of ATXN3 3'UTR *in vivo* and representation of mice stereotaxic

procedure where lentiviral particles encoding for mutATXN3 and mutATXN3-3'UTR were injected bilaterally in the striatum of five-week-old C57/BL6 mice at the following coordinates (x: + 0.6; y: +/- 1.8; z: -3.3). **(B)** QPCR analysis of gDNA transduction rates of both LV-mutATXN3 and LV-mutATXN3-3'UTR after infection of HEK293T cells (n=3). **(C-E)** Immunohistochemical peroxidase staining using anti-ATXN3 antibody (1H9 ab), 5 weeks post-injection. Control mutATXN3 injected animals displayed a large number of mutant ATXN3 inclusions **(C)** which was significantly decreased in the mutATXN3-3'UTR transduced striatum **(D)** as quantified in **E** (n=4). QPCR analysis was normalized with endogenous control (Albumin). Statistical significance was evaluated with paired Student's t-test (***P < 0.001 n = 4). Data are expressed as mean ± SEM. Scale bars represent 40µm.

Importantly, no differences were observed between viral productions regarding their transduction efficiencies after infection of HEK293T cells with equal p24 titers (Fig. 2.7B; LV-mutATXN3: 1.001 ± 0.029 vs LV-mutATXN3-3'UTR: 1.035 ± 0.1295).

In accordance with the *in vitro* data, we observed that the incorporation of the ATXN3 3'UTR drastically reduced the number of mutATXN3 inclusions when compared to the control hemisphere (Fig. 2.7C-E; LV-mutATXN3: 45914 ± 2084 aggregates vs LV-mutATXN3-3'UTR: 5234 ± 306 aggregates).

This model is also characterized by early neuronal dysfunction as shown by a large depleted area of the marker DARPP32 (de Almeida *et al.*, 2002; Alves *et al.*, 2008b; Simoes *et al.*, 2012). In accordance with the observed reduction of mutATXN3 inclusions, immunostaining for DARPP32 revealed a proportionally smaller area of depleted staining (Fig. 2.8A-C; LV-mutATXN3: 0.382 ± 0.041 mm^3 vs LV-mutATXN3-3'UTR: 0.031 ± 0.007 mm^3). Moreover, Iba-1 immunoreactivity which, as previously reported (Goncalves *et al.*, 2013), was strongly exacerbated in the hemisphere injected with LV-mutATXN3, was reduced in the hemisphere injected with LV-mutATXN3-3'UTR (Fig. 2.8D-F; LV-mutATXN3: 1.382 ± 0.013 vs LV-mutATXN3-3'UTR: 1.160 ± 0.030).

These results suggest that, similarly to the previously presented *in vitro* data, ATXN3 3'UTR controls the expression of ATXN3 itself *in vivo*, resulting in a decrease of mutATXN3 inclusions, associated neurodegeneration and neuroinflammation.

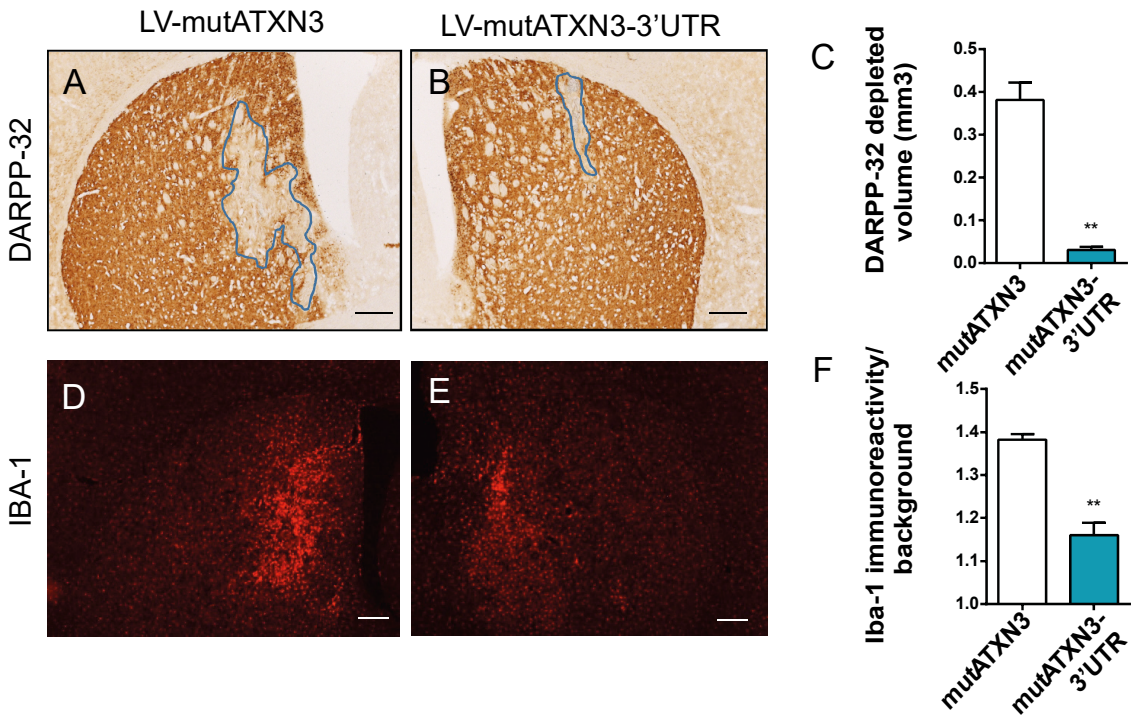

Figure 2.8 – ATXN3 3'UTR reduces associated neuronal dysfunction and neuroinflammation in a lentiviral mouse model of MJD. (A-B) Immunohistochemical analysis using an anti-DARPP32 antibody and lesion identification. mutATXN3-3'UTR injected hemisphere displayed a marked reduction in DARPP-32 depleted volume as quantified in **C** (n=4). **(D-E)** Fluorescent immunohistochemical analysis of Iba-1 immunoreactivity showing a decrease in mutATXN3-3'UTR injected animals as quantified in **F** (n=4). Statistical significance was evaluated with paired Student's t-test (**P < 0.01, n = 4). Data are expressed as mean ± SEM. Scale bars represent 200µm.

2.5 Discussion

In the present study using both *in vitro* and *in vivo* models we show, for the first time, that the human ATXN3 3'UTR plays an important role in the post-transcriptional regulation of ATXN3 itself. Importantly we have done this by developing a new *in vivo* lentiviral mouse model of MJD which should prove useful for the evaluation of ATXN3 3'UTR modulators and for the screening of novel therapeutic approaches for MJD. Moreover, we have provided evidence that endogenous miRNAs strongly regulate ATXN3 expression through an interaction with its 3'UTR.

Despite the efforts that have been made in the development of different MJD animal models for the study of MJD pathogenesis, the vast majority of these have been based on the expression of the CDS of mutant forms of human or mouse ATXN3 (Goti *et al.*, 2004; Bichelmeier *et al.*, 2007; Alves *et al.*, 2008b; Chou *et al.*, 2008; Boy *et al.*, 2009; Boy *et al.*, 2010; Silva-Fernandes *et al.*, 2010). Due to this fact, and regardless of having been effective in the development of promising strategies for the treatment of MJD, these studies lacked in the elucidation of the physiological regulation of ATXN3 expression and how this might be contributing to mutATXN3 toxicity.

In order to understand the post-transcriptional regulatory events modulating ATXN3 mRNA, we decided to focus on its 3'UTR. Human ATXN3 mRNA possesses a long 3'UTR, suggesting it might be a target of post-transcriptional regulators such as miRNAs or RNA-binding proteins. In fact, we observed that the inclusion of a large portion of native human ATXN3 3'UTR was able to mediate a strong decrease in mutATXN3 levels and associated aggregation *in vitro*, in accordance with recent studies suggesting a role for miRNAs as regulators of ATXN3 mRNA through its 3'UTR (Huang *et al.*, 2014; Koscianska and Krzyzosiak, 2014). Additionally, a more recent study described two novel single nucleotide polymorphisms (SNPs) in ATXN3 3'UTR found to modulate disease age-of-onset on MJD patients, highlighting the impact of 3'UTR regulation on disease progression (Long *et al.*, 2015).

On the other hand, our results gain further relevance when aligned with the findings of Ramani and colleagues. The authors observed a retention of intron 10 in mutATXN3 transcripts, reporting that this event leads to an early transcript termination after polyadenylation in intron 10, generating an ATXN3-10e isoform which lacks ATXN3 3'UTR. Furthermore, they report an upregulation of total ATXN3 transcripts in SCA3 knock-in mice, also pointing for likely differences in 3'UTR regulation (Ramani *et al.*,

2015). In the light of our results, we believe this alternative splicing event observed in both YAC ATXN3Q84 and knock-in ATXN3Q82 mice might lead to the expression of an isoform of mutATXN3 that, by lacking the endogenous 3'UTR, will escape endogenous regulatory players such as miRNAs, further contributing for the accumulation of mutATXN3 protein and aggravation of the disease, as supported by our evidence.

MiRNAs represent one of the largest class of endogenous molecules capable of 3'UTR mediated gene expression modulation (He and Hannon, 2004). Considering previous evidence implicating miRNAs in neurodegenerative diseases including MJD (Bilen *et al.*, 2006; Lee *et al.*, 2008; Packer *et al.*, 2008; Miyazaki *et al.*, 2012; Cheng *et al.*, 2013), we sought to investigate if they would be the mediators of ATXN3 3'UTR regulation. Impairment of miRNA biogenesis through combinatorial genetic silencing of hDrosha and hDicer, or pharmacologic inhibition of Dicer-mediated miRNA processing both led to an upregulation of mutATXN3 mRNA and protein levels. Altogether, these results provide strong evidence that endogenous miRNAs might play an important role in the regulation of mutATXN3 through its 3'UTR.

Moreover, the inclusion of ATXN3 3'UTR in our previously characterized lentiviral mouse model of MJD resulted in a remarkable reduction of mutATXN3 aggregates and associated neuropathology. This result suggests that ATXN3 3'UTR is capable of subjecting its mRNA to the regulation of brain miRNAs *in vivo*. Similar results were described by Khodr and colleagues, who observed that the regulation of human alpha-synuclein at its 3′UTR also decreases its levels and toxicity *in vivo* (Khodr *et al.*, 2012).

Interestingly, overexpression of mutATXN3-3'UTR *in vivo* resulted in remarkably low toxicity. This finding is in accordance with the previously mentioned MJD transgenic mouse models that include the 3'UTR of ATXN3. YAC ATXN3Q84, knock-in ATXN3Q82 and Ki91 models are all reportedly described with mild phenotypes, slow progression and modest neuropathology (Cemal *et al.*, 2002; Ramani *et al.*, 2015; Switonski *et al.*, 2015). Being characterized by a moderate yet clear neuropathology, all in a considerably short time frame, we believe our novel mutATXN3-3'UTR lentiviral mouse model of MJD expands the repertoire of existing MJD mouse models, presenting itself as a platform for the study of not only endogenous 3'UTR regulators which might be implicated in MJD pathogenesis, but also novel therapeutic strategies for the treatment of MJD.

CHAPTER 3

MicroRNAs predicted to target human Ataxin-3 are dysregulated in human and mouse Machado-Joseph disease models

3.1 Abstract

Machado-Joseph disease (MJD) is the most common dominantly-inherited ataxia worldwide. Nevertheless, despite being a monogenic disease caused by a mutation in the *ATXN3* gene, the pathogenic events underlying neurodegeneration are still not completely understood. Taking into account that transcriptional dysregulation has been recognized as an important disease pathway in MJD and having provided evidence implicating endogenous microRNAs (miRNAs) in the regulation of ataxin-3 ATXN3 mRNA, in this study we investigated whether miRNAs predicted to target ATXN3 are dysregulated in multiple *in vitro* MJD models including neurons derived from induced pluripotent stem cells (hIPSCs) and *in vivo* in MJD transgenic mice.

We show that specific miRNAs predicted to target ATXN3 3'UTR (mir-9, mir-181a and mir-494) present a general downregulated profile across different MJD models. Moreover, having detected the most severe downregulation for all screened miRNAs in transgenic MJD mice, we took advantage of this model in order to screen the levels of different components of miRNA biogenesis and function genes. In accordance with the results obtained with the mature miRNAs, different genes encoding for miRNA machinery were also found to be downregulated.

All in all, these novel results identified a novel potential role for miRNAs in the pathogenesis of MJD and provide an opportunity for the development of novel therapeutic interventions for this disorder.

3.2 Introduction

Machado-Joseph disease (MJD) or spinocerebellar ataxia type 3, belongs to the group of polyglutamine (polyQ) diseases, dominantly-inherited disorders caused by an expansion of the trinucleotide cytosine-adenine-guanine (CAG) in the genes encoding for polyQ proteins (Bauer and Nukina, 2009). In the case of MJD this mutation occurs in the *ATXN3* gene (Takiyama *et al.*, 1993). MJD is characterized by multiple clinical symptoms such as gait and limb ataxia, peripheral neuropathy, dystonia and dysarthria, altogether leading to a progressive impairment of motor coordination (Kawaguchi *et al.*, 1994; Sudarsky and Coutinho, 1995; Durr *et al.*, 1996). These symptoms develop due to the presence of severe neuronal dysfunction and neurodegeneration in selective brain regions such as the *cerebellum*, *substantia nigra* and *striatum* (Seidel *et al.*, 2012). Although the exact pathological mechanisms underlying MJD are still unclear, it is accepted that the polyQ expansion in the ataxin-3 (ATXN3) protein results in a toxic gain-of-function, involving protein cleavage, oligomerization and aggregation, dysfunction of cellular quality control mechanisms and transcriptional and translational dysregulation, among others (Paulson *et al.*, 1997b; Nascimento-Ferreira *et al.*, 2011; Simoes *et al.*, 2012; Nobrega *et al.*, 2015).

MicroRNAs (miRNAs) are a class of endogenous small non-coding RNAs (containing about 22 nucleotides in size) that mediate post transcriptional gene regulation of their targets, mostly through sequence complementarity to the three prime untranslated region (3'UTR) of messenger RNAs (mRNAs), negatively controlling their translation or causing mRNA degradation (Bartel, 2004).

Recent studies have shown that miRNAs are important players in neurodegenerative diseases and in particular in polyQ disorders. Regarding Huntington's disease (HD), mir-9 was identified to be downregulated in human samples from disease patients. Moreover, this downregulation was correlated with the stage of disease progression (Packer *et al.*, 2008). Interestingly the authors also implicated mir-9 in REST mediated transcriptional dysregulation, a major pathogenic pathway in HD. Besides mir-9, many other miRNAs were shown to be dysregulated in HD patients (Johnson *et al.*, 2008; Packer *et al.*, 2008; Marti *et al.*, 2010). Other studies in animal HD models have also confirmed the presence of miRNA dysregulation. Among many candidates, mir-128a gained significant relevance being downregulated in different animal models such as HD monkeys, YAC128 and R6/2 mice as well as in human samples (Johnson *et al.*, 2008; Marti *et al.*, 2010; Lee *et al.*, 2011).

Nevertheless, the miRNA dysregulation profile in many neurodegenerative diseases appears to be quite dependent on the stage of disease progression and on the animal model being studied. In fact, one study has reported that in different *Drosophila* models of neurodegenerative diseases, no signs of miRNA dysregulation were observed at an early stage of the disease (Reinhardt *et al.*, 2012).

In the case of MJD, studies have reported miRNA dysregulation in both human peripheral serum samples (miR-25, miR-125b, miR-29a and miR-34b) or in MJD transgenic mice brain tissue (miR-15b, miR-181a, miR-361 and mir-674) (Rodriguez-Lebron *et al.*, 2013a; Shi *et al.*, 2014). Even so, the impact of the observed miRNA dysregulation on their targets was not assessed. Moreover, in recent *in vitro* studies, miR-25 and miR-181a were shown to directly target ATXN3 mRNA (Huang *et al.*, 2014; Koscianska and Krzyzosiak, 2014). Nevertheless, whether these miRNAs are dysregulated in the disease remains unclear.

Although miRNA dysregulation has been recognized as an important component in MJD, much of the current research focus has been on the study of mature miRNAs. Therefore, the contribution of other important players involved in miRNA-mediated regulation still remains elusive. In fact, many genes involved in miRNA biogenesis and function have been implicated in other diseases (Hebert and De Strooper, 2009; Mulligan *et al.*, 2013; Hata and Lieberman, 2015). Moreover, dysregulation of miRNA biogenesis genes has in fact been observed in a HD mouse model (Lee *et al.*, 2011). Bilen and colleagues have also reported how the lack of Dicer, one of the major components of the miRNA pathway, aggravates MJD in *Drosophila* (Bilen *et al.*, 2006). Nevertheless, whether MJD is associated with a dysregulation or impairment of this enzyme still remained unadressed.

More recently, our group has shown that Ataxin-2 (ATXN2), a major component of the translational machinery, is decreased in human brain samples of MJD patients, and mouse models (Nobrega *et al.*, 2015). Furthermore, the reestablishment of ATXN2 levels was capable of ammeliorating disease manifestations in different MJD mouse models. Interestingly, ATXN2 has been identified as a major component of the miRNA-mediated repression system (McCann *et al.*, 2011).

Based on the previous evidence implicating endogenous miRNAs in the regulation of ATXN3 through its 3'UTR, in this study we took advantage of bioinformatic algorithms to identify which specific miRNAs were predicted to target ATXN3 mRNA. Furthermore, taking advantage of multiple MJD models, including hIPSCs derived neurons and MJD transgenic mice, we characterized the miRNA profile of our candidate

miRNAs in the context of MJD. Finally, we profiled the levels of genes involved in miRNA biogenesis and function, linking miRNA downregulation with mRNA dysregulation in MJD.

3.3 Materials and methods

3.3.1 SH-SY5Y cell line culture and transduction

SH-SY5Y cells were maintained in DMEM/F12 (Gibco) medium supplemented with 10% fetal bovine serum (FBS) (Life Technologies) and 1% Penicillin/Streptomycin (Gibco).

For the transduction of SH-SY5Y cells, 24 hours after plating, the culture medium was replaced with fresh medium containing lentivirus (400ng of P24 per 200 000 cells). Twelve hours later the medium was replaced with regular complete medium and cells were cultured and expanded in standard conditions.

3.3.2 Neurosphere culture and neuronal differentiation

Human neurospheres derived from hIPSCs generated from MJD (male, 22 years, 80/23 CAGs) or CTRL (female, 52 years, 22/23 CAGs) fibroblasts (Onofre *et al.*, 2016) were maintained in neural expansion media containing Dulbecco's Modified Eagle Medium Nutrient Mixture F-12 (DMEM/F12), B27 supplement (1:50 Invitrogen), Modified Eagle Medium (MEM) non-essential amino acid solution (1:100 Sigma-Aldrich), 20ng/mL epidermal growth factor (EGF), 20 ng/mL basic fibroblast growth factor (bFGF) (Peprotech), 1% Penicillin/Streptomycin (Gibco) and 5µg/mL Heparin (Sigma-Aldrich).

To initiate neuronal differentiation, neurospheres were manually dissociated with a pipette in small aggregates and plated in poly-ornithin/laminin (Sigma-Aldrich) coated plates as small droplets. Neuronal differentiation was performed during 18 days on DMEM/F12 and Neurobasal (mixed 1:1), B27 supplement (1:100 Invitrogen), N2 supplement (1:200 Invitrogen), L-glutamine (1:100 Life Technologies), 20ng/mL brain derived neurotrophic factor (BDNF) (Peprotech), 1% Penicillin/Streptomycin (Gibco), 0.1µM retinoic acid (Sigma-Aldrich), 200nM ascorbic acid (Sigma-Aldrich), 0.5mM Dibutyryl-cAMP (Sigma-Aldrich) and 10µM forskolin (Sigma-Aldrich). Medium was half-changed twice per week or as needed (Onofre, 2016).

3.3.3 Human brain tissue

Post mortem human brain tissue from dentate nucleus was obtained from the "Tissue donation program of the National Ataxia Foundation", Minneapolis, USA (3 MJD and 4 Controls) and from the University of Groningen, The Netherlands (3 MJD and 1 Control).

3.3.4 Fluorescence immunocytochemistry

Cell cultures were washed with Phosphate-buffered saline (PBS) and fixed with PBS/4% paraformaldehyde (PFA). After permeabilization in PBS/1% Triton X-100 solution for 5 minutes and blocking in PBS/3% bovine serum albumin (BSA), cells were incubated overnight at 4ºC with a combination of the following primary antibodies: mouse anti-myc tag clone 4A6 (1:1000, Millipore), mouse anti-βIII tubulin clone 38F4 (1:1000, Life Technologies), rabbit anti-glial fibrillary protein (GFAP) Z0334 (1:1000, Dako), chicken anti-microtubule-associated protein 2 (MAP2) clone ab5392 (1:5000, Abcam), rabbit anti-NeuN clone ABN78 (1:1000, Millipore), mouse anti-SRY-box 2 (SOX2) clone MAB2018 (1:200, R&D), rabbit anti-Nestin AB5922 (1:500, Millipore), diluted in PBS/3% BSA. On the next day, cells were washed and incubated for 2h at room temperature with the secondary antibody: goat anti-mouse/rabbit/chicken Alexa Fluor 488/568/647 (1:250, Molecular Probes-Invitrogen, Eugene). Cells were washed and incubated during 5 min with 4',6'-diamidino-2-phenylindole DAPI (1:5000, Sigma), washed and mounted in mowiol on gelatin-coated slides. Staining was visualized with Zeiss Axioskop 2 imaging microscope (Carl Zeiss MicroImaging) equipped with AxioCam HR color digital cameras (Carl Zeiss Microimaging) and Plan-Neofluar 5x/0.15 Ph 1 (440321), Plan-Neofluar 20x/0.50 Ph 2 (1004-989), Plan-Neofluar 40x/0.75 Ph 2 (440351) and Plan-Neofluar 63x/1.25 Oil (440460-0000) objectives using the AxioVision 4.7 software package (Carl Zeiss Microimaging) or with a Zeiss Axio Imager Z2 imaging microscope (Carl Zeiss MicroImaging) equipped with EC Plan-Neofluar 5x/0.16 M27 (420330-9901), Plan-Apochromat 20x/0.8 M27 (420650-9901), Plan-Apochromat 40x/1.3 Oil DIC M27 (420762-9800) and Plan-Apochromat 63x/1.40 Oil DIC M27 (420782-9900) using ZEN software.

3.3.5 Isolation of total RNA from cells and mouse tissue

Total RNA was isolated with miRCURY RNA isolation kit (Exiqon) according to manufacturer's instructions. Monolayer cell cultures were washed with PBS and stored at -80ºC before extraction. For the extraction from mouse tissue, mice were sacrificed with a lethal dose of avertin. Striatum of mice was dissected and stored at -80ºC until RNA isolation. All samples were submitted to on-column DNAse I digestion (QIAGEN) during isolation. Total amount of RNA was quantified by optical density (OD) using a Nanodrop 2000 Spectrophotometer (Thermo Scientific) and RNA was stored at -80ºC.

3.3.6 cDNA synthesis and quantitative real time polymerase-chain reaction

Specific complementary DNA (cDNA) for miRNA quantification were synthetized using a TaqMan MicroRNA Reverse Transcription Kit combined with specific TaqMan MicroRNA Assays (Applied Biosystems) for each miRNA (mir-103-3p ID000439; mir-9-5p ID000583; mir-181a-5p ID000480; mir-494-3p ID002365; U6 snRNA ID001973) according to manufacturer's instructions. qPCR was performed using TaqMan® Universal PCR Master Mix II with UNG (Applied Biosystems), combined with the previously described TaqMan MicroRNA Assays, following manufacturer's recommended cycling conditions, in a StepOne Plus Real-Time PCR System (Applied Biosystems).

cDNA for mRNA quantification was obtained by conversion of total RNA with iScript cDNA Synthesis kit (Bio-Rad) according to manufacturer's. qPCR was performed in the StepOne Plus Real-Time PCR System (Applied Biosystems) and SsoAdvanced SYBR Green Supermix (Bio-Rad). Primers for mouse DICER, DROSHA and GAPDH genes were pre-designed and validated by QIAGEN (QuantiTect Primers, QIAGEN). Primers for mouse TARBP2, DDX6, Ago2, DGCR8 and FMR1 were designed using PrimerBlast Software (Table 3.1). Appropriate negative controls were also prepared. All reactions were performed in duplicate and using the following cycling conditions: 95ºC for 30 sec, followed by 45 cycles at 95ºC for 5 sec and 58ºC for 30 sec. The amplification rate for each target was evaluated from the cycle threshold (Ct) numbers obtained with cDNA dilutions. Differences between control and experimental samples were calculated using the $2^{-\Delta\Delta Ct}$ method.

Table 3.1 - List of custom designed oligonucleotide sequences used in qPCR analysis

Gene		Primer Sequence	Amplicon size
mDGCR8	Forward	GCGAAGAATAAAGCTGCCCG	112
	Reverse	TGTGGTTAAAATACTCCAGTTCTTC	
mFMR1	Forward	AAAGCGAGCCCACATGTTGAT	109
	Reverse	CTGCCTTGAACTCTCCAGTTG	
mDDX6	Forward	GAGTCGAGCTACTCGCCAAG	88
	Reverse	CGATTTCGATGTTCCTGCCTC	
mAgo2	Forward	ACGCTCTGTGTCAATACCCG	100
	Reverse	TCCTTCAGCGCTGTCATGTT	
mTARBP2	Forward	GGACACTCCTGTCGTTGCTG	73
	Reverse	CATGGGAGGGCTCCTGGTTA	

3.3.7 MJD transgenic mice and genotyping

C57Bl/6-background transgenic mouse model expressing the C-terminal-truncated ATXN3 with 69 glutamine repeats and an N-terminal haemagglutinin (HA) epitope driven by Purkinje-cell-specific L7 promoter were initially obtained from Gunma University Graduate School of Medicine (Torashima *et al.*, 2008). The mice used in this study were obtained from parallel breeding at the CNC animal facilities. All animals used in this study were age matched transgenic (Tg) and wild-type (WT) littermates at 8 weeks of age.

The experiments were carried out in accordance with the European Community directive (2010/63/EU) covering the protection of animals used for scientific purposes. The researchers received adequate training (FELASA-certified course) and certification to perform the experiments from the Portuguese authorities (Direcção Geral de Alimentação e Veterinária).

For mouse genotyping, genomic DNA was isolated from collected animal ear tissue, using a Genomic DNA Purification Kit (Thermo scientific). The presence of the transgene was validated by PCR amplification using DreamTaq (Thermo Scientific) using standard amplification conditions and the following primers Fwd: ATGTACCCATACGATGTTCC; Rev: CTAGCGAGGGAATGAAGAAT.

3.4 Results

3.4.1 Prediction of miRNAs predicted to target ATXN3 3'UTR

Building on the hypothesis that miRNAs were modulating ATXN3 mRNA levels through binding sequences in the 3'UTR (as demonstrated in chapter 1), we screened target prediction databases to identify miRNA candidates (Krek *et al.*, 2005; Betel *et al.*, 2010; Paraskevopoulou *et al.*, 2013; Agarwal *et al.*, 2015). After identification of a first set of highly scored candidates, this information was crossed with data regarding miRNA sequence conservation and expression data of miRNAs in the brain to select those with higher relevance for MJD pathogenesis (Boudreau *et al.*, 2014) (Fig. 3.1A). Three distinct miRNAs (hsa-mir-9-5p, MIMAT0000441; hsa-mir-181a-5p, MIMAT0000256; and hsa-mir-494-3p, MIMAT0002816) were identified as conserved miRNAs targeting the ATXN3 3'UTR, with simultaneously high expression in brain (Fig. 3.1B).

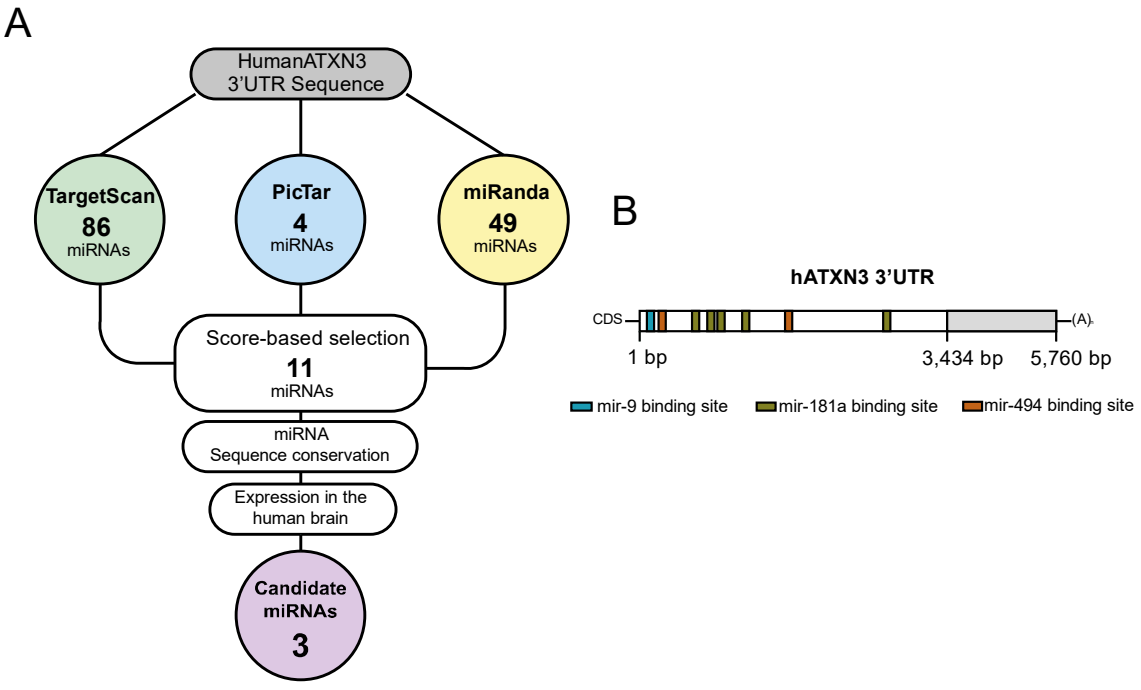

Figure 3.1 – Prediction of miRNAs targeting ATXN3 3'UTR. (A) Schematic representation of the workflow used to identify candidate miRNAs targeting the 3'UTR of human ATXN3. **(B)** Schematic representation of human ATXN3 3'UTR with identification of predicted miRNA target sites for hsa-mir-9-5p, hsa-mir-181a-5p and hsa-mir-494-3p.

While mir-9 was only predicted to bind to ATXN3 3'UTR at one seed site, interestingly, both mir-181a and mir-494 were predicted to bind at multiple sites. More specifically, five seed sites were identified for mir-181a and two different seed sites were identified for mir-494 (Table 3.2). Moreover, many of the predicted miRNA binding sites are located in proximity with other which might suggest the occurrence of miRNA cooperativity (Saetrom *et al.*, 2007).

Table 3.2 – Binding sites of miRNAs predicted to bind to ATXN3 3'UTR

MiRNA	Binding site	3'UTR position
hsa-mir-9-5p	CDS ··· UUAGCCAAAGAG ··· Poly(A) 3' ··· UCUAUUGGUUUCU - 5' miRNA	**190-196**
hsa-mir-181a-5p	CDS ···CUUUAUGAAUGUC··· Poly(A) 3' ··· UCGCAACUUACAA 5' miRNA	**770-776**
hsa-mir-181a-5p	CDS ···CACCAUGAAUGUA··· Poly(A) 3' ··· UCGCAACUUACAA 5' miRNA	**929-936**
hsa-mir-181a-5p	CDS ···UCUUUUGAAUGUU··· Poly(A) 3' ··· UCGCAACUUACAA 5' miRNA	**1033-1039**
hsa-mir-181a-5p	CDS ···GCGUUUGAAUGUG··· Poly(A) 3' ··· UCGCAACUUACAA 5' miRNA	**1381-1387**
hsa-mir-181a-5p	CDS ···UCAUGGAAUGUAG··· Poly(A) 3' ··· UCGCAACUUACAA 5' miRNA	**2393-2399**
hsa-mir-494-3p	CDS ··· UAAAAAUGUUUCA··· Poly(A) 3' ··· GCACAUACAAAGU- 5' miRNA	**236-242**
hsa-mir-494-3p	CDS ···UCUAAAUGUUUCU··· Poly(A) 3' ··· GCACAUACAAAGU- 5' miRNA	**1696-1703**

3.4.2 MiRNA expression profiling in human disease samples and in MJD *in vitro* models

In order to evaluate the role of the miRNAs predicted to target ATXN3 mRNA in the context of MJD, we started by screening the levels of mir-9, mir-181a and mir-494 in human disease samples.

QPCR analysis of mature miRNA levels in *post-mortem* samples from the dentate nucleus of a small number of patients revealed a tendency for decreased miRNA

expression in MJD patient samples (Fig. 3.2A; mir-9 CTRL: 1.138 ± 0.306 vs mir-9 MJD: 0.736 ± 0.129; mir-181a CTRL: 1.118 ± 0.262 vs mir-181a MJD: 0.669 ± 0.116; mir-494 CTRL: 1.069 ± 0.181 vs mir-494 MJD: 0.816 ± 0.067). Although not statistically significant, these samples were obtained from patients with different age and disease progression stages, hence the observed high variability.

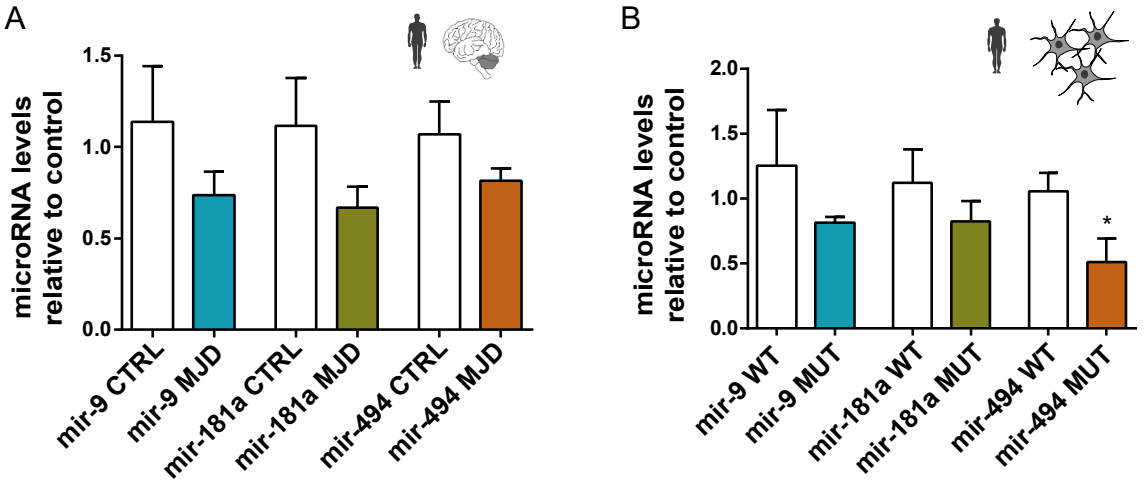

Figure 3.2 – MiRNA profiling in human brain samples and *in vitro* cell line. (A) MiRNA qPCR quantification of mir-9, mir-181a and mir-494 performed in *post-mortem* human samples from the dentate nuclei of control (CTRL) or MJD patients (MJD) (n=6/5) displaying a tendency for a general downregulation profile for all miRNAs. **(B)** MiRNA qPCR quantification of mir-9, mir-181a and mir-494 performed in RNA extracted from SH-SY5Y cells stably expressing wtATXN3 (WT) or mutATXN3 (MUT) (n=6). Mir-494 was found to be significantly reduced in SH-SY5Y stably expressing mutATXN3. QPCR analysis for miRNA was normalized with endogenous control (mir-103-3p). Statistical significance was evaluated with unpaired Student's t-test (*P < 0.05). Data are expressed as mean ± SEM.

To corroborate these results, we screened the same miRNA levels in an *in vitro* model of MJD. Total RNA was isolated from SH-SY5Y human neuroblastoma cells stably expressing either wild-type ataxin-3 (wtATXN3) with a 27 glutamines polyQ stretch or mutant ataxin-3 (mutATXN3). MiRNA levels were evaluated by qPCR and, as observed in the human brain samples, only a tendency for decreased mir-9 and mir-181a expression was observed in cells expressing mutATXN3 compared with wtATXN3 (Fig. 3.2B; mir-9 WT: 1.256 ± 0.427 vs mir-9 Mut: 0.812 ± 0.051; mir-181a WT: 1.122 ± 0.257 vs mir-181a Mut: 0.825 ± 0.158). However, the levels of mir-494 were significantly down-regulated in SH-SY5Y cells expressing mutATXN3 when compared to wtATXN3 (Fig. 3.2B; mir-494 WT: 1.056 ± 0.141 vs mir-494 Mut: 0.509 ± 0.183).

3.4.3 miRNA profiling in human neurospheres derived from hIPSCs

Although the dysregulation in the expression levels of mir-494, obtained on a SH-SY5Y genetically modified cell line, illustrates the value of this expanded CAG mutATXN3 *in vitro* model, it relies on non-endogenous ATXN3 overexpression, driven by an artificial promoter, outside the context of its native regulatory elements. In order to overcome these limitations, we took advantage of hIPSCs technology. hIPSCs generated from reprogramed fibroblasts isolated from MJD or CTRL patients were differentiated into neurospheres and successfully maintained under suspension culture conditions. Upon formation of large dense spheres, mechanical dissociation was effective for cell expansion and maintenance during multiple passages (Fig. 3.3A-B).

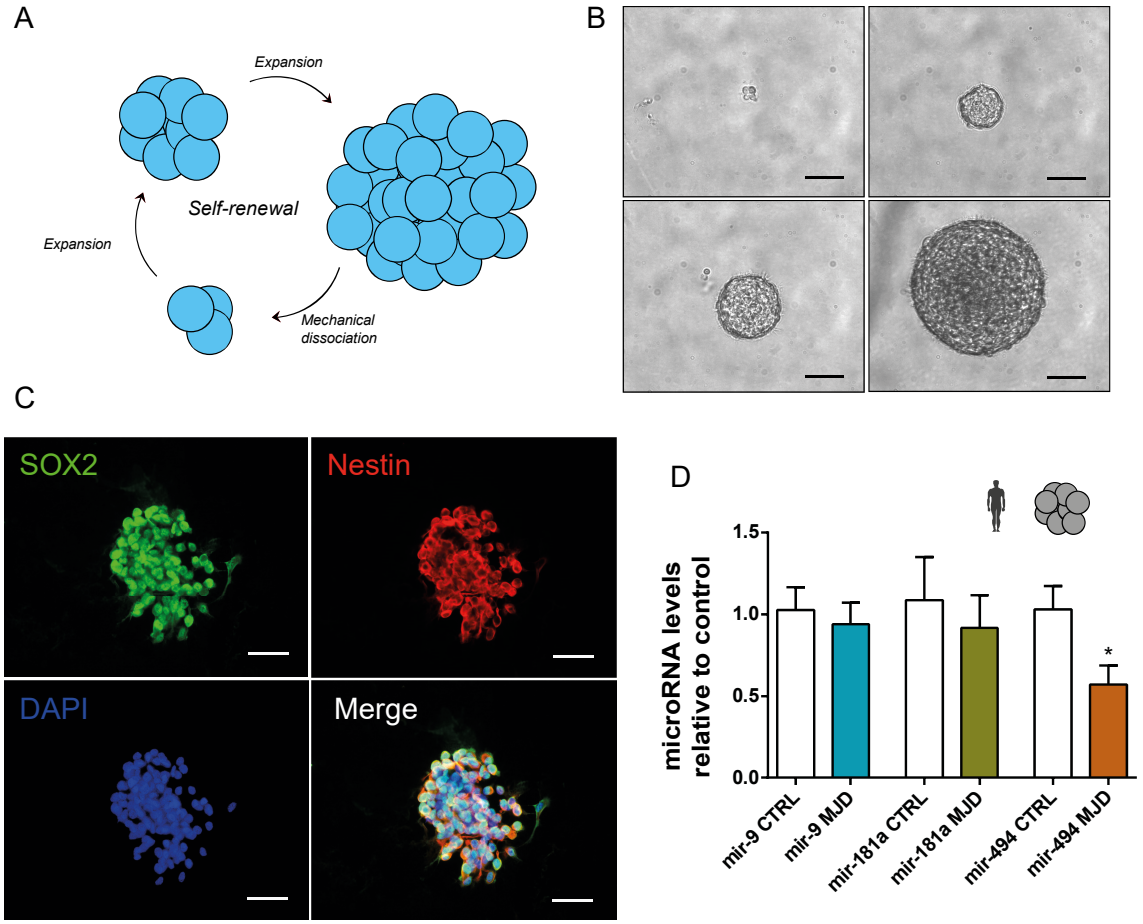

Figure 3.3 – MJD neurosphere system establishment and characterization. (A) Schematic representation of neurosphere expansion protocol. **(B)** Visible microscopy of human neurosphere at different growth stages. **(C)** Fluorescence immunocytochemistry of human neurospheres against SOX2 (green), Nestin (red) and nuclei (blue). **(D)** MiRNA qPCR quantification of mir-9,

mir-181a and mir-494 performed in human neurospheres (n=4/5). Mir-494 was found to be significantly reduced in MJD neurospheres. QPCR analysis for miRNA was normalized with endogenous control (U6). Statistical significance was evaluated with unpaired Student's t-test (*P<0.05). Data are expressed as mean ± SEM. Scale bars represent 100μm (B) and 50μm (C).

Neurospheres immunostained against pluripotency markers Nestin and SOX2 showed strong expression of these markers confirming the neural stem cell phenotype of the cultures (Fig. 3.3C).

After total RNA isolation of neurospheres from both MJD or CTRL patients, the levels of mir-9, mir-181a and mir-494 were evaluated by qPCR. MiRNA profiling revealed a significant downregulation in the levels of mir-494 (Fig. 3.3D; mir-494 CTRL: 1.028 ± 0.146 vs mir-494 MJD: 0.569 ± 0.118). However, again no significant differences were observed in the levels of mir-9 and mir-181a (Fig. 3.3D; mir-9 CTRL: 1.026 ± 0.139 vs mir-9 MJD: 0.938 ± 0.134; mir-181a CTRL: 1.085 ± 0.263 vs mir-181a MJD: 0.916 ± 0.200).

3.4.3 miRNA profiling in human neurons derived from hIPSCs

Even though the human neurosphere system provides important clues for the elucidation of pathological mechanisms at the neurodevelopmental stage, MJD is characterized as a late onset neurodegenerative disease. Therefore, we wanted to evaluate the miRNA profile in differentiated neurons, as this would be a model more relatable to the human condition. In order to do this, neurospheres from both CTRL and MJD patients were subjected to a monolayer differentiation protocol during 18 days in order to promote differentiation into mature neurons (Fig. 3.4A). Following 18 days of neurosphere differentiation, both cultures generated a high fraction of β-III tubulin positive neurons (Fig. 3.4B). Moreover, immunostaining for neuronal maturation markers revealed that the neuronal population was positive for MAP2 and NeuN indicating a good degree of neuronal maturation (Fig. 3.4C).

MiRNA profiling from these cells revealed a significant downregulation in the levels of mir-181a and mir-494 (Fig. 3.4D; mir-181a CTRL: 1.016 ± 0.086 vs mir-181a MJD: 0.705 ± 0.041; mir-494 CTRL: 1.022 ± 0.112 vs mir-494 MJD: 0.599 ± 0.077) whereas no significant differences were obtained for mir-9 (Fig. 3.4D; mir-9 CTRL: 1.057 ± 0.170 vs mir-9 MJD: 0.917 ± 0.198).

Altogether, this data suggests that miRNAs predicted to target mutATXN3 are in fact dysregulated in human *in vitro* MJD models. Moreover, while mir-494 was observed to be downregulated in all the *in vitro* models suggesting an earlier role in the development of the disease, mir-181a was only found to be significantly downregulated upon neuronal differentiation and maturation, linking its role to a more neuron specific neurodegenerative profile.

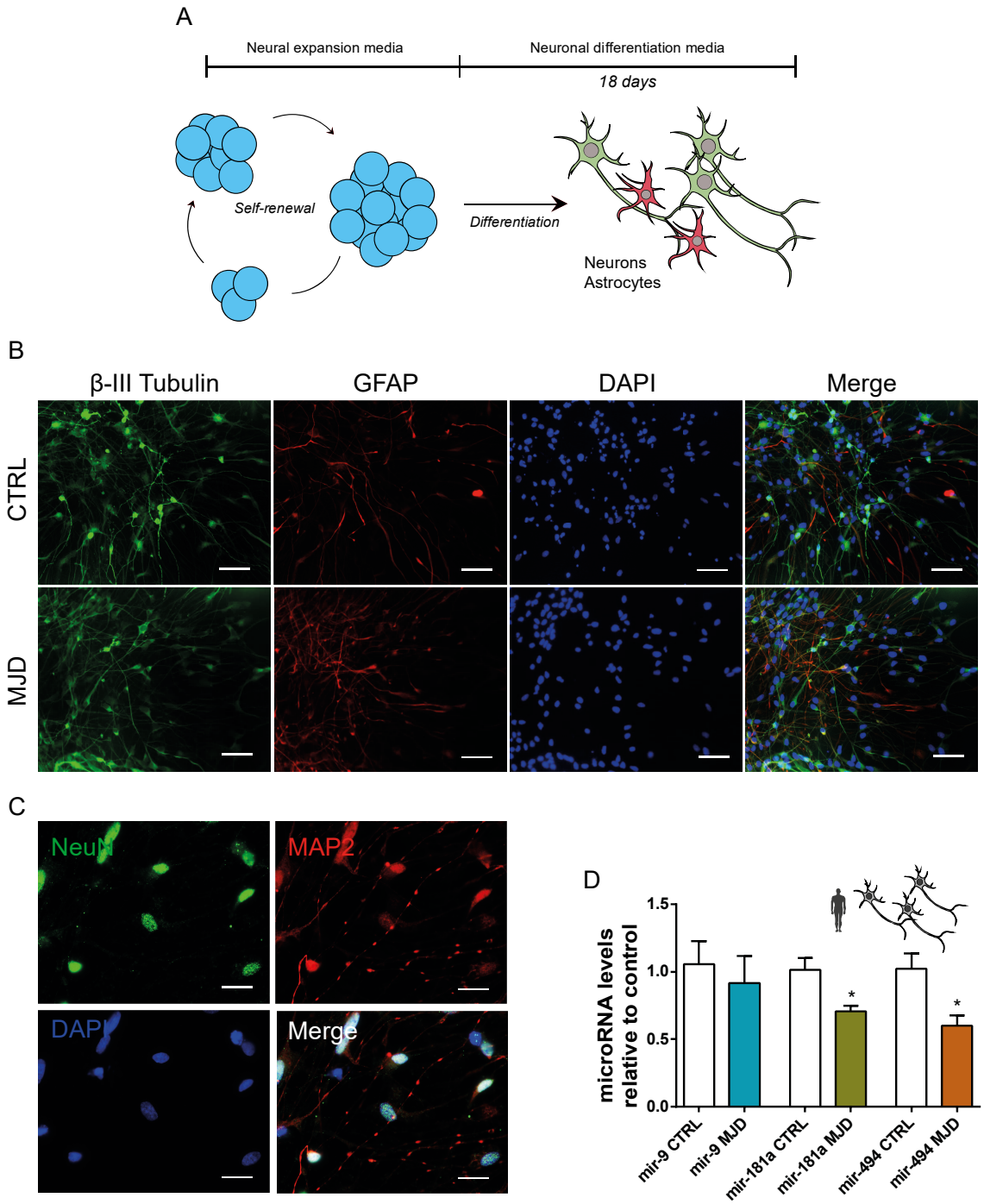

Figure 3.4 – Neuronal differentiation and miRNA profiling in neurons derived from hIPSCs. **(A)** Schematic representation of the neuronal differentiation protocol used in this study. **(B)** Immunocytochmistry against β-III tubulin (green), GFAP (red) and nuclei (blue). Both CTRL and

MJD cultures presented simillar diferentiation profiles. **(C)** Immunostaining against neuronal maturation markers: NeuN (green), MAP2 (red) and nuclei (blue). Neurons in culture were positive for NeuN and MAP2, indicating a good degree of maturation. **(D)** MiRNA qPCR quantification of mir-9, mir-181a and mir-494 performed in human neurons (n=4/5). Mir-181a and mir-494 were found to be significantly reduced in MJD neurons. QPCR analysis for miRNA was normalized with endogenous control (U6). Statistical significance was evaluated with unpaired Student's t-test (*P<0.05). Data are expressed as mean ± SEM. Scale bars represent 40μm (B) and 20μm (C).

3.4.4 Expression profiling of miRNAs and genes involved in miRNA biogenesis and function in MJD transgenic mice

In order to strengthen the results obtained in the miRNA profiling using human *in vitro* MJD models, we took advantage of a transgenic mouse model of MJD (Torashima *et al.*, 2008). This MJD mouse model is characterized by a robust phenotype with severe cerebellar atrophy. Therefore, this model can correlate to a late stage neurodegenerative profile observed in MJD patients where cerebellar degeneration and atrophy is characteristic. Interestingly, analysis of the miRNA profile in samples from transgenic MJD mice cerebella showed a significant decrease in the levels of all miRNAs (Fig. 3.5A: mir-9 WT: 1.051 ± 0.125 vs mir-9 TG: 0.4566 ± 0.042; mir-181a WT: 1.077 ± 0.150 vs mir-181a TG: 0.2345 ± 0.031; mir-494 WT: 1.039 ± 0.106 vs mir-494 TG: 0.3606 ± 0.044).

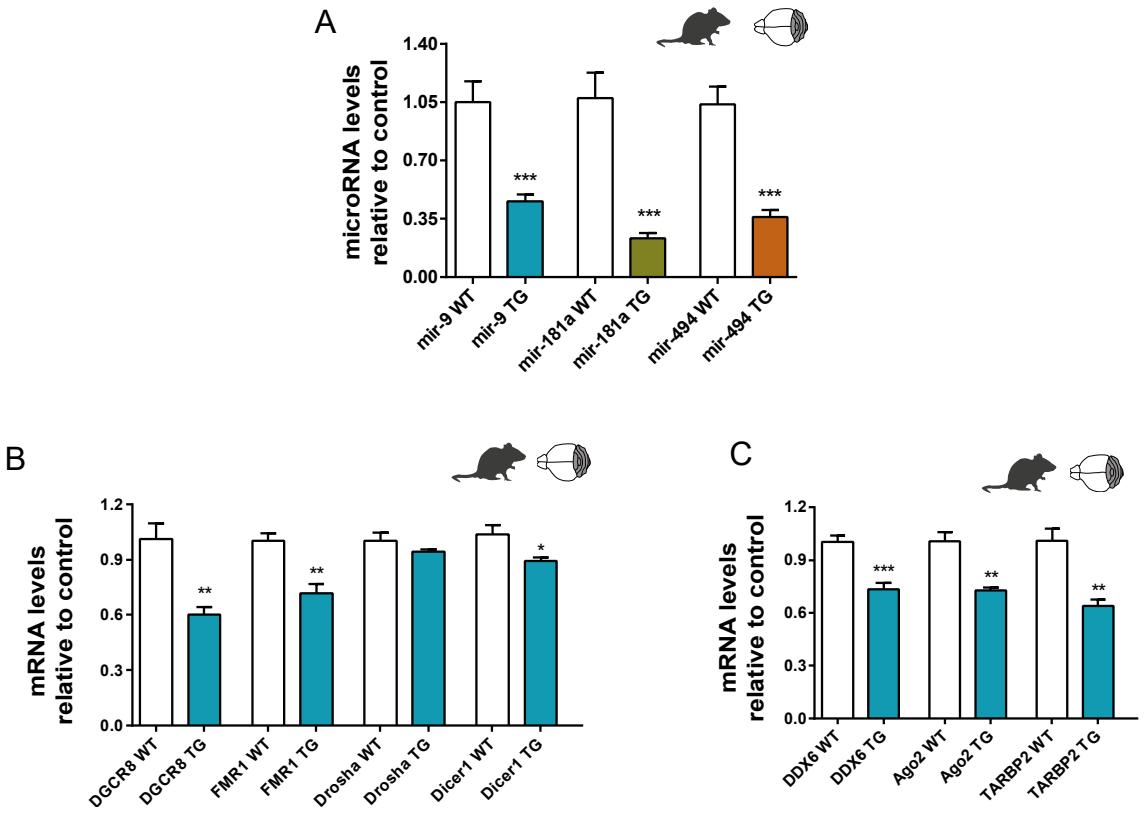

Figure 3.5 – Profiling of miRNAs and associated genes in MJD transgenic mice. (A) MiRNA qPCR quantification of mir-9, mir-181a and mir-494 performed in cerebellar tissue from MJD transgenic mice (TG) or littermate controls (WT) with 8 weeks of age (n=8/14). **(B-C)** Expression profiling of genes involved in the biogenesis and function of miRNAs (DGCR8, FMR1, Drosha, Dicer, DDX6, Ago2 and TARBP) in cerebellum samples from MJD transgenic mice (TG) or littermate controls (WT) with 8 weeks of age (n=5). A general downregulation profile for most of the evaluated genes was observed. QPCR analysis for miRNA was normalized with endogenous control (U6). QPCR analysis for mRNA was normalized with endogenous control (GAPDH). Statistical significance was evaluated with unpaired Student's t-test (*P<0.05, **P < 0.01, ***P < 0.001). Data are expressed as mean ± SEM.

Taken together, these results indicate a general downregulation profile for mir-9, mir-181a and mir-494 in human samples and in MJD *in vitro* and *in vivo* models.

Given the observed miRNA expression changes, we hypothesized that this dysregulation could be associated with an impairment in the expression of genes coding for components of the miRNA biogenesis pathway. Taking into account that the most significant changes in miRNA expression were the ones observed in transgenic MJD mice, we used this model to screen the levels of genes involved in miRNA biogenesis and function. qPCR analysis revealed a significant downregulation of genes implicated in miRNA biogenesis such as DGCR8, Dicer and FMR1 (Fig. 3.5B; DGCR8 WT: 1.013 ± 0.082 vs DGCR8 TG: 0.602 ± 0.040; Dicer WT: 1.037 ± 0.051 vs Dicer Tg: 0.891 ± 0.020; FMR1 WT: 1.003 ± 0.039 vs FMR1 TG: 0.716 ± 0.052) whereas no significant differences were observed for Drosha levels (Fig. 3.5B; Drosha WT: 1.004 ± 0.042 vs Drosha TG: 0.943 ± 0.013). Moreover, we also evaluated the expression levels of genes involved in miRNA silencing machinery and found a significant downregulation of mRNA levels for Ago2, TARBP2 and DDX6 (Fig. 3.5C; Ago2 WT: 1.006 ± 0.053 vs Ago2 TG: 0.727 ± 0.016; TARBP2 WT: 1.010 ± 0.067 vs TARBP2 TG: 0.637 ± 0.038; DDX6 WT: 1.003 ± 0.036 vs DDX6 TG: 0.735 ± 0.036).

All in all, these results suggest not only an impairment in the miRNA biogenesis pathway, which could be related with the observed miRNA dysregulation, but also an impairment in miRNA function, which might contribute for a disturbance in normal post-transcriptional regulatory events.

3.5 Discussion

In the present study, using both *in vitro* and *in vivo* MJD models, we show that miRNAs predicted to target the human ATXN3 3'UTR are dysregulated in MJD. Moreover, we present compelling evidence that implicates different genes involved in miRNA biogenesis and function, whose dysregulation may be contributing to the disruption of the endogenous miRNA profile and consequently to the disease pathogenesis.

After having demonstrated that miRNAs have a role on ATXN3 3'UTR regulation (Chapter 2), we wanted to pinpoint which specific miRNAs would be mediating this effect. To do this we started by performing a bioinformatic screening in order to identify a selection of candidate miRNAs which were predicted to target ATXN3 3'UTR. After narrowing the results list to three brain expressed miRNAs (mir-9, mir-181a and mir-494), we profiled the levels of these miRNAs in *post-mortem* human samples of MJD patients. Despite not obtaining significant results, this could have been due to the very limited sample number in combination with high variability in the disease progression levels of each patient. Nevertheless, a tendency for downregulation of all miRNAs was observed. Although recent studies have approached the topic of miRNA dysregulation in MJD, our study is the first to evaluate miRNA dysregulation in human samples isolated from the dentate nucleus, a region known to be highly degenerated in MJD patients, whereas other studies have focused only on human serum samples (Shi *et al.*, 2014).

In order to strengthen the human samples data, we decided to explore miRNA dysregulation in three *in vitro* human models. In the case of SH-SY5Y cells genetically modified to stably overexpress mutATXN3, mir-494 was the only miRNA observed to be downregulated. Similar results were obtained after screening the levels of mir-9, mir-181a and mir-494 in human neurospheres derived from hIPSCs, which did also present a significant downregulation for mir-494. Interestingly, after neuronal differentiation of human neurospheres into mature neurons, there was a change in miRNA levels of mir-181a, which turned to be significantly downregulated in MJD neurons, while mir-494 was maintained downregulated. These results suggest that while mir-494 downregulation is closely related to the polyQ expansion even outside a mature neuronal environment, implicating mir-494 in a neural developmental context, mir-181a expression is only disrupted in fully mature neurons linking its dysregulation closer to a progressive neurodegenerative scenario. Nevertheless, further studies accessing miRNA

dysregulation across multiple stages of neuronal development, maturation and degeneration in the context of MJD will be required to confirm this hypothesis.

Although miRNA profiling of neurons derived from hIPSCs has been performed in Frontotemporal dementia (FTD) patient cells, where mir-9 downregulation was observed in neurons carrying a TDP-43 mutation (Zhang *et al.*, 2013b), this study was the first to evaluate miRNA dysregulation in human neurons derived from MJD hIPSCs. We believe that our results represent on more contribution to the establishment of hIPSC technology as a model of neurodegenerative diseases, revealing specific defects of human patient neurons in their native genetic context.

To further investigate our data in an *in vivo* transgenic MJD model we profiled the levels of mir-9, mir-181a and mir-494 in the cerebellum of MJD transgenic mice. Interestingly we observed a very significant downregulation in the levels of all miRNAs. We believe this could be associated with the highly severe phenotype of these mice and correspondent marked cerebellar degeneration. Another study has previously evaluated the endogenous miRNA profile in a MJD transgenic model (Rodriguez-Lebron *et al.*, 2013a). At two months-old YAC ATXN3Q84 mice, the authors observed a downregulation of six different miRNAs (mir-101a, mir-146b, mir-324, mir-361, mir-365 and mir-674) and upregulation of four miRNAs (mir-15b, mir-181a, mir-342 and mir-467). However, at six months-old, only mir-181a was still upregulated in MJD mice. In contrast, our results support a downregulation of mir-181a in MJD. Nevertheless, unlike the severe phenotype of the transgenic mice used in our study, the YAC ATXN3Q84 mice is largely asymptomatic at both two and six months-old, hence justifying the differences in the observed results.

Besides targeting ATXN3 mRNA (as will be demonstrated in chapter 4), mir-9, mir-181a and mir-494 are involved in other cellular processes. Mir-9 is a highly conserved neuronal miRNA involved in the neuronal development and neuronal differentiation (Coolen *et al.*, 2013). Moreover, not only it is downregulated in HD and FTD, as mentioned before, but it is also dysregulated in other neurodegenerative diseases such as Alzheimer's, Parkinson's disease and Spinal Muscular Atrophy (Kim *et al.*, 2007; Cogswell *et al.*, 2008; Catapano *et al.*, 2016). Mir-181a, also highly enriched in the brain, has been involved in axon development, localizing strongly to growth cones of developing neurons (Sasaki *et al.*, 2014). Moreover, this miRNA has been suggested to play a role in Purkinje cell maintenance (Schaefer *et al.*, 2007). Finally, regarding mir-494, this miRNA has been observed to be dysregulated in the rat hippocampus following chronic lead exposure and in a macaque model of Creutzfeldt-Jakob disease (Montag *et*

al., 2009; An *et al.*, 2014). Taking this into account we believe that in the future, miRNA dysregulation and its impact on other targets should be further assessed.

In accordance with the observed miRNA profiling data, we observed a general downregulation in the expression of genes controlling the biogenesis and function of miRNAs. This is in line with a decrease in miRNA maturation and with the observed reduction in their levels. Moreover, an impairment in endogenous RNA interference (RNAi) mechanisms, might not only disturb the regulation of mutATXN3 but also other genes. Interestingly it has been previously reported that Dicer deficiency in Purkinje cells leads to cerebellar degeneration and the development of ataxia (Schaefer *et al.*, 2007). Moreover, in a transgenic mouse model of HD, it has been shown that the miRNA biogenesis machinery is also dysregulated (Lee *et al.*, 2011). Importantly, the changes in the levels of these genes could also be correlated with changes in miRNA expression. All in all, our data strongly suggests that the dysregulation of both miRNAs and miRNA biogenesis enzymes could be a novel pathogenic mechanism in the development of MJD. In any case, we believe individual modulation of key RNAi mediators should be performed in order to properly evaluate their role in MJD pathogenesis.

CHAPTER 4

MicroRNAs targeting Ataxin-3 - A gene therapy tool for Machado-Joseph disease

4.1 Abstract

Machado-Joseph disease (MJD) is a fatal, dominant neurodegenerative disorder. MJD is caused by a cytosine-adenine-guanine (CAG) repeat expansion in the *ATXN3* gene, conferring a toxic gain of function to the ataxin-3 (AXTN3) protein. Accordingly, one promising therapeutic approach for MJD is based on the usage of RNA interference (RNAi) in order to silence the expression of the mutant protein. In fact, promising studies have demonstrated the potential application of RNAi in multiple models of MJD. However, all of these studies were based in the usage of artificial sequences not taking advantage of the endogenous RNAi players such as microRNAs (miRNAs).

In this study we sought to exploit miRNA regulation of ATXN3 mRNA as a novel therapeutic approach for the treatment of MJD. This was achieved by employing our previously described lentiviral model together with a lentiviral system for efficient in vivo overexpression of miRNAs targeting ATXN3 3'UTR.

Our results show that the ATXN3 3'UTR is a direct target of mir-9, mir-181a and mir-494 and that overexpression of these miRNAs resulted in a decrease of mutATXN3 levels *in vitro*. Importantly, lentiviral mediated overexpression of each miRNA effectively reduced the levels of mutATXN3 and associated neuropathology *in vivo,* in a genetic mouse model of MJD.

In conclusion, gene therapy applications based on miRNA-mediated silencing of mutATXN3 may be a promising therapeutic approach for MJD.

4.2 Introduction

Machado-Joseph disease (MJD), also known as spinocerebellar ataxia type 3 (SCA3), is a neurodegenerative disease caused by a cytosine-adenine-guanine (CAG) trinucleotide expansion in the *ATXN3* gene (Takiyama *et al.*, 1993; Kawaguchi *et al.*, 1994). This expansion leads to the expression of a mutant ataxin-3 (mutATXN3) protein with an overlong polyglutamine (polyQ) tract. Currently, MJD is a fatal disorder without any disease-modifying treatments available. Despite the current progress in understanding the pathogenesis of MJD, there is no available treatment to cure or delay the progression of the disease.

Taking into account the toxic gain-of-function acquired by ATXN3 upon the CAG expansion, this disease comes to light as one disorder that could benefit from the application of a gene silencing strategy. In fact, promising results were observed in animal models of MJD upon *in vivo* genetic silencing of mutATXN3. Our group has previously demonstrated that the delivery of lentiviral encoded short-hairpin RNAs (shRNAs) specifically targeting mutATXN3 was capable of decreasing the levels of the mutant protein and associated neuropathology in both lentiviral and transgenic mouse models of MJD (Alves *et al.*, 2008a; Nobrega *et al.*, 2013b; Nobrega *et al.*, 2014). Interestingly, in another study, our group has demonstrated that non-allele specific silencing of mutATXN3 was also very effective and well tolerated (Alves *et al.*, 2010). More recently, and taking advantage of targeted stable nucleic acids lipoparticles encapsulating siRNAs against mutATXN3 mRNA, our group has successfully implemented a non-viral strategy which could efficiently reduce the levels of mutATXN3 and associated neuropathology in both lentiviral and transgenic MJD mouse models (Conceição *et al.*, 2015).

Nonetheless, expression of conventional shRNAs in the brain has been associated with toxicity problems, particularly when under control of strong promoters (McBride *et al.*, 2008; Boudreau *et al.*, 2009; Martin *et al.*, 2011). In order to overcome this limitation, the authors developed an artificial microRNA (miRNA) molecule which would include designed silencing sequences inside a miRNA backbone. When compared to shRNAs, artificial miRNAs induced a much reduced neurotoxicity without compromising silencing efficacy (McBride *et al.*, 2008). Taking advantage of this technology, an artificial miRNA-based silencing strategy of mutATXN3 has already been recently employed (Costa Mdo *et al.*, 2013; Rodriguez-Lebron *et al.*, 2013a). The authors observed efficient silencing of mutATXN3 in transgenic MJD mice. However, this

strategy was not effective enough to rescue the behavioral phenotype of these mice. Even so, the authors proposed that the delivery of the silencing sequences at an earlier time point or into a larger extent of the brain might improve the already encouraging results (Costa Mdo *et al.*, 2013).

Although artificial molecules such as siRNAs, shRNAs, artificial miRNAs and antisense oligonucleotides have been the mostly studied tools for gene therapy applications, endogenous miRNAs also offer the potential for silencing mutated genes. MiRNAs, a class of small RNAs discovered in 1993, have since gained momentum and became one of the largest group of molecules studied in gene regulatory events (Lee *et al.*, 1993; He and Hannon, 2004). Due to their gene silencing capabilities and advantages when compared to other molecules such as shRNAs, they are now being tested as a tool for the treatment of neurodegenerative diseases for instance the polyglutamine (polyQ) diseases.

In fact, many polyQ proteins have been described to be the direct target of miRNAs. Ataxin-1 was the first described polyQ protein to be regulated by miRNAs (Lee *et al.*, 2008). Lee and colleagues demonstrated that ATXN1 3'UTR was the target of at least three different miRNAs (mir-19, mir-101 and mir-130). Despite showing that overexpression of these miRNAs led to a decrease in the levels of mutATXN1 and to an improvement of cell viability, no further *in vivo* studies were performed to evaluate the therapeutic potential of these miRNAs in the context of spinocerebellar ataxia type 1 (SCA1). More recently it was demonstrated that the androgen receptor (AR) mRNA, which when containing an expanded polyQ tract is responsible for the development of spinal and bulbar muscular atrophy (SBMA), is also a target of mir-298 (Pourshafie *et al.*, 2016). Moreover, the authors took advantage of mir-298 AR regulation to develop a gene therapy approach for SBMA. Upon AAV mediated overexpression of mir-298, transgenic SBMA mice showed improvements in their disease phenotype.

Moreover, in recent *in vitro* studies, miRNAs were shown to directly target ATXN3 mRNA. Huang and colleagues were the first to identify mir-25 as a regulator of human ATXN3 through interaction with its 3'UTR. Upon *in vitro* overexpression, mir-25 was capable of reducing mutATXN3 levels and improve cell viability (Huang *et al.*, 2014). In another study, mir-181a was also identified to target ATXN3 mRNA, nevertheless this study was limited to target validation (Koscianska and Krzyzosiak, 2014).

In this study, we exploit ATNX3 miRNA based regulation in MJD, assessing the therapeutic potential of *in vivo* delivery of endogenous miRNAs in a lentiviral mouse model of MJD. We prove that the miRNAs predicted in chapter 3 can be used to reduce

mutATXN3 levels. Moreover, we demonstrate that reinstating the levels of miRNAs targeting the 3'UTR of ATXN3 allows robust improvements in MJD neuropathology *in vivo*.

4.3 Materials and methods

4.3.1 Vector construction

Human ATXN3 3'UTR (1-3,434bp) was obtained by restriction digestion of the dual luciferase vector clone HmiT054676a-MT01 (Genecopoeia) using EcoRI and XhoI enzymes (New England Biolabs). The insert was gel purified using a DNA gel extraction kit (Macherey-Nagel), blunted using Klenow Polymerase (New England Biolabs), and later inserted into the previously described LTR-SIN-PGK-mutATXN3-LTR vector (Alves *et al.*, 2008b) using a SmaI site downstream of the mutATXN3 CDS in order to generate the LTR-SIN-PGK-mutATXN3-3'UTR-LTR vector (Fig. 2.1).

For the construction of plasmids encoding for mir-9, mir-181a and mir-494 based on CMV driven expression of a fused GFP-miRNA transcript a series of oligonucleotides were designed (Table 4.1). Top and bottom oligonucleotides were annealed and cloned into pcDNA6.2-GW/ EmGFP-miR backbone using T4 DNA ligase (Life Technologies) and transformed into TOP10 competent cells (Life Technologies). pcDNA6.2-GW/miR-neg vector (Life Technologies) was used as negative control.

Table 4.1 – Oligonucleotide sequences used for miRNA oligonucleotide based cloning

Oligonucleotide	Sequence
Mir-9 TOP	TGCT GA TCTT TGGT TATC TAGC TGTA TGA GTTT TGGC CACT GACT GAC TCAT AAAG CTAG ATAA CCGA AAGT
Mir-9 BOT	CCTG ACTT TCGG TTAT CTAG CTTT ATGA GTC AGTC AGTG GCCA AAAC TCA TACA GCTA GATA ACCA AAGA TC
Mir-181a TOP	TGCT GG AACA TTCA ACGC TGTC GGTG AGT GTTT TGGC CACT GACT GAC ACCA CTGA CCGT TGAC TGTA CC
Mir-181a BOT	CCTG GG TACA GTCA ACGG TCAG TGGT GTC AGTC AGTG GCCA AAAC ACT CACC GACA GCGT TGAA TGTT CC
Mir-494 TOP	TGCT GGAG GTTG TCCG TGTT GTCT TC GTTT TGGC CACT GACT GAC TGAA ACAT ACAC GGGA AACC TC
Mir-494 BOT	CCTG GA GGTT TCCC GTGT ATGT TTCA GTC AGTC AGTG GCCA AAAC GA AGAC AACA CGGA CAAC CTCC

For the construction of the lentiviral plasmids encoding for endogenous precursor miRNAs (pre-miRNAs), a series of oligonucleotides (Life Technologies) was designed in order to amplify the corresponding genomic region encoding for the pre-miRNAs, plus the endogenous flanking sequences in the total range of approximately 400bp (Table 4.2). Amplified inserts were then digested with BglII and HindIII enzymes (New England BioLabs) and ligated into pENTR/pSUPER+ (Addgene plasmid # 17338) using T4 DNA ligase (Life Technologies). The H1-miRNA expression cassettes were then transferred into LTR-SIN-PGK-GFP-AttL1-ccdB-AttL2-LTR destination vector using a Gateway LR recombination reaction (Life Technologies), in order to generate LTR-SIN-PGK-GFP-H1-miRNA-LTR plasmids. The mir-Neg lentiviral vector was generated through PCR amplification of the mir-Neg cassette plus flanking sequences from the pcDNA6.2-GW/miR-neg vector (Life Technologies), ligated into pENTR/pSUPER+ and gateway recombined, as previously described, in order to generate LTR-SIN-PGK-GFP-H1-mir-Neg-LTR.

Table 4.2 – Oligonucleotide sequences used for PCR based pre-miRNA cloning

miRNA		Primer Sequence (BglII/HindIII)	Amplicon size
hsa-mir-9	**Forward**	GTGAT AGATCT GAAATGTCGCCCGAACCAGT	399
	Reverse	GTGAT AAGCTT TTGTTGTTTTGTCTCGGACTTCA	
hsa-mir-181a	**Forward**	TGATCAGATCTACTGCACAGTCTATCCCACAGTT	400
	Reverse	TGATCAAGCTTAGGAACAGTGAGCAGTAGGAATAA	
hsa-mir-494	**Forward**	GTGAT AGATCT GACACGCAAATAGAAGCCATCTG	350
	Reverse	GTGAT AAGCTT GCCACACCCCCACGAC	
mir-neg	**Forward**	GTGAT AGATCT CTGGAGGCTTGCTGAAGGCT	132
	Reverse	GTGAT AAGCTT GGCCATTTGTTCCATGTGAG	

4.3.2 Cell culture, transfection, and transduction

HEK293T were maintained in standard DMEM (Sigma) supplemented with 10% fetal bovine serum (Life Technologies) and 1% Penicillin/Streptomycin (Life Technologies).

For the transfection of HEK293T cell line, 2.75X104 cells were initially plated on 12-well cell culture treated multiwell plates (Fisher Scientific). After 24 hours, medium was changed and cells were transfected with a mixture of DNA/ polethyleneimine (PEI) complexes (MW40000, PolySciences) diluted in complete DMEM. Complex formation was performed by combining 750ng of plasmid DNA in 60µl of serum free DMEM and 4.5µl of PEI (1mg/ml) per well. This mixture was vortexed for 10 seconds and incubated at room temperature for 10 minutes. After that, DNA/PEI complexes were diluted in complete DMEM and added to cell culture. Cell collection was performed 48 hours post-transfection.

4.3.3 Dual luciferase assay

A dual luciferase reporter construct including the 3'UTR of ATXN3 (FLuc-3'UTR) and a control vector (FLuc-CTRL) clone pEZX-MT01 were purchased from GeneCopoeia. To evaluate the direct targeting of miRNAs to ATXN3 3'UTR, 2.75X104 HEK293T cells were seeded per well in 12-well plates (Fisher Scientific). In the next day, cells were transfected with 375ng of the luciferase reporter vector and 375ng of miRNA constructs per well (in triplicates). Forty-eight hours after transfection, cells were washed with 1x Phosphate-buffered saline (PBS) and frozen at -80ºC. Collected cells were lysed with 100 µl of Firefly luciferase assay reagent – 0.1 %Triton (FLAR-T) buffer per well containing 20mM tricine, 100 µM Ethylenediamine tetraacetic acid (EDTA), 25 µM MgCl2, 2.67 mM MgSO4, 17 mM ditiotreitol (DTT) and 0.1% Triton in milli-Q grade water pH 7.8. For the luminescent reaction, 30 µl of cell lysates were loaded on an opaque 96well plate (Corning) and the firefly luminescence activity was measured on a LMax II 384 Luminometer (Molecular Devices) after automatic injection of 100 µl of FLAR buffer containing 20mM tricine, 100 µM EDTA, 25 µM MgCl2, 2.67 mM MgSO4, 17 mM DTT, 250 µM Adenosine triphosphate (ATP) and 250 µM D-luciferin (Synchem). Renilla luminescence activity was used as a normalization control and was measured after automatic injection of 100 µl of renilla assay buffer (RAB) buffer containing 1.1 M NaCl, 2.2 mM Na2EDTA, 0.22 M KxPO4, 0.44 mg/ml bovine serum albumin (BSA), 1.3 mM NaN3, and 1.43 mM coelenterazine (Life Technologies) in milli-Q grade water pH 5.0 to 30 µl of cell lysate per microplate well. Integration times were 10 seconds for firefly luciferase signal capture and 5 seconds for renilla luciferase signal capture. Unless stated, all reagents were purchased from Sigma-Aldrich.

4.3.4 Lentivirus production, purification, and titer assessment

Lentiviral vectors encoding for human mutATXN3, mutATXN3-3'UTR or miRNAs (mir-9, mir-181a, mir-494 and mir-Neg) were produced in HEK293T cells with a four-plasmid system, as previously described (de Almeida *et al.*, 2002). The lentiviral particles were resuspended in 1% bovine serum albumin in PBS. The viral particle content of batches was determined by assessing HIV-1 p24 antigen levels (Retro Tek, Gentaur). Viral stocks were stored at -80ºC.

4.3.5 Animals

Four-week-old C57BL/6J mice were obtained from Charles River. The animals were housed in a temperature-controlled room maintained on a 12 h light/12 h dark cycle. Food and water were provided ad libitum. The experiments were carried out in accordance with the European Union Directive 2010/63/EU covering the protection of animals used for scientific purposes. The researchers received adequate training (FELASA certified course) and certification to perform the experiments from Portuguese authorities (Direção Geral de Veterinária).

4.3.6 Mouse surgery

Five-week-old C57BL/6J mice were anesthetized by intraperitoneal administration of avertin (14 µL/g, 250 mg/Kg). Mice were injected into the striatum in the following coordinates calculated from bregma: anteroposterior: +0.6 mm; lateral: ±1.8 mm; ventral: -3.3 mm; tooth bar: 0, by receiving a single injection of concentrated lentiviral vectors in a final volume of 2 µL containing 400ng of p24 antigen for each vector encoding for the specific transgenes, at an infusion rate of 0.25 µl/min using a 10-µl Hamilton syringe. Five minutes after the infusion was completed the needle was retracted 0.3 mm and allowed to remain in place for an additional 3 minutes prior to its complete removal from the mouse brain.

4.3.7 Immunohistochemical analysis

4.3.7.1 Tissue preparation

Mice were sacrificed with an overdose of avertin (35 µl/g, 625 mg/kg, intraperitoneally), transcardially perfused with PBS and fixed with 4% paraformaldehyde (PFA). Brains were collected and post-fixed in 4% PFA for 24 hours, cryoprotected by incubation in 25% sucrose/PBS and frozen at -80ºC. Coronal sections of 25 µm thickness were obtained using a cryostat equipment (LEICA CM3050S, Leica Microsystems).

4.3.7.2 Bright-field Immunohistochemistry

Free-floating brain coronal sections were treated with a 0.1% phenylhidrazyne/PBS solution for the blockage of endogenous peroxidases for 30 minutes at 37ºC. After permeabilization in PBS/0.1% Triton X-100 with 10% normal goat serum (Gibco), sections were incubated overnight at 4ºC in blocking solution with primary antibodies: mouse monoclonal anti-ataxin 3 antibody (1H9; 1:5000; Merck Millipore), rabbit anti-dopamine and cyclic AMP-regulated neuronal phosphoprotein 32 (DARPP-32) antibody (1:1000; Merck Millipore); followed by incubation with respective biotinylated secondary goat anti-mouse or anti-rabbit antibodies (1:200; Vector Laboratoires). Bound antibodies were visualized using the VECTASTAIN® ABC kit, with 3',3'-diaminobenzidine tetrahydrocloride (DAB metal concentrate; Pierce) as substrate. Dry sections were mounted in gelatin-coated slides, dehydrated with ethanol solutions and Xylene Substitute (Sigma-Aldrich) and mounted in Eukit quick-hardening mounting medium (Sigma-Aldrich). Staining was visualized with Zeiss Axioskop 2 imaging microscope (Carl Zeiss MicroImaging) equipped with AxioCam HR color digital cameras (Carl Zeiss Microimaging) and Plan-Neofluar 5x/0.15 Ph 1 (440321), Plan-Neofluar 20x/0.50 Ph 2 (1004-989), Plan-Neofluar 40x/0.75 Ph 2 (440351) and Plan-Neofluar 63x/1.25 Oil (440460-0000) objectives using the AxioVision 4.7 software package (Carl Zeiss Microimaging).

4.3.8 Isolation of total RNA from cells and mouse tissue

Total RNA was isolated with miRCURY RNA isolation kit (Exiqon) according to manufacturer's instructions. Monolayer cell cultures were washed with PBS and stored at -80ºC before extraction. For the extraction from mouse tissue, mice were sacrificed with a lethal dose of avertin. Striatum of mice was dissected and stored at -80ºC until RNA isolation. All samples were submitted to on-column DNAse I digestion (QIAGEN) during isolation. Total amount of RNA was quantified by optical density (OD) using a Nanodrop 2000 Spectrophotometer (Thermo Scientific) and RNA was stored at -80ºC.

4.3.9 cDNA synthesis and quantitative real time polymerase-chain reaction

Specific complementary DNAs (cDNAs) for miRNA quantification were synthetized using a TaqMan MicroRNA Reverse Transcription Kit combined with specific TaqMan MicroRNA Assays (Applied Biosystems) for each miRNA (mir-9-5p ID000583; mir-181a-5p ID000480; mir-494-3p ID002365; U6 snRNA ID001973; snoRNA202 ID001232) according to manufacturer's instructions. qPCR was performed using TaqMan® Universal PCR Master Mix II with UNG (Applied Biosystems), combined with the previously described TaqMan MicroRNA Assays, following manufacturer's recommended conditions, in a StepOne Plus Real-Time System (Applied Biosystems).

cDNA for mRNA quantification was obtained by conversion of total RNA with iScript cDNA Synthesis kit (Bio-Rad) according to manufacturer's. qPCR was performed in the StepOne Plus Real-Time PCR System (Applied Biosystems) and SsoAdvanced SYBR Green Supermix (Bio-Rad). Primers for human ACTB and mouse ATXN3 genes were pre-designed and validated by QIAGEN (QuantiTect Primers, QIAGEN). Primers for 18S (Forward: CTCAACACGGGAAACCTCAC; Reverse: CGCTCCACCAACTAAGAACG) and human ATXN3-3'UTR (Forward: ACAGCATAGGGTCCACTTTGG; Reverse: CAACCGACGCATTGTTCCAC) were designed using PrimerBlast Software. Appropriate negative controls were also prepared. All reactions were performed in duplicate and using the following cycling conditions: 95ºC for 30 sec, followed by 45 cycles at 95ºC for 5 sec and 58ºC for 30 sec. The amplification rate for each target was evaluated from the cycle threshold (Ct) numbers obtained with cDNA dilutions. Differences between control and experimental samples were calculated using the $2^{-\Delta\Delta Ct}$ method.

4.3.10 Protein extraction and western blotting

Monolayer cells were scraped in radioimmunoprecipitation lysis buffer (50mM Tris HCl, pH 8, 150mM NaCl, 1% NP-40, 0.5% sodium deoxycholate, 0.1% sodium dodecyl sulphate) containing protease inhibitors (Roche) followed by sonication by 2 series of 4s pulses. Protein lysates were stored at -20ºC and protein concentration was determined with Bio-Rad Protein Assay. Protein samples were denatured with 6x sample buffer (0.375M Tris pH 6.8 (Sigma-Aldrich), 12% SDS (Sigma-Aldrich), 60% glycerol (Sigma-Aldrich), 0.6M DTT (Sigma-Aldrich), 0.06% bromophenol blue (Sigma-Aldrich)) and 40 µg were resolved by electrophoresis on 12% SDS-PAGE and transferred onto polyvinylidene fluoride (PVDF) membranes (GE Healthcare). Membranes were blocked by incubation in 5% non-fat milk powder in 0.1% Tween 20 in Tris buffered saline (TBS-T), and incubated overnight at 4°C with primary antibody: mouse monoclonal anti-ATXN3 (antibody (1H9; 1:5000; Merck Millipore); mouse monoclonal antibody anti-myc tag (4A6; 1:1000; Merck Millipore) and mouse anti-β-actin antibody (AC74; 1:10.000; Sigma-Aldrich), followed by the incubation with alkaline phosphatase-linked secondary goat anti-mouse antibody (1:10.000; Thermo Scientific Pierce). Bands were visualized with Enhanced Chemifluorescence substrate (ECF) (GE Healthcare) and chemifluorescence imaging (Chemidoc Imaging System, Bio-Rad). Semi-quantitative analysis was carried out based on the optical density of scanned membranes (ImageLab version 5.2.1; Bio-Rad). The specific optical density was then normalized with respect to the amount of β-actin loaded in the corresponding lane of the same gel.

4.4 Results

4.4.1 Development of an efficient system for miRNA overexpression *in vitro* and *in vivo*

In order to evaluate whether mir-9, mir-181a and mir-494 regulate ATXN3 expression, we first developed a lentiviral vector system for the overexpression of these candidate miRNAs *in vitro.* The first strategy employed was based on the construction of a vector system encoding for CMV driven expression of a single transcript including GFP and each interest miRNA. This system takes advantage of an artificial hairpin structure with a mir-155 backbone modified to include the mature sequences of our interest miRNAs (Fig. 4.1A). However, transfection of these vectors into HEK293T cells could only generate strong miRNA overexpression for mir-9 (Fig. 4.1B; mir-neg: 1.034 ± 0.263 vs mir-9: 54.59 ± 39.63) whereas it was either low for mir-494 (Fig. 4.1B; mir-neg: 1.074 ± 0.391 vs mir-494: 7.436 ± 3.324) or non-existent for mir-181a (Fig. 4.1B; mir-neg: 1.519 ± 1.144 vs mir-181a: 1.800 ± 0.654).

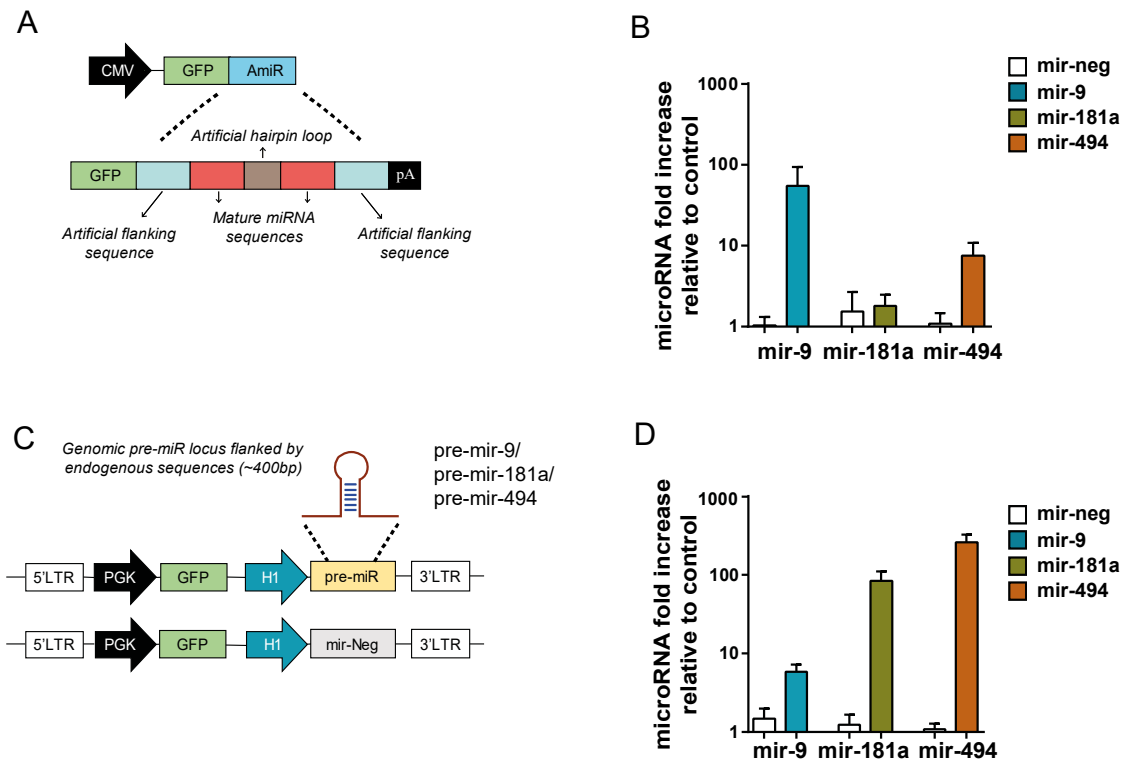

Figure 4.1 – Design and validation of a miRNA overexpression system. (A) Schematic representation of a miRNA overexpression system based on CMV driven expression of a fused

transcript encoding for GFP and an artificial miRNA composed of the 5p and 3p mature miRNA sequences flanked by artificial sequences and including an artificial loop based on the sequence of mir-155. **(B)** MiRNA overexpression in HEK293T cells transfected with an artificial miRNA expression system revealing inconsistent overexpression among mir-9, mir-181a and mir-494 (n=2). **(C)** Schematic representation of a miRNA overexpression system based on H1 mediated expression of endogenous miRNA sequences. **(D)** MiRNA overexpression in HEK293T cells transfected with plasmid DNA encoding for endogenous miRNA sequences revealing higher consistency in the overexpression of mir-9, mir-181a and mir-494 when compared to mir-neg (n=6). QPCR analysis for miRNA was normalized with endogenous control (snoRNA202 and U6). Data are expressed as mean ± SEM.

In order to improve the previously described miRNA overexpression system, we developed a new system based on PCR cloning of the human genomic locus encoding for pre-miRNAs. In order to ensure proper processing of the endogenous hairpin, the genomic sequences flanking the pre-miRNA were also included in a total transcript size up to 400bp. Furthermore, taking into account that miRNAs do not require their expression to be driven by RNA Pol II promoters, we cloned our interest miRNAs downstream of a RNA Pol III promoter (H1) in order to drive stronger miRNA expression (Maczuga *et al.*, 2012). GFP expression was maintained through an independent expression cassette under the control of PGK promoter (Fig. 4.1C). After transfection of these miRNA-encoding vectors in HEK293T cells, we could successfully validate a modest overexpression for mir-9 (Fig. 4.1D; mir-neg: 1.478 ± 0.504 vs mir-9: 5.855 ± 1.359) and very high overexpression for mir-181a (Fig. 4.1D; mir-neg: 1.245 ± 0.414 vs mir-181a: 84.64 ± 26.32) and mir-494 (Fig 4.1D: mir-neg: 1.087 ± 0.189 vs mir-494: 258.7 ± 69.56).

4.4.2 Overexpression of mir-9, mir-181a or mir-494 leads to a reduction in the levels of mutATXN3

QPCR analysis of mutATXN3 mRNA levels showed a significant downregulation in mutATXN3 expression for both mir-181a and mir-494 transfected cells when compared to mir-neg (Fig. 4.2A; mir-neg: 1.001 ± 0.018 vs mir-181a: 0.626 ± 0.051 vs mir-494: 0.701 ± 0.023). However, no difference was observed in cells co-transfected with mutATXN3 and mir-9 when compared to control. Analysis of mutATXN3 at the protein level revealed similar results, but with a significant downregulation of mutATXN3 protein levels for all miRNAs including mir-9 (Fig. 4.2B-C; mir-neg: 1.000 ± 0.005 vs mir-9: 0.674 ± 0.041 vs mir-181a: 0.741 ± 0.092 vs mir-494: 0.569 ± 0.008).

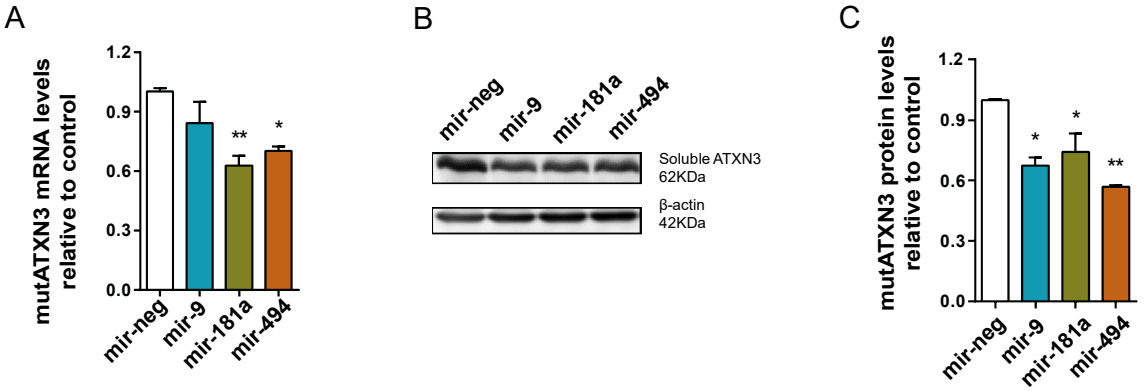

Figure 4.2 – Overexpression of mir-9, mir-181a and mir-494 leads to a reduction in human mutATXN3 levels. (A) MutAtxn3 mRNA levels in HEK293T co-transfected with miRNA constructs and mutATXN3-3'UTR (n=4). Mir-181a and mir-494 significantly reduced mutATXN3 mRNA levels. **(B-C)** Western blot analysis of HEK293T cells transfected with mutATXN3-3'UTR and different miRNA constructs. Optical densitometry analysis of mutATXN3 protein levels normalized with actin. Results are expressed as ratio ATXN3/actin relative to mir-neg control (n=3). All miRNAs significantly reduced mutATXN3 protein levels. QPCR analysis for mRNA was normalized with endogenous control (ACTB). Statistical significance was evaluated with One-way ANOVA (*P < 0.05, **P < 0.01). Data are expressed as mean ± SEM.

These results suggest that, *in vitro*, mir-181a and mir-494 downregulate mutATXN3 expression either by inducing the degradation of its mRNA or by inhibiting its translation, while mir-9 acts mostly through translational inhibition.

4.4.3 ATXN3 3'UTR is the direct target of mir-9, mir-181a and mir-494

Nevertheless, it is known that miRNAs can modulate the expression of multiple genes at the same time. Therefore, a dual luciferase assay was performed to confirm that mir-9, mir-181a and mir-494 directly bind to ATXN3 3'UTR in order to downregulate its expression. All candidate miRNAs significantly reduced luciferase activity when co-transfected with a vector encoding for a luciferase gene bound to ATXN3 3'UTR (Fig. 4.3A; Luc-3'UTR: mir-neg: 104.0 ± 2.400 vs mir-9: 80.00 ± 4.864, mir-181a: 83.56 ± 2.245 and mir-494: 79.98 ± 2.137) but not when a control vector was used (Fig. 4.3A; Luc-CTRL: mir-neg: 97.908 ± 4.121 vs mir-9: 97.447 ± 4.437, mir-181a: 123.055 ± 3.733 and mir-494: 103.670 ± 1.040.

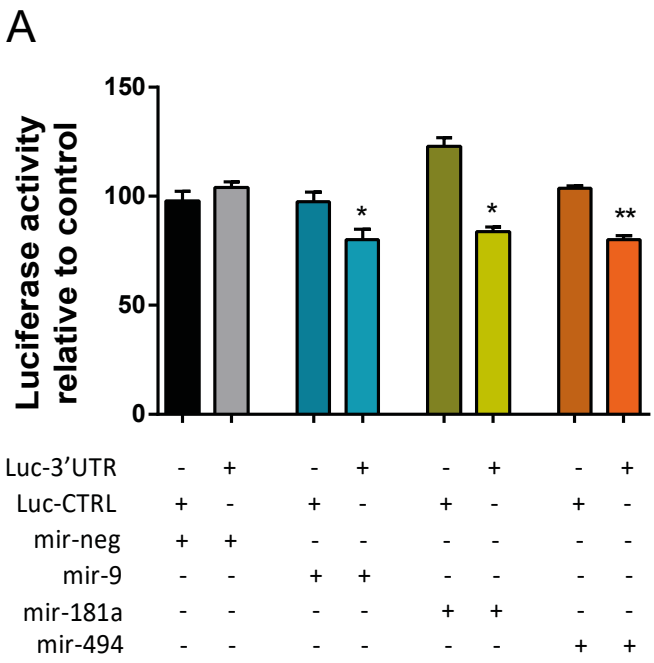

Figure 4.3 – Direct interaction of mir-9, mir-181a and mir-494 with ATXN3 3'UTR. (A) Validation of direct interaction between miRNAs and ATXN3 3'UTR using a dual luciferase assay. Luminescence activity from HEK293T cells co-transfected with a dual luciferase construct containing ATXN3 3'UTR or a control luciferase vector and miRNA / mir-neg encoding constructs. Results are expressed as a ratio of Firefly luminescence / Renilla luminescence (FL/RL) relative to control (LucCTRL) (n=4). All miRNAs specifically reduced Luc-3'UTR activity. Statistical significance was evaluated with One-way ANOVA comparing all miRNAs to mir-neg in the Luc-3'UTR condition (*P < 0.05, **P < 0.01). Data are expressed as mean ± SEM.

Altogether, these results indicate that ATXN3 3'UTR is a validated target of mir-9, mir-181a and mir-494. Although it's likely that other miRNAs might be involved in ATXN3 mRNA regulation, genetic modulation of these particular miRNAs can be seen as a potential tool for the manipulation of mutATXN3 levels in the disease.

4.4.4 *In vivo* overexpression of mir-9, mir-181a and mir-494 in a lentiviral mouse model of MJD reduces the levels of mutATXN3

In order to evaluate the therapeutic potential of mir-9, mir-181a and mir-494 *in vivo,* we stereotaxically co-injected lentiviral vectors encoding for mutATXN3-3'UTR with either mir-neg or each miRNA in the striatum of five-week-old mice (Fig. 4.4A). Lentiviral vectors encoding for the miRNAs of interest and EGFP, efficiently transduced a large area of the striatum (Fig. 4.4B). Analysis of miRNA expression levels from transduced striatum tissue shows effective overexpression of all miRNAs, although at different

magnitudes, probably due to differences in pre-miRNA processing efficiencies and in the endogenous levels of each miRNA (Fig. 4.4C; mir-9 LV-Neg: 1.001 ± 0.028 vs mir-9 LV-mir-9: 1.237 ± 0.124; mir-181a LV-Neg: 1.032 ± 0.138 vs mir-181a LV-181a: 1.547 ± 0.116; mir-494 LV-Neg: 1.047 ± 0.178 vs mir-494 LV-494: 2.197 ± 0.176).

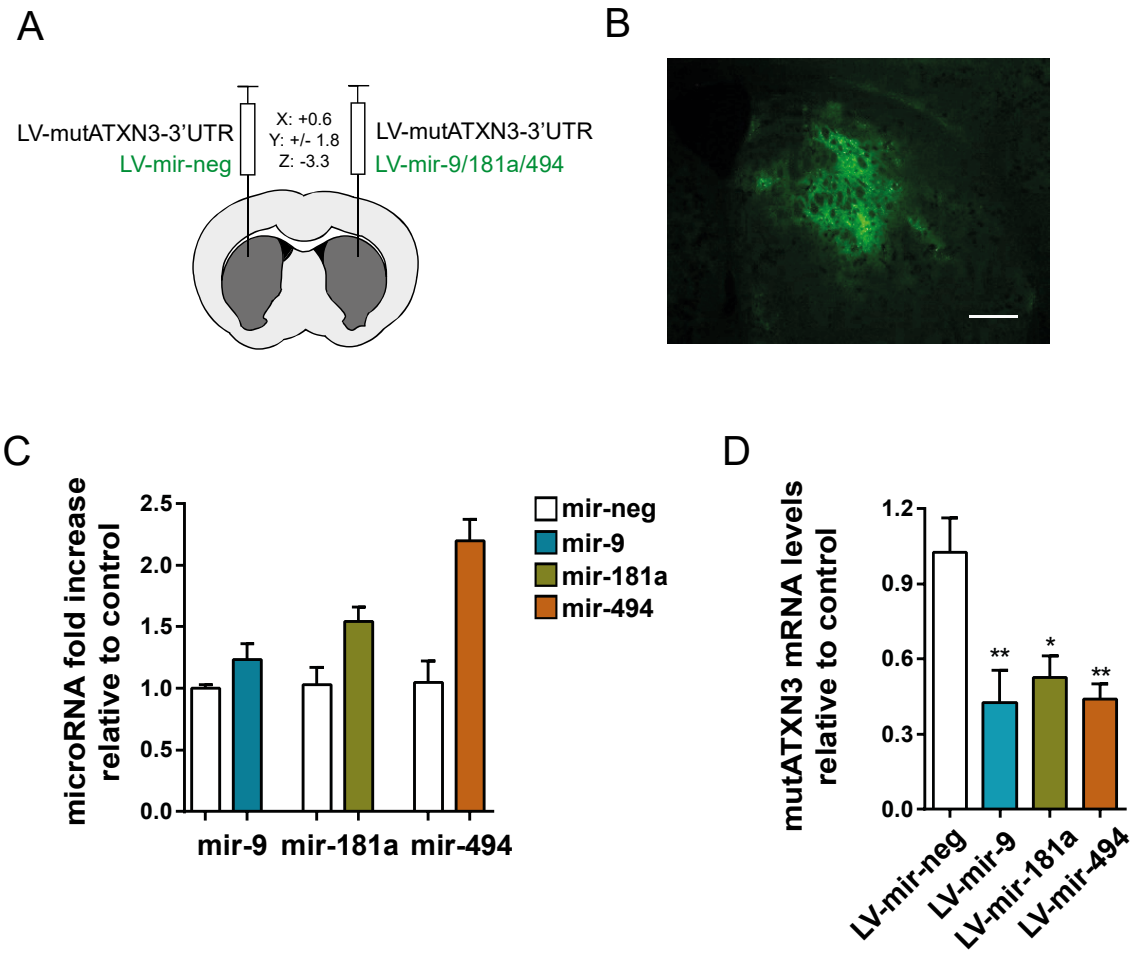

Figure 4.4 – *In vivo* overexpression of mir-9, mir-181a and mir-494 reduce mutATXN3 levels. (A) Schematic representation of the stereotaxic procedure. Lentivirus encoding for mutATXN3-3'UTR were injected bilaterally in the striatum of five-week-old C57/BL6 mice. Simultaneously, lentivirus encoding for mir-9, mir-181a or mir-494 were co-injected with mutATXN3 while mir-Neg was co-injected as control. **(B)** Lentivirus encoding for interest miRNAs efficiently mediate *in vivo* transduction of mouse striatum, as can be seen through reporter expression of GFP. **(C)** QPCR analysis confirmed miRNA overexpression levels for each miRNA in injected striatum tissue compared to control. **(D)** MutATXN3 mRNA levels quantification after miRNA co-injection. LV-mir-9, LV-mir-181a, and LV-mir-494, significantly reduced the levels of mutATXN3 *in vivo* (n=4-5). QPCR analysis for mRNA was normalized with endogenous control (18S). QPCR analysis for miRNA was normalized with endogenous control (U6). Statistical significance was evaluated with One-way ANOVA (*P<0.05, **P < 0.01). Data are expressed as mean ± SEM. Scale bar represents 200µm.

Analysis of mutATXN3 mRNA levels showed a marked reduction after miRNA overexpression (Fig. 4.4D; LV-neg: 1.027 ± 0.136 vs LV-9: 0.427 ± 0.128, LV-181a:

0.526 ± 0.085, LV-494: 0.440 ± 0.062). Altogether, these results clearly demonstrate the efficiency of *in vivo* silencing of mutATXN3.

4.4.5 *In vivo* overexpression of mir-9, mir-181a and mir-494 alleviates neuropathology in a lentiviral mouse model of MJD

Immunohistochemical analysis of coronal sections obtained from injected mice showed a marked reduction in the total number of 1H9 reactive mutATXN3 inclusions in the hemispheres injected with miRNA-encoding lentivirus when compared to the control hemisphere. (Fig. 4.5A, C, E, G, I; LV-neg: 13966 ± 1122 aggregates vs LV-9: 8899 ± 849.8 aggregates, LV-181a: 8832 ± 784.1 aggregates, LV-494: 9662 ± 996.7 aggregates). Furthermore, and in accordance with the previous results, total DARPP-32 depleted volume was also significantly reduced after overexpression of the studied miRNAs (Fig. 4.5B, D, F, H, J; LV-neg: 0.082 ± 0.012 mm^3 vs LV-9: 0.043 ± 0.007 mm^3 , LV-181a: 0.034 ± 0.007 mm^3, LV-494: 0.037 ± 0.007 mm^3).

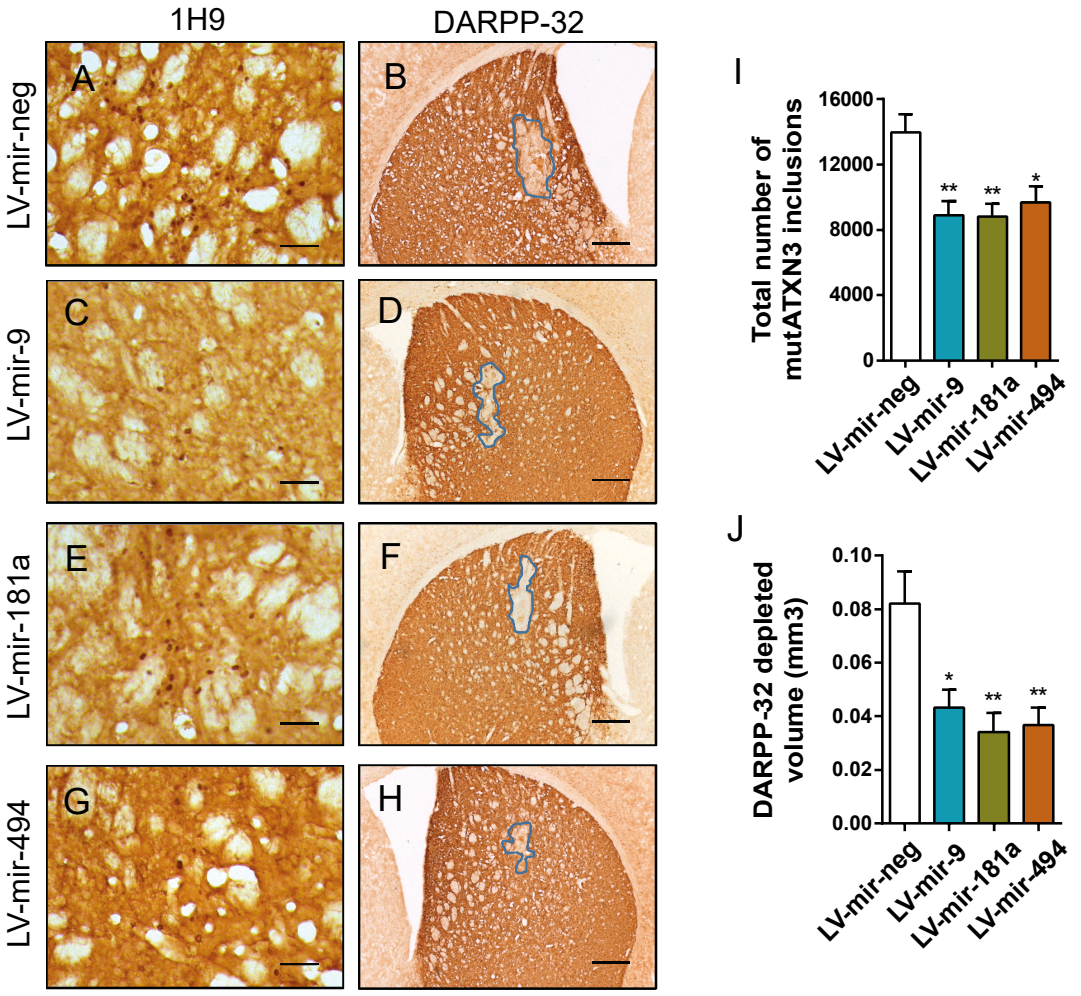

Figure 4.5 - Mir-9, mir-181a and mir-494 lentiviral overexpression reduce neuropathology in a lentiviral model of MJD. (A) Immunohistochemical peroxidase staining using anti-ATXN3 antibody (1H9 ab), 5 weeks post-injection. Control mutATXN3-3'UTR / LV-mir-Neg injected animals displayed a large number of mutATXN3 inclusions **(A)** which was significantly decreased after co-injection with any of the study miRNAs **(C, E, G)** as quantified in **I** (n=4-5). **(B)** Immunohistochemical analysis using an anti-DARPP32 antibody and lesion identification. MutATXN3-3'UTR / LV-mir-Neg injected hemisphere displayed a higher depletion in DARPP-32 volume when compared to miRNA injected hemispheres **(D, F, H)**, as quantified in **J** (n=5). Statistical significance was evaluated with One-way ANOVA (*P < 0.05, **P < 0.01). Data are expressed as mean ± SEM. Scale bars A, C, E and G represent 50µm. Scale bars B, D, F and H represent 200µm.

4.4.6 Mouse endogenous ATXN3 regulation by miRNAs

Moreover, to evaluate if these miRNAs would modulate endogenous mouse Atxn3 (mAtxn3), qPCR for mAtxn3 mRNA was performed in the same samples. We observed a significant reduction for mAtxn3 mRNA levels for both LV-9 and LV-181a (Fig. 4.6B: LV-neg: 1.002 ± 0.029 vs LV-9: 0.818 ± 0.045, LV-181a: 0.769 ± 0.008) but not for LV-494 (Fig. 4.6B; LV-neg: 1.002 ± 0.028 vs LV-494: 0.969 ± 0.068). Note that mAtxn3 3'UTR is considerably different from the human sequence. Still, when in comparison with the human 3'UTR, it contains an identical mir-9 binding site and other non-conserved binding sites for mir-181a and mir-494, which fit with the observed results (Fig. 4.6A).

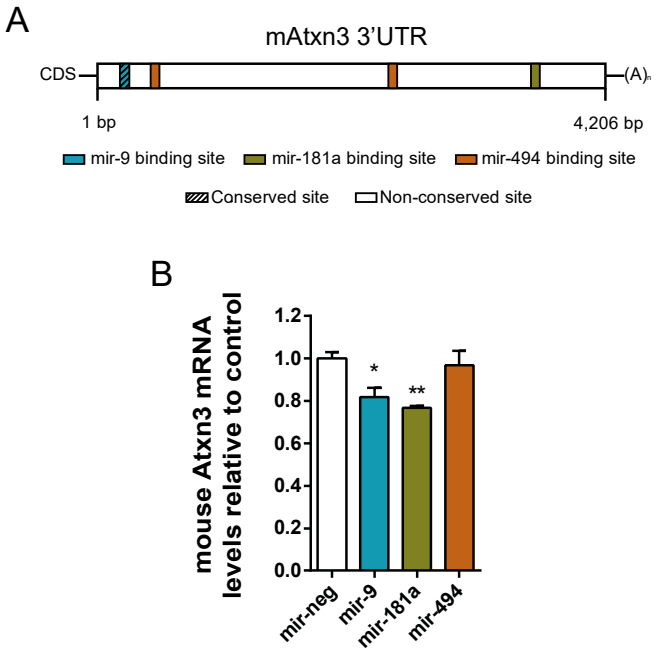

Figure 4.6 – Effects of miRNA overexpression in mouse ATXN3 mRNA. (A) Schematic representation of mATXN3 3'UTR and predicted miRNA binding sites for mir-9, mir-181a and mir-

494. **(B)** QPCR analysis of endogenous mouse ATXN3 mRNA levels. Both mir-9 and mir-181a induced a significant downregulation in the levels of mouse ATXN3. No differences were observed for mir-494. QPCR analysis for mRNA was normalized with endogenous control (18S). Statistical significance was evaluated with One-way ANOVA (*P < 0.05, **P < 0.01). Data are expressed as mean ± SEM.

4.5 Discussion

In chapter 2 we provided evidence implicating endogenous miRNAs in the regulation of ATXN3 mRNA through its 3'UTR, while in chapter 3 we have assessed miRNA dysregulation in multiple MJD models. In this chapter, we validated ATXN3 miRNA based regulation in MJD, confirming that mir-9, mir-181a and mir-494 reduce mutATXN3 levels *in vitro*. Moreover, we assessed the therapeutic potential of *in vivo* delivery of endogenous miRNAs in a lentiviral mouse model of MJD, demonstrating that reinstating the levels of miRNAs targeting the 3'UTR of ATXN3 allows dramatic improvements in MJD neuropathology *in vivo.*

Taking into account the previously observed downregulated miRNA profile in MJD models (chapter 3), we anticipated that the overexpression of these endogenous miRNAs targeting ATXN3 could be a promising approach for the reduction of mutATXN3 levels. In order to pursue this objective, we developed a lentiviral based system for the overexpression of our interest miRNAs, demonstrating that it was able to efficiently increase the levels of mir-9, mir-181a and mir-494 in the mouse striatum upon stereotaxic injection.

Taking advantage of this technology, we have not only validated mir-181a interaction with ATXN3 3'UTR, but we also identified two novel regulatory miRNAs regulating mutATXN3 expression (mir-9 and mir-494), all of them confirmed to directly interact with ATXN3 3'UTR.

Other studies have identified miRNAs targeting ATXN3 mRNA, with mir-25 being the first miRNA known to target ATXN3 3'UTR. Interestingly, overexpression of this miRNA was capable of reducing the levels of mutATXN3 and concomitantly reduce apoptosis *in vitro* (Huang *et al.*, 2014). Nevertheless, no further attempts to pursue an *in vivo* application of mir-25 in MJD animal models were made. Moreover, mir-25 has been strongly related to cancer due to the binding of mir-25 to the 3'UTR of the tumor suppressor p53 (Kumar *et al.*, 2011). Even more, high expression levels of miR-25 have been correlated with poor survival in cancer patients (Qu *et al.*, 2015), limiting its therapeutic value for the treatment of MJD.

More recently, another study has shown that ATXN3 3'UTR is also targeted by mir-181a. However, the authors only assessed the interaction of mir-181a and the 3'UTR of ATXN3, not addressing whether mir-181a could effectively reduce mutATXN3 levels in the context of MJD (Koscianska and Krzyzosiak, 2014).

In this study, this approach was successfully employed for the first time for *in vivo* silencing of mutATXN3, effectively reducing the levels of mutATXN3 and associated neuropathological features in a lentiviral mouse model of MJD.

Although our strategy based of miRNA regulation does not allow for specific silencing of the mutATXN3 allele, our group has previously demonstrated that non allele-specific silencing of ATXN3 *in vivo* was effective and well tolerated in mice (Alves *et al.*, 2010). Moreover, ATXN3 knock-out mice revealed no signs of neurodegeneration or ataxia phenotype, suggesting that therapies based on non-allele-specific silencing of ATXN3 might be safe (Schmitt *et al.*, 2007). Furthermore, compared to other RNA inhibition strategies such as shRNAs, miRNAs are likely less toxic and immunogenic (Bridge *et al.*, 2003; Sledz *et al.*, 2003; McBride *et al.*, 2008).

Taking into account that each miRNA targets multiple mRNAs, we anticipate that other eventual transcripts targeted by mir-9, mir-181a and mir-494 will likely see their levels restored from the reestablishment of these miRNAs, leading to an improvement of the transcriptional dysregulated profile in MJD. In any case, whether the usage of endogenous miRNAs will be beneficial over the usage of artificial miRNAs, a strategy already employed by others (Costa Mdo *et al.*, 2013; Rodriguez-Lebron *et al.*, 2013a), will likely depend on the required silencing potency and off-targeting characteristics of each sequence. Furthermore, detailed analysis of the mRNA targets of mir-9, mir-181a and mir-494 should be further assessed.

Although lentiviruses are characterized by excellent neuronal tropism and sustained CNS expression making them an adequate tool for a proof of concept study regarding the use of therapeutic miRNAs in MJD mouse models, we anticipate that, from a translational perspective, other approaches will have significant advantages, especially considering that miRNAs are excellent candidates for both non-viral and AAV delivery, both of which could be applied with non-invasive procedures. In fact, miRNA delivery can take advantage of our previously demonstrated liposome technology which enables the delivery of silencing sequences to the brain after intravenous administration (Conceição *et al.*, 2015). Moreover, this strategy could be combined with miRNA chemical modifications, such as the use of locked nucleic acids, conferring both higher stability and specificity to these molecules (Wahlestedt *et al.*, 2000). Furthermore, due to their small size, miRNA sequences can easily be incorporated into the AAV genome, allowing the combination of AAV non integrative miRNA gene delivery, with AAV capsid mediated tropism flexibility (Wu *et al.*, 2006). In fact, recent advances have led to the development of AAV serotypes with modified capsids which enable efficient transgene delivery to the

brain after intravenous administration (Deverman *et al.*, 2016). These modifications continue to improve AAVs profile, making it a safer and more efficient gene therapy vector for the treatment of neurodegenerative diseases.

Another step that will be critical for the application of endogenous miRNAs as a therapeutic approach will be to assess their beneficial effects in a transgenic mouse model of MJD. Among existing mouse models of MJD, the YAC ATXN3Q84 currently comes up as the prime candidate for assessing the therapeutic potential of miRNAs targeting the 3'UTR, since it contains all the native human regulatory elements (Cemal *et al.*, 2002). Nevertheless, this model is characterized by a slowly progressive mild phenotype which will hamper the screening of multiple candidates. Moreover, although previous silencing attempts on this model resulted in an amelioration of the molecular phenotype, those were not translatable into an improvement of motor performance (Costa Mdo *et al.*, 2013; Rodriguez-Lebron *et al.*, 2013a). Even so, the combination of our miRNA therapy with enhanced delivery techniques such as whole brain AAV transduction could prove to be more efficient.

In conclusion, the encouraging results here described with lentiviral delivery of mir-9, mir-181a and mir-494 in a lentiviral mouse model of MJD, provide evidence that gene delivery of endogenous miRNAs targeting ATXN3 may be a promising strategy for the treatment of MJD. In the future, this strategy can and should be further associated with state of the art technologies for safe and efficient gene delivery to the CNS, pushing MJD gene therapy one step closer to the patients.

CHAPTER 5

Final conclusions and future perspectives

5. Final conclusions and future perspectives

This thesis focused on the microRNA (miRNA) mediated regulation of human ataxin-3 (ATXN3) through its 3' untranslated region (3'UTR), in the assessment of miRNA expression levels in the context of Machado-Joseph disease (MJD) and in the evaluation of miRNA overexpression as a therapeutic approach for the treatment of MJD. Our results demonstrate that the 3'UTR of ATXN3 plays a crucial role in the control of the levels of ATXN3 by enabling the regulatory function of endogenous miRNAs. Moreover, we showed that lentiviral overexpression of specific miRNAs targeting ATXN3 3'UTR, which are downregulated in different MJD models, efficiently reduced the levels of mutant ataxin-3 (mutATXN3) and associated neuropathology *in vivo* (Fig. 5.1).

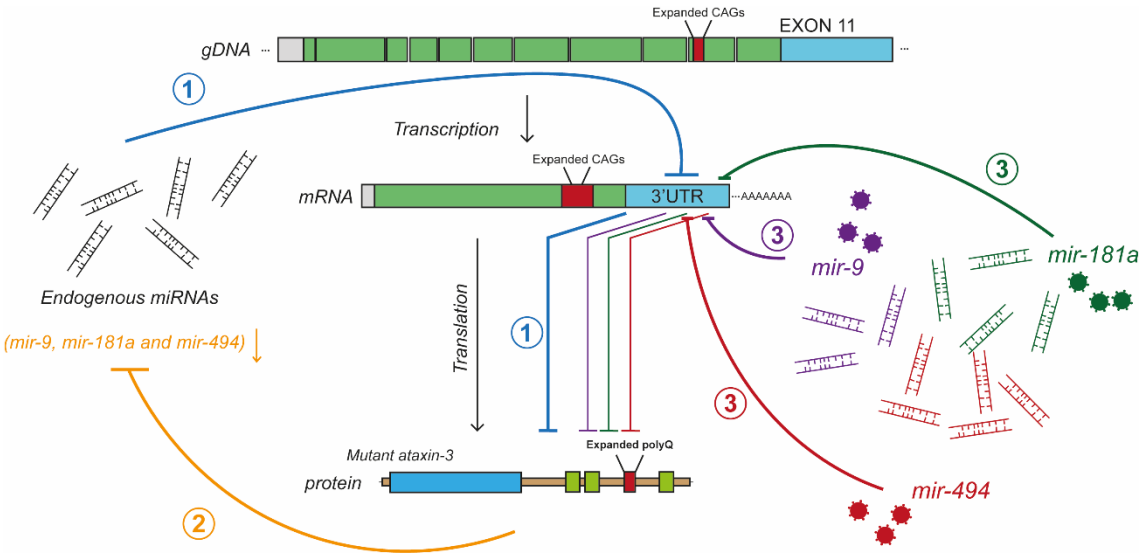

Figure 5.1 – Schematic representation of our findings. (1) ATXN3 3'UTR controls the stability and translation of ATXN3 mRNA leading to a reduction in the levels of mutATXN3 *in vitro* and *in vivo*. Endogenous miRNAs are responsible for the observed 3'UTR effect, leading to a reduction in mutATXN3 levels. **(2)** MiRNA profiling in different human brain samples and in MJD *in vitro* and *in vivo* models revealed a general downregulated profile for miRNAs: mir-9, mir-181a and mir-494. QPCR analysis revealed transcriptional impairments in genes involved in miRNA biogenesis and function, explaining the observed changes at the mature miRNA levels. **(3)** Lentiviral delivery of mir-9, mir-181a and mir-494 was able to reduce the levels of mutATXN3 and associated neuropathology *in vivo*, by directly targeting ATXN3 3'UTR. This strategy represents a novel therapeutic approach for the treatment of MJD.

Although 3'UTRs have been recognized to play very critical and diverse roles in the control of gene expression (Matoulkova *et al.*, 2012), the function of ATXN3 3'UTR has remained largely unaddressed, since research has been mainly focused in the role of the ATXN3 coding sequence. Therefore, in the first part of this project, we started by generating a novel modified lentiviral mouse model of MJD by introducing the 3'UTR sequence of human ATXN3 in our previously characterized lentiviral model (Alves *et al.*, 2008b). Strikingly, the introduction of this sequence induced a robust decrease in the levels of mutATXN3 *in vitro* and *in vivo* while being associated with a concomitant reduction in the associated neuropathology. Moreover, we provide evidence implicating the endogenous miRNAs as responsible for this effect, by employing a genetic and pharmacologic blockage of the endogenous miRNA biogenesis pathway, which resulted in an increase in the levels of mutATXN3.

Overall, these results clearly demonstrate that ATXN3 3'UTR has a major regulatory function over the stability and translation of the ATXN3 mRNA. This is particular relevant to understand MJD pathogenesis especially taking into account how diverse the transcriptomic profile of ATXN3 is, which includes not only transcripts with 3'UTRs of different length, but also transcripts where this region is completely excluded (Ichikawa *et al.*, 2001; Bettencourt *et al.*, 2010). Moreover, one study has previously detected an increased production of a splicing variant upon the presence of the CAG expansion (Ramani *et al.*, 2015). Interestingly, besides encoding for a shorter isoform of ATXN3 protein which appears to have a higher toxicity profile, this mRNA isoform lacks exon 11 due to the use of an early poly(A) termination signal. Combined with the evidence presented it this thesis, we believe this aberrant splicing event may be contributing for the disease pathogenesis. This creates an opportunity for the development of a novel therapeutic approach based on antisense splicing modulation of the ATXN3 gene in order to prevent the exclusion of exon 11.

Nevertheless, 3'UTRs are regulated by a complex network of different players other than miRNAs. Concomitantly, many different RNA binding proteins (RBPs) may be co-responsible for the observed effects at the 3'UTR level (Gerstberger *et al.*, 2014). Therefore, further studies will be required to completely characterize the interactome of ATXN3 3'UTR. One experimental approach could be based on the proteomic and transcriptomic characterization of the protein and RNA fractions crosslinked to ATXN3 3'UTR and isolated after pull-down of ATXN3 mRNA using oligonucleotide probes. Eventually, the modulation of key interacting partners of ATXN3 3'UTR may be the basis of novel therapeutic approaches for MJD. However, we decided to focus on the study of miRNA regulation of ATXN3, not only due to the important functions of miRNAs at the

regulation of gene expression through 3'UTRs, but also based on our evidence suggesting a specific role for endogenous miRNAs on the 3'UTR of ATXN3.

Therefore, in the second part of this project, we started by identifying which particular miRNAs were predicted to target ATXN3 3'UTR and by evaluating their expression status in the context of MJD. Bioinformatic analysis suggested a great number of candidates which were later restricted to three high scoring miRNAs with higher probability to regulate ATXN3 3'UTR: hsa-mir-9-5p, hsa-mir-181a-5p and hsa-mir-494-3p. Importantly all of these miRNAs are conserved between human and mouse, and expressed in the brain. Interestingly, profiling the levels of these miRNAs across multiple MJD models revealed a general downregulation in their levels. This is particular relevant for MJD pathogenesis since an impairment of these miRNAs may not only cause an upregulation of mutATXN3, but may also be contributing for a global transcriptomic dysregulation of multiple other targets.

Moreover, we wondered what would be the mechanism behind this general downregulated profile observed for our candidate miRNAs. Quantitative PCR analysis revealed significant impairments for multiple genes involved in miRNA biogenesis and function, which line up with the results observed at the miRNA levels. Although the status of the miRNA machinery has never been previously evaluated in MJD, this has been recognized as core component in the pathogenesis of other diseases, including Huntington's disease (HD) (Lee *et al.*, 2011). Moreover, transcriptional dysregulation has been previously implicated in MJD (McCampbell *et al.*, 2000; Evert *et al.*, 2006a). Nevertheless, future studies will be required to isolate the individual impact of each component in miRNA dysregulation and in the pathogenesis of MJD. Genetic modulation of these components might be a promising therapeutic approach for the treatment of MJD. Moreover, an increase in the global levels of miRNAs can be achieved through pharmacological therapy. Enoxacin is a small molecule which enhances RNA interference by increasing Dicer-mediated miRNA processing (Shan *et al.*, 2008). Furthermore, in a recent study, *in vivo* administration of enoxacin efficiently increased the levels of miRNAs in the brain, ameliorating the behavioral phenotype in a mouse model of depression characterized by decreased miRNA expression (Smalheiser *et al.*, 2014). Accordingly, enoxacin may be a promising therapeutic agent for MJD, leading to a reinstatement of the levels of endogenous miRNAs, and therefore enhancing their activity over ATXN3 3'UTR and their associated target transcriptome.

Taking into account the previous results, in chapter 4 we started by validating the direct regulation of ATXN3 3'UTR by our candidate miRNAs, which did in fact

downregulate the levels of mutATXN3 *in vitro*. Subsequently we took advantage of a lentiviral miRNA overexpression system and of our novel lentiviral MJD mouse model in order to assess the potential of these miRNAs as a therapeutic approach for the alleviation of MJD *in vivo*. As expected, lentiviral overexpression of each miRNA led to a reduction of mutATXN3 mRNA levels while decreasing the number of mutATXN3 inclusions and associated neuropathology. However, although the lentiviral model used in this study offers great advantages for the screening of multiple therapeutic approaches, it is also limited in other different aspects, such as in the absence of an observable behavioral phenotype. Therefore, it will be critical to evaluate the potential of our miRNA sequences in different MJD models with 3'UTR regulation such as the YAC ATXN3Q84 and knock-in Ki91 models, which present mild behavioral impairments (Cemal *et al.*, 2002; Switonski *et al.*, 2015). Although miRNA regulation of ATXN3 through its 3'UTR has been previously demonstrated (Huang *et al.*, 2014), no previous studies have assessed their potential as a therapeutic approach *in vivo.* Moreover, taking into account the general downregulated profile of our miRNAs, we expect that the reinstatement of the levels of each miRNA may not only reduce the levels of mutATXN3 but also restore their target transcriptomes, which may be disrupted in MJD.

Nevertheless, before being translated into the clinics, this approach will need to overcome different hurdles. First we will need to evaluate whether the modulation of other targets by our miRNAs will not be prejudicial for the treatment of MJD as each miRNA can target hundreds of genes simultaneously (Peter, 2010). Moreover, our miRNA-based strategy will not mediate an allele-specific silencing of mutATXN3. However, based on previous evidence suggesting that non allele specific silencing of ATXN3 is not toxic (Alves *et al.*, 2010), together with the data provided by ATXN3 knock-out mice (Schmitt *et al.*, 2007), our strategy may be feasible for a clinical application. Secondly, we will need to evaluate the toxicity of RNA interference silencing approach. Although miRNAs are presumably less toxic than short-hairpin RNAs (shRNAs), a careful evaluation of promoters and transgene sequences will be required to minimize these previously described effects (McBride *et al.*, 2008). Moreover, although our lentiviral vectors performed well in our study, the delivery system for our studied miRNA sequences can still benefit from improvements when envisioning a clinical application. Recent advances on adeno-associated viral (AAV) vectors technology with genetically engineered capsids may allow for a non-invasive brain-targeted delivery of miRNAs through intravenous injection (Deverman *et al.*, 2016). Moreover, AAV's generally safer profile should ease their approval for a clinical application (Daya and Berns, 2008). A different yet promising approach will be to combine our miRNA silencing sequences with

the administration of brain-targeted stable nucleic acid lipid particles technology recently developed by our group (Conceição *et al.*, 2015), bypassing the safety limitations of viral vectors.

All in all, in this thesis we have evaluated the regulatory role of ATXN3 3'UTR by developing and characterizing a novel lentiviral model of MJD. Moreover, we have provided important clues for miRNA-associated MJD pathogenesis and opened new avenues for the evaluation of novel miRNA based therapeutic strategies for MJD. Altogether, this study has contributed for further understanding of MJD and represents one more step forward toward the development of an effective therapy for the treatment of MJD.

References

Abrahante JE, Daul AL, Li M, Volk ML, Tennessen JM, Miller EA*, et al.* The Caenorhabditis elegans hunchback-like gene lin-57/hbl-1 controls developmental time and is regulated by microRNAs. Developmental cell 2003; 4(5): 625-37.

Agarwal V, Bell GW, Nam JW, Bartel DP. Predicting effective microRNA target sites in mammalian mRNAs. eLife 2015; 4.

Albrecht M, Golatta M, Wullner U, Lengauer T. Structural and functional analysis of ataxin-2 and ataxin-3. European journal of biochemistry / FEBS 2004; 271(15): 3155-70.

Alves S, Nascimento-Ferreira I, Auregan G, Hassig R, Dufour N, Brouillet E*, et al.* Allele-specific RNA silencing of mutant ataxin-3 mediates neuroprotection in a rat model of Machado-Joseph disease. PloS one 2008a; 3(10): e3341.

Alves S, Nascimento-Ferreira I, Dufour N, Hassig R, Auregan G, Nobrega C*, et al.* Silencing ataxin-3 mitigates degeneration in a rat model of Machado-Joseph disease: no role for wild-type ataxin-3? Human molecular genetics 2010; 19(12): 2380-94.

Alves S, Regulier E, Nascimento-Ferreira I, Hassig R, Dufour N, Koeppen A*, et al.* Striatal and nigral pathology in a lentiviral rat model of Machado-Joseph disease. Human molecular genetics 2008b; 17(14): 2071-83.

Ambros V, Bartel B, Bartel DP, Burge CB, Carrington JC, Chen X*, et al.* A uniform system for microRNA annotation. Rna 2003; 9(3): 277-9.

An J, Cai T, Che H, Yu T, Cao Z, Liu X*, et al.* The changes of miRNA expression in rat hippocampus following chronic lead exposure. Toxicology Letters 2014; 229(1): 158-66.

Andrew SE, Goldberg YP, Kremer B, Telenius H, Theilmann J, Adam S*, et al.* The relationship between trinucleotide (CAG) repeat length and clinical features of Huntington's disease. Nature genetics 1993; 4(4): 398-403.

Araujo J, Breuer P, Dieringer S, Krauss S, Dorn S, Zimmermann K*, et al.* FOXO4-dependent upregulation of superoxide dismutase-2 in response to oxidative stress is impaired in spinocerebellar ataxia type 3. Human molecular genetics 2011; 20(15): 2928-41.

Avior Y, Sagi I, Benvenisty N. Pluripotent stem cells in disease modelling and drug discovery. Nature reviews Molecular cell biology 2016; 17(3): 170-82.

Bader AG, Brown D, Winkler M. The promise of microRNA replacement therapy. Cancer research 2010; 70(18): 7027-30.

Baek D, Villen J, Shin C, Camargo FD, Gygi SP, Bartel DP. The impact of microRNAs on protein output. Nature 2008; 455(7209): 64-71.

Bak RO, Hollensen AK, Primo MN, Sorensen CD, Mikkelsen JG. Potent microRNA suppression by RNA Pol II-transcribed 'Tough Decoy' inhibitors. Rna 2013; 19(2): 280-93.

Banasik MB, McCray PB, Jr. Integrase-defective lentiviral vectors: progress and applications. Gene therapy 2010; 17(2): 150-7.

Banez-Coronel M, Porta S, Kagerbauer B, Mateu-Huertas E, Pantano L, Ferrer I*, et al.* A pathogenic mechanism in Huntington's disease involves small CAG-repeated RNAs with neurotoxic activity. PLoS genetics 2012; 8(2): e1002481.

Bankiewicz KS, Forsayeth J, Eberling JL, Sanchez-Pernaute R, Pivirotto P, Bringas J*, et al.* Long-term clinical improvement in MPTP-lesioned primates after gene therapy with AAV-hAADC. Molecular therapy : the journal of the American Society of Gene Therapy 2006; 14(4): 564-70.

Bartel DP. MicroRNAs: genomics, biogenesis, mechanism, and function. Cell 2004; 116(2): 281-97.

Bartel DP. MicroRNAs: target recognition and regulatory functions. Cell 2009; 136(2): 215-33.

Bauer PO, Nukina N. The pathogenic mechanisms of polyglutamine diseases and current therapeutic strategies. Journal of neurochemistry 2009; 110(6): 1737-65.

Behlke MA. Chemical modification of siRNAs for in vivo use. Oligonucleotides 2008; 18(4): 305-19.

Bennett CF, Swayze EE. RNA targeting therapeutics: molecular mechanisms of antisense oligonucleotides as a therapeutic platform. Annual review of pharmacology and toxicology 2010; 50: 259-93.

Berke SJ, Chai Y, Marrs GL, Wen H, Paulson HL. Defining the role of ubiquitin-interacting motifs in the polyglutamine disease protein, ataxin-3. The Journal of biological chemistry 2005; 280(36): 32026-34.

Berke SJ, Schmied FA, Brunt ER, Ellerby LM, Paulson HL. Caspase-mediated proteolysis of the polyglutamine disease protein ataxin-3. Journal of neurochemistry 2004; 89(4): 908-18.

Bessis N, GarciaCozar FJ, Boissier MC. Immune responses to gene therapy vectors: influence on vector function and effector mechanisms. Gene therapy 2004; 11 Suppl 1: S10-7.

Betel D, Koppal A, Agius P, Sander C, Leslie C. Comprehensive modeling of microRNA targets predicts functional non-conserved and non-canonical sites. Genome biology 2010; 11(8): R90.

Bettencourt C, Santos C, Kay T, Vasconcelos J, Lima M. Analysis of segregation patterns in Machado-Joseph disease pedigrees. Journal of human genetics 2008; 53(10): 920-3.

Bettencourt C, Santos C, Montiel R, Costa Mdo C, Cruz-Morales P, Santos LR*, et al.* Increased transcript diversity: novel splicing variants of Machado-Joseph disease gene (ATXN3). Neurogenetics 2010; 11(2): 193-202.

Bevivino AE, Loll PJ. An expanded glutamine repeat destabilizes native ataxin-3 structure and mediates formation of parallel beta -fibrils. Proceedings of the National Academy of Sciences of the United States of America 2001; 98(21): 11955-60.

Bichelmeier U, Schmidt T, Hubener J, Boy J, Ruttiger L, Habig K*, et al.* Nuclear localization of ataxin-3 is required for the manifestation of symptoms in SCA3: in vivo evidence. The Journal of neuroscience : the official journal of the Society for Neuroscience 2007; 27(28): 7418-28.

Bienroth S, Keller W, Wahle E. Assembly of a processive messenger RNA polyadenylation complex. The EMBO journal 1993; 12(2): 585-94.

Bilen J, Liu N, Burnett BG, Pittman RN, Bonini NM. MicroRNA pathways modulate polyglutamine-induced neurodegeneration. Molecular cell 2006; 24(1): 157-63.

Bird TD. Hereditary Ataxia Overview. In: Pagon RA, Adam MP, Ardinger HH, Wallace SE, Amemiya A, Bean LJH*, et al.*, editors. GeneReviews(R). Seattle (WA); 1993.

Boudreau RL, Jiang P, Gilmore BL, Spengler RM, Tirabassi R, Nelson JA*, et al.* Transcriptome-wide discovery of microRNA binding sites in human brain. Neuron 2014; 81(2): 294-305.

Boudreau RL, Martins I, Davidson BL. Artificial microRNAs as siRNA shuttles: improved safety as compared to shRNAs in vitro and in vivo. Molecular therapy : the journal of the American Society of Gene Therapy 2009; 17(1): 169-75.

Boy J, Schmidt T, Schumann U, Grasshoff U, Unser S, Holzmann C*, et al.* A transgenic mouse model of spinocerebellar ataxia type 3 resembling late disease onset and gender-specific instability of CAG repeats. Neurobiology of disease 2010; 37(2): 284-93.

Boy J, Schmidt T, Wolburg H, Mack A, Nuber S, Bottcher M*, et al.* Reversibility of symptoms in a conditional mouse model of spinocerebellar ataxia type 3. Human molecular genetics 2009; 18(22): 4282-95.

Brawerman G. The Role of the poly(A) sequence in mammalian messenger RNA. CRC critical reviews in biochemistry 1981; 10(1): 1-38.

Bridge AJ, Pebernard S, Ducraux A, Nicoulaz AL, Iggo R. Induction of an interferon response by RNAi vectors in mammalian cells. Nature genetics 2003; 34(3): 263-4.

Burnett B, Li F, Pittman RN. The polyglutamine neurodegenerative protein ataxin-3 binds polyubiquitylated proteins and has ubiquitin protease activity. Human molecular genetics 2003; 12(23): 3195-205.

Burnett BG, Pittman RN. The polyglutamine neurodegenerative protein ataxin 3 regulates aggresome formation. Proceedings of the National Academy of Sciences of the United States of America 2005; 102(12): 4330-5.

Cai X, Hagedorn CH, Cullen BR. Human microRNAs are processed from capped, polyadenylated transcripts that can also function as mRNAs. Rna 2004; 10(12): 1957-66.

Catapano F, Zaharieva I, Scoto M, Marrosu E, Morgan J, Muntoni F*, et al.* Altered Levels of MicroRNA-9, -206, and -132 in Spinal Muscular Atrophy and Their Response to Antisense Oligonucleotide Therapy. Molecular Therapy—Nucleic Acids 2016; 5(7): e331.

Cemal CK, Carroll CJ, Lawrence L, Lowrie MB, Ruddle P, Al-Mahdawi S*, et al.* YAC transgenic mice carrying pathological alleles of the MJD1 locus exhibit a mild and slowly progressive cerebellar deficit. Human molecular genetics 2002; 11(9): 1075-94.

Chai Y, Koppenhafer SL, Bonini NM, Paulson HL. Analysis of the role of heat shock protein (Hsp) molecular chaperones in polyglutamine disease. The Journal of neuroscience : the official journal of the Society for Neuroscience 1999a; 19(23): 10338-47.

Chai Y, Koppenhafer SL, Shoesmith SJ, Perez MK, Paulson HL. Evidence for proteasome involvement in polyglutamine disease: localization to nuclear inclusions in SCA3/MJD and suppression of polyglutamine aggregation in vitro. Human molecular genetics 1999b; 8(4): 673-82.

Chai Y, Wu L, Griffin JD, Paulson HL. The role of protein composition in specifying nuclear inclusion formation in polyglutamine disease. The Journal of biological chemistry 2001; 276(48): 44889-97.

Chang WH, Tien CL, Chen TJ, Nukina N, Hsieh M. Decreased protein synthesis of Hsp27 associated with cellular toxicity in a cell model of Machado-Joseph disease. Neuroscience letters 2009; 454(2): 152-6.

Cheloufi S, Dos Santos CO, Chong MM, Hannon GJ. A dicer-independent miRNA biogenesis pathway that requires Ago catalysis. Nature 2010; 465(7298): 584-9.

Chen CZ, Li L, Lodish HF, Bartel DP. MicroRNAs modulate hematopoietic lineage differentiation. Science 2004; 303(5654): 83-6.

Chen X, Tang TS, Tu H, Nelson O, Pook M, Hammer R*, et al.* Deranged calcium signaling and neurodegeneration in spinocerebellar ataxia type 3. The Journal of neuroscience : the official journal of the Society for Neuroscience 2008; 28(48): 12713-24.

Cheng PH, Li CL, Chang YF, Tsai SJ, Lai YY, Chan AW*, et al.* miR-196a ameliorates phenotypes of Huntington disease in cell, transgenic mouse, and induced pluripotent stem cell models. American journal of human genetics 2013; 93(2): 306-12.

Chi SW, Hannon GJ, Darnell RB. An alternative mode of microRNA target recognition. Nature structural & molecular biology 2012; 19(3): 321-7.

Chorn G, Klein-McDowell M, Zhao L, Saunders MA, Flanagan WM, Willingham AT*, et al.* Single-stranded microRNA mimics. Rna 2012; 18(10): 1796-804.

Chou AH, Lin AC, Hong KY, Hu SH, Chen YL, Chen JY*, et al.* p53 activation mediates polyglutamine-expanded ataxin-3 upregulation of Bax expression in cerebellar and pontine nuclei neurons. Neurochemistry international 2011; 58(2): 145-52.

Chou AH, Yeh TH, Kuo YL, Kao YC, Jou MJ, Hsu CY*, et al.* Polyglutamine-expanded ataxin-3 activates mitochondrial apoptotic pathway by upregulating Bax and downregulating Bcl-xL. Neurobiology of disease 2006; 21(2): 333-45.

Chou AH, Yeh TH, Ouyang P, Chen YL, Chen SY, Wang HL. Polyglutamine-expanded ataxin-3 causes cerebellar dysfunction of SCA3 transgenic mice by inducing transcriptional dysregulation. Neurobiology of disease 2008; 31(1): 89-101.

Choudhury SR, Harris AF, Cabral DJ, Keeler AM, Sapp E, Ferreira JS*, et al.* Widespread Central Nervous System Gene Transfer and Silencing After Systemic Delivery of Novel AAV-AS Vector. Molecular therapy : the journal of the American Society of Gene Therapy 2016; 24(4): 726-35.

Cogswell JP, Ward J, Taylor IA, Waters M, Shi Y, Cannon B*, et al.* Identification of miRNA changes in Alzheimer's disease brain and CSF yields putative biomarkers and insights into disease pathways. Journal of Alzheimer's disease : JAD 2008; 14(1): 27-41.

Colomer Gould VF, Goti D, Pearce D, Gonzalez GA, Gao H, Bermudez de Leon M*, et al.* A mutant ataxin-3 fragment results from processing at a site N-terminal to amino acid 190 in brain of Machado-Joseph disease-like transgenic mice. Neurobiology of disease 2007; 27(3): 362-9.

Conceição M, Mendonça L, Nóbrega C, Gomes C, Costa P, Hirai H*, et al.* Intravenous administration of brain-targeted stable nucleic acid lipid particles alleviates Machado-Joseph disease neurological phenotype. Biomaterials 2015.

Conne B, Stutz A, Vassalli JD. The 3' untranslated region of messenger RNA: A molecular 'hotspot' for pathology? Nature medicine 2000; 6(6): 637-41.

Coolen M, Katz S, Bally-Cuif L. miR-9: a versatile regulator of neurogenesis. Frontiers in cellular neuroscience 2013; 7: 220.

Correia M, Coutinho P, Silva MC, Guimaraes J, Amado J, Matos E. Evaluation of the effect of sulphametoxazole and trimethoprim in patients with Machado-Joseph disease. Revista de neurologia 1995; 23(121): 632-4.

Costa Mdo C, Luna-Cancalon K, Fischer S, Ashraf NS, Ouyang M, Dharia RM*, et al.* Toward RNAi therapy for the polyglutamine disease Machado-Joseph disease. Molecular therapy : the journal of the American Society of Gene Therapy 2013; 21(10): 1898-908.

Costa Mdo C, Paulson HL. Toward understanding Machado-Joseph disease. Progress in neurobiology 2012; 97(2): 239-57.

Coutinho P, Andrade C. Autosomal dominant system degeneration in Portuguese families of the Azores Islands. A new genetic disorder involving cerebellar, pyramidal, extrapyramidal and spinal cord motor functions. Neurology 1978; 28(7): 703-9.

Couto LB, High KA. Viral vector-mediated RNA interference. Current opinion in pharmacology 2010; 10(5): 534-42.

Cummings CJ, Zoghbi HY. Trinucleotide repeats: mechanisms and pathophysiology. Annual review of genomics and human genetics 2000; 1: 281-328.

Cunha-Santos J, Duarte-Neves J, Carmona V, Guarente L, Pereira de Almeida L, Cavadas C. Caloric restriction blocks neuropathology and motor deficits in Machado-Joseph disease mouse models through SIRT1 pathway. Nature communications 2016; 7: 11445.

D'Abreu A, Franca MC, Jr., Paulson HL, Lopes-Cendes I. Caring for Machado-Joseph disease: current understanding and how to help patients. Parkinsonism & related disorders 2010; 16(1): 2-7.

Davies BP, Arenz C. A fluorescence probe for assaying micro RNA maturation. Bioorganic & medicinal chemistry 2008; 16(1): 49-55.

Davies SW, Turmaine M, Cozens BA, DiFiglia M, Sharp AH, Ross CA*, et al.* Formation of neuronal intranuclear inclusions underlies the neurological dysfunction in mice transgenic for the HD mutation. Cell 1997; 90(3): 537-48.

Davis S, Lollo B, Freier S, Esau C. Improved targeting of miRNA with antisense oligonucleotides. Nucleic acids research 2006; 34(8): 2294-304.

Daya S, Berns KI. Gene therapy using adeno-associated virus vectors. Clinical microbiology reviews 2008; 21(4): 583-93.

de Almeida LP, Ross CA, Zala D, Aebischer P, Deglon N. Lentiviral-mediated delivery of mutant huntingtin in the striatum of rats induces a selective neuropathology modulated by polyglutamine repeat size, huntingtin expression levels, and protein length. The Journal of neuroscience : the official journal of the Society for Neuroscience 2002; 22(9): 3473-83.

Deglon N, Hantraye P. Viral vectors as tools to model and treat neurodegenerative disorders. The journal of gene medicine 2005; 7(5): 530-9.

Derti A, Garrett-Engele P, Macisaac KD, Stevens RC, Sriram S, Chen R*, et al.* A quantitative atlas of polyadenylation in five mammals. Genome research 2012; 22(6): 1173-83.

Deverman BE, Pravdo PL, Simpson BP, Kumar SR, Chan KY, Banerjee A*, et al.* Cre-dependent selection yields AAV variants for widespread gene transfer to the adult brain. Nature biotechnology 2016; 34(2): 204-9.

Durr A, Stevanin G, Cancel G, Duyckaerts C, Abbas N, Didierjean O*, et al.* Spinocerebellar ataxia 3 and Machado-Joseph disease: clinical, molecular, and neuropathological features. Annals of neurology 1996; 39(4): 490-9.

Ebert MS, Neilson JR, Sharp PA. MicroRNA sponges: competitive inhibitors of small RNAs in mammalian cells. Nature methods 2007; 4(9): 721-6.

Ebert MS, Sharp PA. MicroRNA sponges: progress and possibilities. Rna 2010; 16(11): 2043-50.

Edwalds-Gilbert G, Veraldi KL, Milcarek C. Alternative poly(A) site selection in complex transcription units: means to an end? Nucleic acids research 1997; 25(13): 2547-61.

Eliseeva IA, Lyabin DN, Ovchinnikov LP. Poly(A)-binding proteins: structure, domain organization, and activity regulation. Biochemistry Biokhimiia 2013; 78(13): 1377-91.

Erson-Bensan AE. Alternative polyadenylation and RNA-binding proteins. Journal of molecular endocrinology 2016; 57(2): F29-34.

Esau CC. Inhibition of microRNA with antisense oligonucleotides. Methods 2008; 44(1): 55-60.

Eulalio A, Huntzinger E, Izaurralde E. GW182 interaction with Argonaute is essential for miRNA-mediated translational repression and mRNA decay. Nature structural & molecular biology 2008; 15(4): 346-53.

Evers MM, Toonen LJ, van Roon-Mom WM. Ataxin-3 protein and RNA toxicity in spinocerebellar ataxia type 3: current insights and emerging therapeutic strategies. Molecular neurobiology 2014; 49(3): 1513-31.

Evert BO, Araujo J, Vieira-Saecker AM, de Vos RA, Harendza S, Klockgether T*, et al.* Ataxin-3 represses transcription via chromatin binding, interaction with histone deacetylase 3, and histone deacetylation. The Journal of neuroscience : the official journal of the Society for Neuroscience 2006a; 26(44): 11474-86.

Evert BO, Schelhaas J, Fleischer H, de Vos RA, Brunt ER, Stenzel W*, et al.* Neuronal intranuclear inclusions, dysregulation of cytokine expression and cell death in spinocerebellar ataxia type 3. Clinical neuropathology 2006b; 25(6): 272-81.

Evert BO, Vogt IR, Kindermann C, Ozimek L, de Vos RA, Brunt ER*, et al.* Inflammatory genes are upregulated in expanded ataxin-3-expressing cell lines and spinocerebellar ataxia type 3 brains. The Journal of neuroscience : the official journal of the Society for Neuroscience 2001; 21(15): 5389-96.

Evert BO, Vogt IR, Vieira-Saecker AM, Ozimek L, de Vos RA, Brunt ER*, et al.* Gene expression profiling in ataxin-3 expressing cell lines reveals distinct effects of normal and mutant ataxin-3. Journal of neuropathology and experimental neurology 2003; 62(10): 1006-18.

Evert BO, Wullner U, Schulz JB, Weller M, Groscurth P, Trottier Y*, et al.* High level expression of expanded full-length ataxin-3 in vitro causes cell death and formation of intranuclear inclusions in neuronal cells. Human molecular genetics 1999; 8(7): 1169-76.

Fabian MR, Sonenberg N. The mechanics of miRNA-mediated gene silencing: a look under the hood of miRISC. Nature structural & molecular biology 2012; 19(6): 586-93.

Filipowicz W, Bhattacharyya SN, Sonenberg N. Mechanisms of post-transcriptional regulation by microRNAs: are the answers in sight? Nature reviews Genetics 2008; 9(2): 102-14.

Fire A, Xu S, Montgomery MK, Kostas SA, Driver SE, Mello CC. Potent and specific genetic interference by double-stranded RNA in Caenorhabditis elegans. Nature 1998; 391(6669): 806-11.

Flynt AS, Lai EC. Biological principles of microRNA-mediated regulation: shared themes amid diversity. Nature reviews Genetics 2008; 9(11): 831-42.

Freeman W, Wszolek Z. Botulinum toxin type A for treatment of spasticity in spinocerebellar ataxia type 3 (Machado-Joseph disease). Movement disorders : official journal of the Movement Disorder Society 2005; 20(5): 644.

Furukawa N, Sakurai F, Katayama K, Seki N, Kawabata K, Mizuguchi H. Optimization of a microRNA expression vector for function analysis of microRNA. Journal of controlled release : official journal of the Controlled Release Society 2011; 150(1): 94-101.

Gaspar C, Lopes-Cendes I, Hayes S, Goto J, Arvidsson K, Dias A*, et al.* Ancestral origins of the Machado-Joseph disease mutation: a worldwide haplotype study. American journal of human genetics 2001; 68(2): 523-8.

Gaughwin PM, Ciesla M, Lahiri N, Tabrizi SJ, Brundin P, Bjorkqvist M. Hsa-miR-34b is a plasma-stable microRNA that is elevated in pre-manifest Huntington's disease. Human molecular genetics 2011; 20(11): 2225-37.

Gerstberger S, Hafner M, Tuschl T. A census of human RNA-binding proteins. Nature reviews Genetics 2014; 15(12): 829-45.

Ghatak S, Raha S. Micro RNA-214 contributes to proteasome independent downregulation of beta catenin in Huntington's disease knock-in striatal cell model STHdhQ111/Q111. Biochemical and biophysical research communications 2015; 459(3): 509-14.

Ginn SL, Alexander IE, Edelstein ML, Abedi MR, Wixon J. Gene therapy clinical trials worldwide to 2012 - an update. The journal of gene medicine 2013; 15(2): 65-77.

Goncalves N, Simoes AT, Cunha RA, de Almeida LP. Caffeine and adenosine A(2A) receptor inactivation decrease striatal neuropathology in a lentiviral-based model of Machado-Joseph disease. Annals of neurology 2013; 73(5): 655-66.

Gonitel R, Moffitt H, Sathasivam K, Woodman B, Detloff PJ, Faull RL*, et al.* DNA instability in postmitotic neurons. Proceedings of the National Academy of Sciences of the United States of America 2008; 105(9): 3467-72.

Goti D, Katzen SM, Mez J, Kurtis N, Kiluk J, Ben-Haiem L*, et al.* A mutant ataxin-3 putative-cleavage fragment in brains of Machado-Joseph disease patients and transgenic mice is cytotoxic above a critical concentration. The Journal of neuroscience : the official journal of the Society for Neuroscience 2004; 24(45): 10266-79.

Goto J, Watanabe M, Ichikawa Y, Yee SB, Ihara N, Endo K*, et al.* Machado-Joseph disease gene products carrying different carboxyl termini. Neuroscience research 1997; 28(4): 373-7.

Graber JH, Cantor CR, Mohr SC, Smith TF. In silico detection of control signals: mRNA 3'-end-processing sequences in diverse species. Proceedings of the National Academy of Sciences of the United States of America 1999; 96(24): 14055-60.

Grimson A, Farh KK, Johnston WK, Garrett-Engele P, Lim LP, Bartel DP. MicroRNA targeting specificity in mammals: determinants beyond seed pairing. Molecular cell 2007; 27(1): 91-105.

Grishok A, Pasquinelli AE, Conte D, Li N, Parrish S, Ha I*, et al.* Genes and mechanisms related to RNA interference regulate expression of the small temporal RNAs that control C. elegans developmental timing. Cell 2001; 106(1): 23-34.

Gruber AR, Martin G, Muller P, Schmidt A, Gruber AJ, Gumienny R*, et al.* Global 3' UTR shortening has a limited effect on protein abundance in proliferating T cells. Nature communications 2014; 5: 5465.

Gu S, Jin L, Zhang F, Sarnow P, Kay MA. Biological basis for restriction of microRNA targets to the 3' untranslated region in mammalian mRNAs. Nature structural & molecular biology 2009; 16(2): 144-50.

Gunawardena S, Her LS, Brusch RG, Laymon RA, Niesman IR, Gordesky-Gold B*, et al.* Disruption of axonal transport by loss of huntingtin or expression of pathogenic polyQ proteins in Drosophila. Neuron 2003; 40(1): 25-40.

Gusella JF, MacDonald ME. Molecular genetics: unmasking polyglutamine triggers in neurodegenerative disease. Nature reviews Neuroscience 2000; 1(2): 109-15.

Haacke A, Hartl FU, Breuer P. Calpain inhibition is sufficient to suppress aggregation of polyglutamine-expanded ataxin-3. The Journal of biological chemistry 2007; 282(26): 18851-6.

Hacein-Bey-Abina S, Von Kalle C, Schmidt M, McCormack MP, Wulffraat N, Leboulch P*, et al.* LMO2-associated clonal T cell proliferation in two patients after gene therapy for SCID-X1. Science 2003; 302(5644): 415-9.

Han J, Lee Y, Yeom KH, Nam JW, Heo I, Rhee JK*, et al.* Molecular basis for the recognition of primary microRNAs by the Drosha-DGCR8 complex. Cell 2006; 125(5): 887-901.

Hara T, Nakamura K, Matsui M, Yamamoto A, Nakahara Y, Suzuki-Migishima R*, et al.* Suppression of basal autophagy in neural cells causes neurodegenerative disease in mice. Nature 2006; 441(7095): 885-9.

Haraguchi T, Ozaki Y, Iba H. Vectors expressing efficient RNA decoys achieve the long-term suppression of specific microRNA activity in mammalian cells. Nucleic acids research 2009; 37(6): e43.

Harris GM, Dodelzon K, Gong L, Gonzalez-Alegre P, Paulson HL. Splice isoforms of the polyglutamine disease protein ataxin-3 exhibit similar enzymatic yet different aggregation properties. PloS one 2010; 5(10): e13695.

Hata A, Lieberman J. Dysregulation of microRNA biogenesis and gene silencing in cancer. Science signaling 2015; 8(368): re3.

He L, Hannon GJ. MicroRNAs: small RNAs with a big role in gene regulation. Nature reviews Genetics 2004; 5(7): 522-31.

Hebert SS, De Strooper B. Alterations of the microRNA network cause neurodegenerative disease. Trends in neurosciences 2009; 32(4): 199-206.

Henry JC, Azevedo-Pouly AC, Schmittgen TD. MicroRNA replacement therapy for cancer. Pharmaceutical research 2011; 28(12): 3030-42.

Holmberg M, Duyckaerts C, Durr A, Cancel G, Gourfinkel-An I, Damier P*, et al.* Spinocerebellar ataxia type 7 (SCA7): a neurodegenerative disorder with neuronal intranuclear inclusions. Human molecular genetics 1998; 7(5): 913-8.

Holzer SE, Ludlow CL. The swallowing side effects of botulinum toxin type A injection in spasmodic dysphonia. The Laryngoscope 1996; 106(1 Pt 1): 86-92.

Hoss AG, Labadorf A, Latourelle JC, Kartha VK, Hadzi TC, Gusella JF*, et al.* miR-10b-5p expression in Huntington's disease brain relates to age of onset and the extent of striatal involvement. BMC medical genomics 2015; 8: 10.

Huang F, Zhang L, Long Z, Chen Z, Hou X, Wang C*, et al.* miR-25 alleviates polyQ-mediated cytotoxicity by silencing ATXN3. FEBS letters 2014.

Hubener J, Riess O. Polyglutamine-induced neurodegeneration in SCA3 is not mitigated by non-expanded ataxin-3: conclusions from double-transgenic mouse models. Neurobiology of disease 2010; 38(1): 116-24.

Hubener J, Vauti F, Funke C, Wolburg H, Ye Y, Schmidt T*, et al.* N-terminal ataxin-3 causes neurological symptoms with inclusions, endoplasmic reticulum stress and ribosomal dislocation. Brain : a journal of neurology 2011; 134(Pt 7): 1925-42.

Huen NY, Chan HY. Dynamic regulation of molecular chaperone gene expression in polyglutamine disease. Biochemical and biophysical research communications 2005; 334(4): 1074-84.

Hutvagner G, McLachlan J, Pasquinelli AE, Balint E, Tuschl T, Zamore PD. A cellular function for the RNA-interference enzyme Dicer in the maturation of the let-7 small temporal RNA. Science 2001; 293(5531): 834-8.

Hutvagner G, Zamore PD. A microRNA in a multiple-turnover RNAi enzyme complex. Science 2002; 297(5589): 2056-60.

Hydbring P, Badalian-Very G. Clinical applications of microRNAs. F1000Research 2013; 2: 136.

Ichikawa Y, Goto J, Hattori M, Toyoda A, Ishii K, Jeong SY*, et al.* The genomic structure and expression of MJD, the Machado-Joseph disease gene. Journal of human genetics 2001; 46(7): 413-22.

Ikeda H, Yamaguchi M, Sugai S, Aze Y, Narumiya S, Kakizuka A. Expanded polyglutamine in the Machado-Joseph disease protein induces cell death in vitro and in vivo. Nature genetics 1996; 13(2): 196-202.

Ishikawa K, Fujigasaki H, Saegusa H, Ohwada K, Fujita T, Iwamoto H*, et al.* Abundant expression and cytoplasmic aggregations of [alpha]1A voltage-dependent calcium channel protein associated with neurodegeneration in spinocerebellar ataxia type 6. Human molecular genetics 1999a; 8(7): 1185-93.

Ishikawa K, Watanabe M, Yoshizawa K, Fujita T, Iwamoto H, Yoshizawa T*, et al.* Clinical, neuropathological, and molecular study in two families with spinocerebellar ataxia type 6 (SCA6). Journal of neurology, neurosurgery, and psychiatry 1999b; 67(1): 86-9.

Jakobsson J, Lundberg C. Lentiviral vectors for use in the central nervous system. Molecular therapy : the journal of the American Society of Gene Therapy 2006; 13(3): 484-93.

Jeub M, Herbst M, Spauschus A, Fleischer H, Klockgether T, Wuellner U*, et al.* Potassium channel dysfunction and depolarized resting membrane potential in a cell model of SCA3. Experimental neurology 2006; 201(1): 182-92.

Jin P, Alisch RS, Warren ST. RNA and microRNAs in fragile X mental retardation. Nature cell biology 2004; 6(11): 1048-53.

Johnson R, Zuccato C, Belyaev ND, Guest DJ, Cattaneo E, Buckley NJ. A microRNA-based gene dysregulation pathway in Huntington's disease. Neurobiology of disease 2008; 29(3): 438-45.

Karres JS, Hilgers V, Carrera I, Treisman J, Cohen SM. The conserved microRNA miR-8 tunes atrophin levels to prevent neurodegeneration in Drosophila. Cell 2007; 131(1): 136-45.

Kawaguchi Y, Okamoto T, Taniwaki M, Aizawa M, Inoue M, Katayama S*, et al.* CAG expansions in a novel gene for Machado-Joseph disease at chromosome 14q32.1. Nature genetics 1994; 8(3): 221-8.

Khan LA, Bauer PO, Miyazaki H, Lindenberg KS, Landwehrmeyer BG, Nukina N. Expanded polyglutamines impair synaptic transmission and ubiquitin-proteasome system in Caenorhabditis elegans. Journal of neurochemistry 2006; 98(2): 576-87.

Khodr CE, Pedapati J, Han Y, Bohn MC. Inclusion of a portion of the native SNCA 3'UTR reduces toxicity of human S129A SNCA on striatal-projecting dopamine neurons in rat substantia nigra. Developmental neurobiology 2012; 72(6): 906-17.

Kieling C, Prestes PR, Saraiva-Pereira ML, Jardim LB. Survival estimates for patients with Machado-Joseph disease (SCA3). Clinical genetics 2007; 72(6): 543-5.

Kim J, Inoue K, Ishii J, Vanti WB, Voronov SV, Murchison E*, et al.* A MicroRNA feedback circuit in midbrain dopamine neurons. Science 2007; 317(5842): 1220-4.

Kim VN. MicroRNA biogenesis: coordinated cropping and dicing. Nature reviews Molecular cell biology 2005; 6(5): 376-85.

Kim YT, Shin SM, Lee WY, Kim GM, Jin DK. Expression of expanded polyglutamine protein induces behavioral changes in Drosophila (polyglutamine-induced changes in Drosophila). Cellular and molecular neurobiology 2004; 24(1): 109-22.

Kirik D, Bjorklund A. Modeling CNS neurodegeneration by overexpression of disease-causing proteins using viral vectors. Trends in neurosciences 2003; 26(7): 386-92.

Kitade Y, Akao Y. MicroRNAs and their therapeutic potential for human diseases: microRNAs, miR-143 and -145, function as anti-oncomirs and the application of chemically modified miR-143 as an anti-cancer drug. Journal of pharmacological sciences 2010; 114(3): 276-80.

Kloosterman WP, Plasterk RH. The diverse functions of microRNAs in animal development and disease. Developmental cell 2006; 11(4): 441-50.

Kocerha J, Xu Y, Prucha MS, Zhao D, Chan AW. microRNA-128a dysregulation in transgenic Huntington's disease monkeys. Molecular brain 2014; 7: 46.

Koch P, Breuer P, Peitz M, Jungverdorben J, Kesavan J, Poppe D*, et al.* Excitation-induced ataxin-3 aggregation in neurons from patients with Machado-Joseph disease. Nature 2011; 480(7378): 543-6.

Komatsu M, Waguri S, Chiba T, Murata S, Iwata J, Tanida I*, et al.* Loss of autophagy in the central nervous system causes neurodegeneration in mice. Nature 2006; 441(7095): 880-4.

Koscianska E, Krzyzosiak WJ. Current understanding of the role of microRNAs in spinocerebellar ataxias. Cerebellum & Ataxias 2014; 1(1): 7.

Kozomara A, Griffiths-Jones S. miRBase: annotating high confidence microRNAs using deep sequencing data. Nucleic acids research 2014; 42(Database issue): D68-73.

Krek A, Grün D, Poy MN, Wolf R, Rosenberg L, Epstein EJ*, et al.* Combinatorial microRNA target predictions. Nature genetics 2005; 37(5): 495-500.

Krutzfeldt J, Rajewsky N, Braich R, Rajeev KG, Tuschl T, Manoharan M*, et al.* Silencing of microRNAs in vivo with 'antagomirs'. Nature 2005; 438(7068): 685-9.

Kumar M, Lu Z, Takwi AA, Chen W, Callander NS, Ramos KS*, et al.* Negative regulation of the tumor suppressor p53 gene by microRNAs. Oncogene 2011; 30(7): 843-53.

La Spada AR, Roling DB, Harding AE, Warner CL, Spiegel R, Hausmanowa-Petrusewicz I*, et al.* Meiotic stability and genotype-phenotype correlation of the trinucleotide repeat in X-linked spinal and bulbar muscular atrophy. Nature genetics 1992; 2(4): 301-4.

La Spada AR, Wilson EM, Lubahn DB, Harding AE, Fischbeck KH. Androgen receptor gene mutations in X-linked spinal and bulbar muscular atrophy. Nature 1991; 352(6330): 77-9.

Lagos-Quintana M, Rauhut R, Lendeckel W, Tuschl T. Identification of novel genes coding for small expressed RNAs. Science 2001; 294(5543): 853-8.

Lagos-Quintana M, Rauhut R, Yalcin A, Meyer J, Lendeckel W, Tuschl T. Identification of tissue-specific microRNAs from mouse. Current biology : CB 2002; 12(9): 735-9.

Lam JK, Chow MY, Zhang Y, Leung SW. siRNA Versus miRNA as Therapeutics for Gene Silencing. Molecular therapy Nucleic acids 2015; 4: e252.

Landau WM, Schmidt RE, McGlennen RC, Reich SG. Hereditary spastic paraplegia and hereditary ataxia, Part 2: A family demonstrating various phenotypic manifestations with the SCA3 genotype. Archives of neurology 2000; 57(5): 733-9.

Lebbink RJ, Lowe M, Chan T, Khine H, Wang X, McManus MT. Polymerase II promoter strength determines efficacy of microRNA adapted shRNAs. PloS one 2011; 6(10): e26213.

Lee RC, Feinbaum RL, Ambros V. The C. elegans heterochronic gene lin-4 encodes small RNAs with antisense complementarity to lin-14. Cell 1993; 75(5): 843-54.

Lee ST, Chu K, Im WS, Yoon HJ, Im JY, Park JE*, et al.* Altered microRNA regulation in Huntington's disease models. Experimental neurology 2011; 227(1): 172-9.

Lee Y, Ahn C, Han J, Choi H, Kim J, Yim J*, et al.* The nuclear RNase III Drosha initiates microRNA processing. Nature 2003; 425(6956): 415-9.

Lee Y, Samaco RC, Gatchel JR, Thaller C, Orr HT, Zoghbi HY. miR-19, miR-101 and miR-130 co-regulate ATXN1 levels to potentially modulate SCA1 pathogenesis. Nature neuroscience 2008; 11(10): 1137-9.

Lei LF, Yang GP, Wang JL, Chuang DM, Song WH, Tang BS*, et al.* Safety and efficacy of valproic acid treatment in SCA3/MJD patients. Parkinsonism & related disorders 2016; 26: 55-61.

Lennox KA, Owczarzy R, Thomas DM, Walder JA, Behlke MA. Improved Performance of Anti-miRNA Oligonucleotides Using a Novel Non-Nucleotide Modifier. Molecular therapy Nucleic acids 2013; 2: e117.

Li F, Macfarlan T, Pittman RN, Chakravarti D. Ataxin-3 is a histone-binding protein with two independent transcriptional corepressor activities. The Journal of biological chemistry 2002; 277(47): 45004-12.

Li LB, Yu Z, Teng X, Bonini NM. RNA toxicity is a component of ataxin-3 degeneration in Drosophila. Nature 2008; 453(7198): 1107-11.

Licatalosi DD, Darnell RB. RNA processing and its regulation: global insights into biological networks. Nature reviews Genetics 2010; 11(1): 75-87.

Lima M, Mayer FM, Coutinho P, Abade A. Origins of a mutation: population genetics of Machado-Joseph disease in the Azores (Portugal). Human biology 1998; 70(6): 1011-23.

Lin SY, Johnson SM, Abraham M, Vella MC, Pasquinelli A, Gamberi C*, et al.* The C elegans hunchback homolog, hbl-1, controls temporal patterning and is a probable microRNA target. Developmental cell 2003; 4(5): 639-50.

Lisowski L, Tay SS, Alexander IE. Adeno-associated virus serotypes for gene therapeutics. Current opinion in pharmacology 2015; 24: 59-67.

Liu CS, Hsu HM, Cheng WL, Hsieh M. Clinical and molecular events in patients with Machado-Joseph disease under lamotrigine therapy. Acta neurologica Scandinavica 2005; 111(6): 385-90.

Liu J, Carmell MA, Rivas FV, Marsden CG, Thomson JM, Song JJ*, et al.* Argonaute2 is the catalytic engine of mammalian RNAi. Science 2004; 305(5689): 1437-41.

Liu T, Im W, Mook-Jung I, Kim M. MicroRNA-124 slows down the progression of Huntington's disease by promoting neurogenesis in the striatum. Neural regeneration research 2015; 10(5): 786-91.

Liu X, Fortin K, Mourelatos Z. MicroRNAs: biogenesis and molecular functions. Brain pathology 2008; 18(1): 113-21.

Long Z, Chen Z, Wang C, Huang F, Peng H, Hou X*, et al.* Two novel SNPs in ATXN3 3' UTR may decrease age at onset of SCA3/MJD in Chinese patients. PloS one 2015; 10(2): e0117488.

Lund E, Guttinger S, Calado A, Dahlberg JE, Kutay U. Nuclear export of microRNA precursors. Science 2004; 303(5654): 95-8.

Macedo-Ribeiro S, Cortes L, Maciel P, Carvalho AL. Nucleocytoplasmic shuttling activity of ataxin-3. PloS one 2009; 4(6): e5834.

Maciel P, Gaspar C, DeStefano AL, Silveira I, Coutinho P, Radvany J*, et al.* Correlation between CAG repeat length and clinical features in Machado-Joseph disease. American journal of human genetics 1995; 57(1): 54-61.

Maczuga P, Koornneef A, Borel F, Petry H, van Deventer S, Ritsema T*, et al.* Optimization and comparison of knockdown efficacy between polymerase II expressed shRNA and artificial miRNA targeting luciferase and Apolipoprotein B100. BMC biotechnology 2012; 12: 42.

Makinen PI, Koponen JK, Karkkainen AM, Malm TM, Pulkkinen KH, Koistinaho J*, et al.* Stable RNA interference: comparison of U6 and H1 promoters in endothelial cells and in mouse brain. The journal of gene medicine 2006; 8(4): 433-41.

Mangiarini L, Sathasivam K, Seller M, Cozens B, Harper A, Hetherington C*, et al.* Exon 1 of the HD gene with an expanded CAG repeat is sufficient to cause a progressive neurological phenotype in transgenic mice. Cell 1996; 87(3): 493-506.

Mao Y, Senic-Matuglia F, Di Fiore PP, Polo S, Hodsdon ME, De Camilli P. Deubiquitinating function of ataxin-3: insights from the solution structure of the Josephin domain. Proceedings of the National Academy of Sciences of the United States of America 2005; 102(36): 12700-5.

Marti E, Pantano L, Banez-Coronel M, Llorens F, Minones-Moyano E, Porta S*, et al.* A myriad of miRNA variants in control and Huntington's disease brain regions detected by massively parallel sequencing. Nucleic acids research 2010; 38(20): 7219-35.

Martin JN, Wolken N, Brown T, Dauer WT, Ehrlich ME, Gonzalez-Alegre P. Lethal toxicity caused by expression of shRNA in the mouse striatum: implications for therapeutic design. Gene therapy 2011; 18(7): 666-73.

Masino L, Musi V, Menon RP, Fusi P, Kelly G, Frenkiel TA*, et al.* Domain architecture of the polyglutamine protein ataxin-3: a globular domain followed by a flexible tail. FEBS letters 2003; 549(1-3): 21-5.

Matos CA, de Macedo-Ribeiro S, Carvalho AL. Polyglutamine diseases: the special case of ataxin-3 and Machado-Joseph disease. Progress in neurobiology 2011; 95(1): 26-48.

Matoulkova E, Michalova E, Vojtesek B, Hrstka R. The role of the 3' untranslated region in post-transcriptional regulation of protein expression in mammalian cells. RNA biology 2012; 9(5): 563-76.

Maziere P, Enright AJ. Prediction of microRNA targets. Drug discovery today 2007; 12(11-12): 452-8.

Mazzucchelli S, De Palma A, Riva M, D'Urzo A, Pozzi C, Pastori V*, et al.* Proteomic and biochemical analyses unveil tight interaction of ataxin-3 with tubulin. The international journal of biochemistry & cell biology 2009; 41(12): 2485-92.

McBride JL, Boudreau RL, Harper SQ, Staber PD, Monteys AM, Martins I*, et al.* Artificial miRNAs mitigate shRNA-mediated toxicity in the brain: implications for the therapeutic development of RNAi. Proceedings of the National Academy of Sciences of the United States of America 2008; 105(15): 5868-73.

McCampbell A, Taylor JP, Taye AA, Robitschek J, Li M, Walcott J*, et al.* CREB-binding protein sequestration by expanded polyglutamine. Human molecular genetics 2000; 9(14): 2197-202.

McCann C, Holohan EE, Das S, Dervan A, Larkin A, Lee JA*, et al.* The Ataxin-2 protein is required for microRNA function and synapse-specific long-term olfactory habituation. Proceedings of the National Academy of Sciences of the United States of America 2011; 108(36): E655-62.

McMurray CT. Mechanisms of trinucleotide repeat instability during human development. Nature reviews Genetics 2010; 11(11): 786-99.

Mendonca LS, Nobrega C, Hirai H, Kaspar BK, Pereira de Almeida L. Transplantation of cerebellar neural stem cells improves motor coordination and neuropathology in Machado-Joseph disease mice. Brain : a journal of neurology 2015; 138(Pt 2): 320-35.

Millar AA, Waterhouse PM. Plant and animal microRNAs: similarities and differences. Functional & integrative genomics 2005; 5(3): 129-35.

Miller VM, Xia H, Marrs GL, Gouvion CM, Lee G, Davidson BL*, et al.* Allele-specific silencing of dominant disease genes. Proceedings of the National Academy of Sciences of the United States of America 2003; 100(12): 7195-200.

Mitchell RS, Beitzel BF, Schroder AR, Shinn P, Chen H, Berry CC*, et al.* Retroviral DNA integration: ASLV, HIV, and MLV show distinct target site preferences. PLoS biology 2004; 2(8): E234.

Miyazaki Y, Adachi H, Katsuno M, Minamiyama M, Jiang YM, Huang Z*, et al.* Viral delivery of miR-196a ameliorates the SBMA phenotype via the silencing of CELF2. Nature medicine 2012; 18(7): 1136-41.

Miyazaki Y, Du X, Muramatsu S, Gomez CM. An miRNA-mediated therapy for SCA6 blocks IRES-driven translation of the CACNA1A second cistron. Science translational medicine 2016; 8(347): 347ra94.

Montag J, Hitt R, Opitz L, Schulz-Schaeffer WJ, Hunsmann G, Motzkus D. Upregulation of miRNA hsa-miR-342-3p in experimental and idiopathic prion disease. Molecular Neurodegeneration 2009; 4(1): 36.

Monte TL, Rieder CR, Tort AB, Rockenback I, Pereira ML, Silveira I*, et al.* Use of fluoxetine for treatment of Machado-Joseph disease: an open-label study. Acta neurologica Scandinavica 2003; 107(3): 207-10.

Mulligan MK, Dubose C, Yue J, Miles MF, Lu L, Hamre KM. Expression, covariation, and genetic regulation of miRNA Biogenesis genes in brain supports their role in addiction, psychiatric disorders, and disease. Frontiers in genetics 2013; 4: 126.

Munoz E, Rey MJ, Mila M, Cardozo A, Ribalta T, Tolosa E*, et al.* Intranuclear inclusions, neuronal loss and CAG mosaicism in two patients with Machado-Joseph disease. Journal of the neurological sciences 2002; 200(1-2): 19-25.

Mykowska A, Sobczak K, Wojciechowska M, Kozlowski P, Krzyzosiak WJ. CAG repeats mimic CUG repeats in the misregulation of alternative splicing. Nucleic acids research 2011; 39(20): 8938-51.

Nagai Y, Inui T, Popiel HA, Fujikake N, Hasegawa K, Urade Y*, et al.* A toxic monomeric conformer of the polyglutamine protein. Nature structural & molecular biology 2007; 14(4): 332-40.

Nakano KK, Dawson DM, Spence A. Machado disease. A hereditary ataxia in Portuguese emigrants to Massachusetts. Neurology 1972; 22(1): 49-55.

Nascimento-Ferreira I, Nobrega C, Vasconcelos-Ferreira A, Onofre I, Albuquerque D, Aveleira C*, et al.* Beclin 1 mitigates motor and neuropathological deficits in genetic mouse models of Machado-Joseph disease. Brain : a journal of neurology 2013; 136(Pt 7): 2173-88.

Nascimento-Ferreira I, Santos-Ferreira T, Sousa-Ferreira L, Auregan G, Onofre I, Alves S*, et al.* Overexpression of the autophagic beclin-1 protein clears mutant ataxin-3 and alleviates Machado-Joseph disease. Brain : a journal of neurology 2011; 134(Pt 5): 1400-15.

Nicastro G, Menon RP, Masino L, Knowles PP, McDonald NQ, Pastore A. The solution structure of the Josephin domain of ataxin-3: structural determinants for molecular recognition. Proceedings of the National Academy of Sciences of the United States of America 2005; 102(30): 10493-8.

Nilsen TW. Mechanisms of microRNA-mediated gene regulation in animal cells. Trends in genetics : TIG 2007; 23(5): 243-9.

Nobrega C, Carmo-Silva S, Albuquerque D, Vasconcelos-Ferreira A, Vijayakumar UG, Mendonca L*, et al.* Re-establishing ataxin-2 downregulates translation of mutant ataxin-3 and alleviates Machado-Joseph disease. Brain : a journal of neurology 2015; 138(Pt 12): 3537-54.

Nobrega C, Nascimento-Ferreira I, Onofre I, Albuquerque D, Conceicao M, Deglon N*, et al.* Overexpression of mutant ataxin-3 in mouse cerebellum induces ataxia and cerebellar neuropathology. Cerebellum 2013a; 12(4): 441-55.

Nobrega C, Nascimento-Ferreira I, Onofre I, Albuquerque D, Deglon N, de Almeida LP. RNA interference mitigates motor and neuropathological deficits in a cerebellar mouse model of Machado-Joseph disease. PloS one 2014; 9(8): e100086.

Nobrega C, Nascimento-Ferreira I, Onofre I, Albuquerque D, Hirai H, Deglon N*, et al.* Silencing mutant ataxin-3 rescues motor deficits and neuropathology in Machado-Joseph disease transgenic mice. PloS one 2013b; 8(1): e52396.

Onofre I. Dissecting the pathogenesis of Machado-Joseph Disease in a new human disease model derived from induced pluripotent stem cells: University of Coimbra; 2016.

Onofre I, Mendonca N, Lopes S, Nobre R, de Melo JB, Carreira IM*, et al.* Fibroblasts of Machado Joseph Disease patients reveal autophagy impairment. Scientific reports 2016; 6: 28220.

Ordway JM, Tallaksen-Greene S, Gutekunst CA, Bernstein EM, Cearley JA, Wiener HW*, et al.* Ectopically expressed CAG repeats cause intranuclear inclusions and a

progressive late onset neurological phenotype in the mouse. Cell 1997; 91(6): 753-63.

Oue M, Mitsumura K, Torashima T, Koyama C, Yamaguchi H, Furuya N*, et al.* Characterization of mutant mice that express polyglutamine in cerebellar Purkinje cells. Brain research 2009; 1255: 9-17.

Packer AN, Xing Y, Harper SQ, Jones L, Davidson BL. The bifunctional microRNA miR-9/miR-9* regulates REST and CoREST and is downregulated in Huntington's disease. The Journal of neuroscience : the official journal of the Society for Neuroscience 2008; 28(53): 14341-6.

Paraskevopoulou MD, Georgakilas G, Kostoulas N, Reczko M, Maragkakis M, Dalamagas TM*, et al.* DIANA-LncBase: experimentally verified and computationally predicted microRNA targets on long non-coding RNAs. Nucleic acids research 2013; 41(Database issue): D239-45.

Pasquinelli AE, Reinhart BJ, Slack F, Martindale MQ, Kuroda MI, Maller B*, et al.* Conservation of the sequence and temporal expression of let-7 heterochronic regulatory RNA. Nature 2000; 408(6808): 86-9.

Paulson H. Spinocerebellar Ataxia Type 3. In: Pagon RA, Adam MP, Ardinger HH, Wallace SE, Amemiya A, Bean LJH*, et al.*, editors. GeneReviews(R). Seattle (WA); 1993.

Paulson H. Machado-Joseph disease/spinocerebellar ataxia type 3. Handbook of clinical neurology 2012; 103: 437-49.

Paulson HL, Das SS, Crino PB, Perez MK, Patel SC, Gotsdiner D*, et al.* Machado-Joseph disease gene product is a cytoplasmic protein widely expressed in brain. Annals of neurology 1997a; 41(4): 453-62.

Paulson HL, Perez MK, Trottier Y, Trojanowski JQ, Subramony SH, Das SS*, et al.* Intranuclear inclusions of expanded polyglutamine protein in spinocerebellar ataxia type 3. Neuron 1997b; 19(2): 333-44.

Peden CS, Burger C, Muzyczka N, Mandel RJ. Circulating anti-wild-type adeno-associated virus type 2 (AAV2) antibodies inhibit recombinant AAV2 (rAAV2)-mediated, but not rAAV5-mediated, gene transfer in the brain. Journal of virology 2004; 78(12): 6344-59.

Pedroso JL, Franca MC, Jr., Braga-Neto P, D'Abreu A, Saraiva-Pereira ML, Saute JA*, et al.* Nonmotor and extracerebellar features in Machado-Joseph disease: a review. Movement disorders : official journal of the Movement Disorder Society 2013; 28(9): 1200-8.

Perez MK, Paulson HL, Pendse SJ, Saionz SJ, Bonini NM, Pittman RN. Recruitment and the role of nuclear localization in polyglutamine-mediated aggregation. The Journal of cell biology 1998; 143(6): 1457-70.

Perron MP, Provost P. Protein interactions and complexes in human microRNA biogenesis and function. Frontiers in bioscience : a journal and virtual library 2008; 13: 2537-47.

Persengiev S, Kondova I, Otting N, Koeppen AH, Bontrop RE. Genome-wide analysis of miRNA expression reveals a potential role for miR-144 in brain aging and

spinocerebellar ataxia pathogenesis. Neurobiology of aging 2011; 32(12): 2316 e17-27.

Peter ME. Targeting of mRNAs by multiple miRNAs: the next step. Oncogene 2010; 29(15): 2161-4.

Philippe S, Sarkis C, Barkats M, Mammeri H, Ladroue C, Petit C*, et al.* Lentiviral vectors with a defective integrase allow efficient and sustained transgene expression in vitro and in vivo. Proceedings of the National Academy of Sciences of the United States of America 2006; 103(47): 17684-9.

Pourshafie N, Lee PR, Chen KL, Harmison GG, Bott LC, Katsuno M*, et al.* MiR-298 Counteracts Mutant Androgen Receptor Toxicity in Spinal and Bulbar Muscular Atrophy. Molecular therapy : the journal of the American Society of Gene Therapy 2016.

Proudfoot NJ, Brownlee GG. 3' non-coding region sequences in eukaryotic messenger RNA. Nature 1976; 263(5574): 211-4.

Qu J, Li M, Zhong W, Hu C. Prognostic role of microRNA-25 in cancers: evidence from a meta-analysis. International journal of clinical and experimental medicine 2015; 8(8): 12921-7.

Rahim AA, Wong AM, Howe SJ, Buckley SM, Acosta-Saltos AD, Elston KE*, et al.* Efficient gene delivery to the adult and fetal CNS using pseudotyped non-integrating lentiviral vectors. Gene therapy 2009; 16(4): 509-20.

Ramani B, Harris GM, Huang R, Seki T, Murphy GG, Costa Mdo C*, et al.* A knockin mouse model of spinocerebellar ataxia type 3 exhibits prominent aggregate pathology and aberrant splicing of the disease gene transcript. Human molecular genetics 2015; 24(5): 1211-24.

Ranum LP, Chung MY, Banfi S, Bryer A, Schut LJ, Ramesar R*, et al.* Molecular and clinical correlations in spinocerebellar ataxia type I: evidence for familial effects on the age at onset. American journal of human genetics 1994; 55(2): 244-52.

Raposo M, Bettencourt C, Maciel P, Gao F, Ramos A, Kazachkova N*, et al.* Novel candidate blood-based transcriptional biomarkers of Machado-Joseph disease. Movement disorders : official journal of the Movement Disorder Society 2015; 30(7): 968-75.

Reina CP, Zhong X, Pittman RN. Proteotoxic stress increases nuclear localization of ataxin-3. Human molecular genetics 2010; 19(2): 235-49.

Reinhardt A, Feuillette S, Cassar M, Callens C, Thomassin H, Birman S*, et al.* Lack of miRNA Misregulation at Early Pathological Stages in Drosophila Neurodegenerative Disease Models. Frontiers in genetics 2012; 3: 226.

Reinhart BJ, Slack FJ, Basson M, Pasquinelli AE, Bettinger JC, Rougvie AE*, et al.* The 21-nucleotide let-7 RNA regulates developmental timing in Caenorhabditis elegans. Nature 2000; 403(6772): 901-6.

Riess O, Rub U, Pastore A, Bauer P, Schols L. SCA3: neurological features, pathogenesis and animal models. Cerebellum 2008; 7(2): 125-37.

Rodrigues AJ, Coppola G, Santos C, Costa Mdo C, Ailion M, Sequeiros J*, et al.* Functional genomics and biochemical characterization of the C. elegans orthologue of the Machado-Joseph disease protein ataxin-3. FASEB journal : official publication of the Federation of American Societies for Experimental Biology 2007; 21(4): 1126-36.

Rodrigues AJ, Neves-Carvalho A, Teixeira-Castro A, Rokka A, Corthals G, Logarinho E*, et al.* Absence of ataxin-3 leads to enhanced stress response in C. elegans. PloS one 2011; 6(4): e18512.

Rodriguez-Lebron E, Costa M, Luna-Cancalon K, Peron TM, Fischer S, Boudreau RL*, et al.* Silencing mutant ATXN3 expression resolves molecular phenotypes in SCA3 transgenic mice. Molecular therapy : the journal of the American Society of Gene Therapy 2013a; 21(10): 1909-18.

Rodriguez-Lebron E, Liu G, Keiser M, Behlke MA, Davidson BL. Altered Purkinje cell miRNA expression and SCA1 pathogenesis. Neurobiology of disease 2013b; 54: 456-63.

Romanul FC, Fowler HL, Radvany J, Feldman RG, Feingold M. Azorean disease of the nervous system. The New England journal of medicine 1977; 296(26): 1505-8.

Rosenberg RN. Machado-Joseph disease: an autosomal dominant motor system degeneration. Movement disorders : official journal of the Movement Disorder Society 1992; 7(3): 193-203.

Rosenberg RN, Nyhan WL, Bay C, Shore P. Autosomal dominant striatonigral degeneration. A clinical, pathologic, and biochemical study of a new genetic disorder. Neurology 1976; 26(8): 703-14.

Rub U, Brunt ER, Deller T. New insights into the pathoanatomy of spinocerebellar ataxia type 3 (Machado-Joseph disease). Current opinion in neurology 2008; 21(2): 111-6.

Rub U, Schols L, Paulson H, Auburger G, Kermer P, Jen JC*, et al.* Clinical features, neurogenetics and neuropathology of the polyglutamine spinocerebellar ataxias type 1, 2, 3, 6 and 7. Progress in neurobiology 2013; 104: 38-66.

Saetrom P, Heale BS, Snove O, Jr., Aagaard L, Alluin J, Rossi JJ. Distance constraints between microRNA target sites dictate efficacy and cooperativity. Nucleic acids research 2007; 35(7): 2333-42.

Saito T, Saetrom P. MicroRNAs--targeting and target prediction. New biotechnology 2010; 27(3): 243-9.

Sakai T, Matsuishi T, Yamada S, Komori H, Iwashita H. Sulfamethoxazole-trimethoprim double-blind, placebo-controlled, crossover trial in Machado-Joseph disease: sulfamethoxazole-trimethoprim increases cerebrospinal fluid level of biopterin. Journal of neural transmission General section 1995; 102(2): 159-72.

Sasaki Y, Gross C, Xing L, Goshima Y, Bassell GJ. Identification of axon-enriched MicroRNAs localized to growth cones of cortical neurons. Developmental neurobiology 2014; 74(3): 397-406.

Saute JA, de Castilhos RM, Monte TL, Schumacher-Schuh AF, Donis KC, D'Avila R*, et al.* A randomized, phase 2 clinical trial of lithium carbonate in Machado-Joseph

disease. Movement disorders : official journal of the Movement Disorder Society 2014; 29(4): 568-73.

Schaefer A, O'Carroll D, Tan CL, Hillman D, Sugimori M, Llinas R*, et al.* Cerebellar neurodegeneration in the absence of microRNAs. The Journal of experimental medicine 2007; 204(7): 1553-8.

Scheel H, Tomiuk S, Hofmann K. Elucidation of ataxin-3 and ataxin-7 function by integrative bioinformatics. Human molecular genetics 2003; 12(21): 2845-52.

Scherr M, Venturini L, Battmer K, Schaller-Schoenitz M, Schaefer D, Dallmann I*, et al.* Lentivirus-mediated antagomir expression for specific inhibition of miRNA function. Nucleic acids research 2007; 35(22): e149.

Schmidt MF. Drug target miRNAs: chances and challenges. Trends in biotechnology 2014; 32(11): 578-85.

Schmidt T, Landwehrmeyer GB, Schmitt I, Trottier Y, Auburger G, Laccone F*, et al.* An isoform of ataxin-3 accumulates in the nucleus of neuronal cells in affected brain regions of SCA3 patients. Brain pathology 1998; 8(4): 669-79.

Schmitt I, Linden M, Khazneh H, Evert BO, Breuer P, Klockgether T*, et al.* Inactivation of the mouse Atxn3 (ataxin-3) gene increases protein ubiquitination. Biochemical and biophysical research communications 2007; 362(3): 734-9.

Schols L, Bauer P, Schmidt T, Schulte T, Riess O. Autosomal dominant cerebellar ataxias: clinical features, genetics, and pathogenesis. The Lancet Neurology 2004; 3(5): 291-304.

Schols L, Haan J, Riess O, Amoiridis G, Przuntek H. Sleep disturbance in spinocerebellar ataxias: is the SCA3 mutation a cause of restless legs syndrome? Neurology 1998; 51(6): 1603-7.

Schroder AR, Shinn P, Chen H, Berry C, Ecker JR, Bushman F. HIV-1 integration in the human genome favors active genes and local hotspots. Cell 2002; 110(4): 521-9.

Schulte T, Mattern R, Berger K, Szymanski S, Klotz P, Kraus PH*, et al.* Double-blind crossover trial of trimethoprim-sulfamethoxazole in spinocerebellar ataxia type 3/Machado-Joseph disease. Archives of neurology 2001; 58(9): 1451-7.

Schulz JB, Borkert J, Wolf S, Schmitz-Hubsch T, Rakowicz M, Mariotti C*, et al.* Visualization, quantification and correlation of brain atrophy with clinical symptoms in spinocerebellar ataxia types 1, 3 and 6. NeuroImage 2010; 49(1): 158-68.

Schwarz DS, Hutvagner G, Du T, Xu Z, Aronin N, Zamore PD. Asymmetry in the assembly of the RNAi enzyme complex. Cell 2003; 115(2): 199-208.

Seidel K, Siswanto S, Brunt ER, den Dunnen W, Korf HW, Rub U. Brain pathology of spinocerebellar ataxias. Acta neuropathologica 2012; 124(1): 1-21.

Selbach M, Schwanhausser B, Thierfelder N, Fang Z, Khanin R, Rajewsky N. Widespread changes in protein synthesis induced by microRNAs. Nature 2008; 455(7209): 58-63.

Senut MC, Suhr ST, Kaspar B, Gage FH. Intraneuronal aggregate formation and cell death after viral expression of expanded polyglutamine tracts in the adult rat brain. The Journal of neuroscience : the official journal of the Society for Neuroscience 2000; 20(1): 219-29.

Sequeiros J, Coutinho P. Epidemiology and clinical aspects of Machado-Joseph disease. Advances in neurology 1993; 61: 139-53.

Seyhan AA. A multiplexed miRNA and transgene expression platform for simultaneous repression and expression of protein coding sequences. Molecular bioSystems 2016; 12(1): 295-312.

Shan G, Li Y, Zhang J, Li W, Szulwach KE, Duan R*, et al.* A small molecule enhances RNA interference and promotes microRNA processing. Nature biotechnology 2008; 26(8): 933-40.

Shao J, Diamond MI. Polyglutamine diseases: emerging concepts in pathogenesis and therapy. Human molecular genetics 2007; 16 Spec No. 2: R115-23.

Shi Y, Huang F, Tang B, Li J, Wang J, Shen L*, et al.* MicroRNA profiling in the serums of SCA3/MJD patients. The International journal of neuroscience 2014; 124(2): 97-101.

Shirasaki H, Ishida C, Nakajima T, Kamei H, Koide T, Fukuhara N. [A quantitative evaluation of spinocerebellar degeneration by an acoustic analysis--the effect of taltirelin hydrate on patients with Machado-Joseph disease]. Rinsho shinkeigaku = Clinical neurology 2003; 43(4): 143-8.

Silva-Fernandes A, Costa Mdo C, Duarte-Silva S, Oliveira P, Botelho CM, Martins L*, et al.* Motor uncoordination and neuropathology in a transgenic mouse model of Machado-Joseph disease lacking intranuclear inclusions and ataxin-3 cleavage products. Neurobiology of disease 2010; 40(1): 163-76.

Silva-Fernandes A, Duarte-Silva S, Neves-Carvalho A, Amorim M, Soares-Cunha C, Oliveira P*, et al.* Chronic treatment with 17-DMAG improves balance and coordination in a new mouse model of Machado-Joseph disease. Neurotherapeutics : the journal of the American Society for Experimental NeuroTherapeutics 2014; 11(2): 433-49.

Silva RC, Saute JA, Silva AC, Coutinho AC, Saraiva-Pereira ML, Jardim LB. Occupational therapy in spinocerebellar ataxia type 3: an open-label trial. Brazilian journal of medical and biological research = Revista brasileira de pesquisas medicas e biologicas / Sociedade Brasileira de Biofisica [et al] 2010; 43(6): 537-42.

Simoes AT, Goncalves N, Koeppen A, Deglon N, Kugler S, Duarte CB*, et al.* Calpastatin-mediated inhibition of calpains in the mouse brain prevents mutant ataxin 3 proteolysis, nuclear localization and aggregation, relieving Machado-Joseph disease. Brain : a journal of neurology 2012; 135(Pt 8): 2428-39.

Simoes AT, Goncalves N, Nobre RJ, Duarte CB, Pereira de Almeida L. Calpain inhibition reduces ataxin-3 cleavage alleviating neuropathology and motor impairments in mouse models of Machado-Joseph disease. Human molecular genetics 2014; 23(18): 4932-44.

Sinn PL, Sauter SL, McCray PB, Jr. Gene therapy progress and prospects: development of improved lentiviral and retroviral vectors--design, biosafety, and production. Gene therapy 2005; 12(14): 1089-98.

Skinner PJ, Koshy BT, Cummings CJ, Klement IA, Helin K, Servadio A*, et al.* Ataxin-1 with an expanded glutamine tract alters nuclear matrix-associated structures. Nature 1997; 389(6654): 971-4.

Sledz CA, Holko M, de Veer MJ, Silverman RH, Williams BR. Activation of the interferon system by short-interfering RNAs. Nature cell biology 2003; 5(9): 834-9.

Smalheiser NR, Zhang H, Dwivedi Y. Enoxacin Elevates MicroRNA Levels in Rat Frontal Cortex and Prevents Learned Helplessness. Frontiers in psychiatry 2014; 5: 6.

Sontheimer EJ. Assembly and function of RNA silencing complexes. Nature reviews Molecular cell biology 2005; 6(2): 127-38.

Sorensen MD, Kvaerno L, Bryld T, Hakansson AE, Verbeure B, Gaubert G*, et al.* alpha-L-ribo-configured locked nucleic acid (alpha-L-LNA): synthesis and properties. Journal of the American Chemical Society 2002; 124(10): 2164-76.

Spies N, Burge CB, Bartel DP. 3' UTR-isoform choice has limited influence on the stability and translational efficiency of most mRNAs in mouse fibroblasts. Genome research 2013; 23(12): 2078-90.

Stark A, Brennecke J, Bushati N, Russell RB, Cohen SM. Animal MicroRNAs confer robustness to gene expression and have a significant impact on 3'UTR evolution. Cell 2005; 123(6): 1133-46.

Stefani G, Slack FJ. A 'pivotal' new rule for microRNA-mRNA interactions. Nature structural & molecular biology 2012; 19(3): 265-6.

Sudarsky L, Corwin L, Dawson DM. Machado-Joseph disease in New England: clinical description and distinction from the olivopontocerebellar atrophies. Movement disorders : official journal of the Movement Disorder Society 1992; 7(3): 204-8.

Sudarsky L, Coutinho P. Machado-Joseph disease. Clinical neuroscience 1995; 3(1): 17-22.

Suenaga T, Matsushima H, Nakamura S, Akiguchi I, Kimura J. Ubiquitin-immunoreactive inclusions in anterior horn cells and hypoglossal neurons in a case with Joseph's disease. Acta neuropathologica 1993; 85(3): 341-4.

Switonski PM, Szlachcic WJ, Krzyzosiak WJ, Figiel M. A new humanized ataxin-3 knock-in mouse model combines the genetic features, pathogenesis of neurons and glia and late disease onset of SCA3/MJD. Neurobiology of disease 2015; 73: 174-88.

Tait D, Riccio M, Sittler A, Scherzinger E, Santi S, Ognibene A*, et al.* Ataxin-3 is transported into the nucleus and associates with the nuclear matrix. Human molecular genetics 1998; 7(6): 991-7.

Takahashi J, Tanaka J, Arai K, Funata N, Hattori T, Fukuda T*, et al.* Recruitment of nonexpanded polyglutamine proteins to intranuclear aggregates in neuronal intranuclear hyaline inclusion disease. Journal of neuropathology and experimental neurology 2001; 60(4): 369-76.

Takahashi K, Yamanaka S. Induction of Pluripotent Stem Cells from Mouse Embryonic and Adult Fibroblast Cultures by Defined Factors. Cell 2006; 126(4): 663-76.

Takahashi T, Kikuchi S, Katada S, Nagai Y, Nishizawa M, Onodera O. Soluble polyglutamine oligomers formed prior to inclusion body formation are cytotoxic. Human molecular genetics 2008; 17(3): 345-56.

Takei A, Fukazawa T, Hamada T, Sohma H, Yabe I, Sasaki H*, et al.* Effects of tandospirone on "5-HT1A receptor-associated symptoms" in patients with Machado-Josephe disease: an open-label study. Clinical neuropharmacology 2004; 27(1): 9-13.

Takiyama Y, Nishizawa M, Tanaka H, Kawashima S, Sakamoto H, Karube Y*, et al.* The gene for Machado-Joseph disease maps to human chromosome 14q. Nature genetics 1993; 4(3): 300-4.

Tan JY, Vance KW, Varela MA, Sirey T, Watson LM, Curtis HJ*, et al.* Cross-talking noncoding RNAs contribute to cell-specific neurodegeneration in SCA7. Nature structural & molecular biology 2014; 21(11): 955-61.

Taniwaki T, Sakai T, Kobayashi T, Kuwabara Y, Otsuka M, Ichiya Y*, et al.* Positron emission tomography (PET) in Machado-Joseph disease. Journal of the neurological sciences 1997; 145(1): 63-7.

Teixeira-Castro A, Ailion M, Jalles A, Brignull HR, Vilaca JL, Dias N*, et al.* Neuron-specific proteotoxicity of mutant ataxin-3 in C. elegans: rescue by the DAF-16 and HSF-1 pathways. Human molecular genetics 2011; 20(15): 2996-3009.

Thomas CE, Ehrhardt A, Kay MA. Progress and problems with the use of viral vectors for gene therapy. Nature reviews Genetics 2003; 4(5): 346-58.

Tian B, Hu J, Zhang H, Lutz CS. A large-scale analysis of mRNA polyadenylation of human and mouse genes. Nucleic acids research 2005; 33(1): 201-12.

Todi SV, Paulson HL. Balancing act: deubiquitinating enzymes in the nervous system. Trends in neurosciences 2011; 34(7): 370-82.

Todi SV, Winborn BJ, Scaglione KM, Blount JR, Travis SM, Paulson HL. Ubiquitination directly enhances activity of the deubiquitinating enzyme ataxin-3. The EMBO journal 2009; 28(4): 372-82.

Torashima T, Koyama C, Iizuka A, Mitsumura K, Takayama K, Yanagi S*, et al.* Lentivector-mediated rescue from cerebellar ataxia in a mouse model of spinocerebellar ataxia. EMBO reports 2008; 9(4): 393-9.

Trottier Y, Cancel G, An-Gourfinkel I, Lutz Y, Weber C, Brice A*, et al.* Heterogeneous intracellular localization and expression of ataxin-3. Neurobiology of disease 1998; 5(5): 335-47.

Tsai HF, Tsai HJ, Hsieh M. Full-length expanded ataxin-3 enhances mitochondrial-mediated cell death and decreases Bcl-2 expression in human neuroblastoma cells. Biochemical and biophysical research communications 2004; 324(4): 1274-82.

Tuite PJ, Rogaeva EA, St George-Hyslop PH, Lang AE. Dopa-responsive parkinsonism phenotype of Machado-Joseph disease: confirmation of 14q CAG expansion. Annals of neurology 1995; 38(4): 684-7.

Uchihara T, Iwabuchi K, Funata N, Yagishita S. Attenuated nuclear shrinkage in neurons with nuclear aggregates--a morphometric study on pontine neurons of Machado-Joseph disease brains. Experimental neurology 2002; 178(1): 124-8.

Wahle E. A novel poly(A)-binding protein acts as a specificity factor in the second phase of messenger RNA polyadenylation. Cell 1991; 66(4): 759-68.

Wahlestedt C, Salmi P, Good L, Kela J, Johnsson T, Hokfelt T*, et al.* Potent and nontoxic antisense oligonucleotides containing locked nucleic acids. Proceedings of the National Academy of Sciences of the United States of America 2000; 97(10): 5633-8.

Wang G, Ide K, Nukina N, Goto J, Ichikawa Y, Uchida K*, et al.* Machado-Joseph disease gene product identified in lymphocytes and brain. Biochemical and biophysical research communications 1997; 233(2): 476-9.

Wang YG, Du J, Wang JL, Chen J, Chen C, Luo YY*, et al.* Six cases of SCA3/MJD patients that mimic hereditary spastic paraplegia in clinic. Journal of the neurological sciences 2009; 285(1-2): 121-4.

Warrick JM, Morabito LM, Bilen J, Gordesky-Gold B, Faust LZ, Paulson HL*, et al.* Ataxin-3 suppresses polyglutamine neurodegeneration in Drosophila by a ubiquitin-associated mechanism. Molecular cell 2005; 18(1): 37-48.

Warrick JM, Paulson HL, Gray-Board GL, Bui QT, Fischbeck KH, Pittman RN*, et al.* Expanded polyglutamine protein forms nuclear inclusions and causes neural degeneration in Drosophila. Cell 1998; 93(6): 939-49.

Wellington CL, Ellerby LM, Hackam AS, Margolis RL, Trifiro MA, Singaraja R*, et al.* Caspase cleavage of gene products associated with triplet expansion disorders generates truncated fragments containing the polyglutamine tract. The Journal of biological chemistry 1998; 273(15): 9158-67.

Wen FC, Li YH, Tsai HF, Lin CH, Li C, Liu CS*, et al.* Down-regulation of heat shock protein 27 in neuronal cells and non-neuronal cells expressing mutant ataxin-3. FEBS letters 2003; 546(2-3): 307-14.

Winborn BJ, Travis SM, Todi SV, Scaglione KM, Xu P, Williams AJ*, et al.* The deubiquitinating enzyme ataxin-3, a polyglutamine disease protein, edits Lys63 linkages in mixed linkage ubiquitin chains. The Journal of biological chemistry 2008; 283(39): 26436-43.

Witkos TM, Koscianska E, Krzyzosiak WJ. Practical Aspects of microRNA Target Prediction. Current molecular medicine 2011; 11(2): 93-109.

Woods BT, Schaumburg HH. Nigro-spino-dentatal degeneration with nuclear ophthalmoplegia. A unique and partially treatable clinico-pathological entity. Journal of the neurological sciences 1972; 17(2): 149-66.

Wu L, Belasco JG. Let me count the ways: mechanisms of gene regulation by miRNAs and siRNAs. Molecular cell 2008; 29(1): 1-7.

Wu Z, Asokan A, Samulski RJ. Adeno-associated virus serotypes: vector toolkit for human gene therapy. Molecular therapy : the journal of the American Society of Gene Therapy 2006; 14(3): 316-27.

Xie J, Ameres SL, Friedline R, Hung JH, Zhang Y, Xie Q*, et al.* Long-term, efficient inhibition of microRNA function in mice using rAAV vectors. Nature methods 2012; 9(4): 403-9.

Yamada M, Tan CF, Inenaga C, Tsuji S, Takahashi H. Sharing of polyglutamine localization by the neuronal nucleus and cytoplasm in CAG-repeat diseases. Neuropathology and applied neurobiology 2004; 30(6): 665-75.

Yanez-Munoz RJ, Balaggan KS, MacNeil A, Howe SJ, Schmidt M, Smith AJ*, et al.* Effective gene therapy with nonintegrating lentiviral vectors. Nature medicine 2006; 12(3): 348-53.

Yang JS, Lai EC. Alternative miRNA biogenesis pathways and the interpretation of core miRNA pathway mutants. Molecular cell 2011; 43(6): 892-903.

Yi R, Qin Y, Macara IG, Cullen BR. Exportin-5 mediates the nuclear export of pre-microRNAs and short hairpin RNAs. Genes & development 2003; 17(24): 3011-6.

Yoshizawa T, Yoshida H, Shoji S. Differential susceptibility of cultured cell lines to aggregate formation and cell death produced by the truncated Machado-Joseph disease gene product with an expanded polyglutamine stretch. Brain research bulletin 2001; 56(3-4): 349-52.

Zesiewicz TA, Greenstein PE, Sullivan KL, Wecker L, Miller A, Jahan I*, et al.* A randomized trial of varenicline (Chantix) for the treatment of spinocerebellar ataxia type 3. Neurology 2012; 78(8): 545-50.

Zhang Y, Wang Z, Gemeinhart RA. Progress in microRNA delivery. Journal of controlled release : official journal of the Controlled Release Society 2013a; 172(3): 962-74.

Zhang Z, Almeida S, Lu Y, Nishimura AL, Peng L, Sun D*, et al.* Downregulation of microRNA-9 in iPSC-derived neurons of FTD/ALS patients with TDP-43 mutations. PloS one 2013b; 8(10): e76055.